To the Graduate Council:

I am submitting herewith a thesis written by Amelia Carol Robinson entitled "A Chronosequence Study of Modern Vertisols and Application to Interpreting the Time Significance of Paleozoic PaleoVertisols." I have examined the final paper of this thesis for form and content and recommend that it be accepted in partial fulfillment of the requirements for the degree of Master of Science, with a major in Geology.

Steven G. Driese, Major Professor

We have read this thesis
And recommend its acceptance:

Claudia I. Mora

Michael E. Essington

Accepted for the Council:

Vice Provost and Dean of Graduate Studies

A CHRONOSEQUENCE STUDY OF MODERN VERTISOLS AND APPLICATION TO INTERPRETING THE TIME SIGNIFICANCE OF PALEOZOIC PALEOVERTISOLS

A Thesis
Presented for the
Master of Science Degree
The University of Tennessee, Knoxville

Amelia Carol Robinson
May, 2002

DEDICATION

This thesis is dedicated in honor of:

Robert A. Robinson

and

Bettie Robinson

And in loving memory of my brother,

Robert Scott Wheatley

ACKNOWLEDGEMENTS

I am grateful to my family and friends for their support through this adventure and their faith in the path that I had chosen. My father, Robert Robinson, was my assistant, working for what seemed endless hours, making thin sections. I would not trade the time for the world, but I think we would have both preferred to be fishing. I could never put into words how thankful I am for the love, time, advice, and friendship that Bettie Robinson has provided. Joshua Johnson deserves many, many thanks for his support, his smile, his computer knowledge and most importantly, his heart. I appreciate Autumn Robinson, Christopher McLeary, and Steven Wheatley and family for your encouragement. Jacob, Averie and Lillian, thank you for providing the sunshine in my life.

Teresa, Denise and Melody have been a source of assistance, friendship and humor during my tenure. Thank you for the laughs at all of the right and not-so-right times! My sincere appreciation goes to Dr. Marvin Bennett for his assistance with computer glitches, laboratory instruction support, and his contribution to the department, as a whole. I am grateful to my students and friends from the P.A.C.E. (UT Martin) and MSRC Upward Bound (UT Knoxville) programs. The interaction with you encouraged me to reach for the goal of my doctorate. Several people have made this chapter in my life particularly interesting and fun. To Dana Miller, I owe a million thanks for all the memories, friendship and encouragement. My appreciation goes to Patrick Schuneman and Tabbatha Cavendish for keeping me well fed, encouraged and laughing regardless of the stress! I would like to thank Ellen Robey for her assistance with my research and especially for her friendship. Jennifer Whisner and Keith Milam have been a source of inspiration for their knowledge, their dedication and their contribution to the Department. I would also like to acknowledge Melanie Stewart, Heather Gastineau, Mark Pollock, Janna Peevler, Elizabeth Humbert, Sandra Smith, Peter Nester, and many others for their contribution to my days here at UT. I appreciate your friendship and support.

My research was supported by an NSF Grant to Driese and Mora, a research grant from Southeast GSA, Science Alliance Fellowship, and Discretionary Funds of the Department of Geological Sciences at the University of Tennessee. I appreciate the time and effort of Larry Wilding (TAMU), Warren Lynn (NRCS), and John Wiedenfeld (NRCS) for their support and assistance with sample selection and field reconnaissance. In addition, I would like to thank the members of my committee, Dr. Claudia Mora and Dr. Michael Essington, for their support of this research. In particular, I would like to express sincere gratitude to my thesis advisor, Steven G. Driese. Your encouragement of my work and ideas is greatly appreciated. I would like to acknowledge Cathy Jahr, my high school math teacher, for she was a role model and inspiration early on.

Lastly, I would like to thank the doctors and nurses at Baptist East Hospital (Memphis, TN) for taking care of my dad so that he could see the day that this research reached fruition. It has been a struggle, but to have him at my defense was nothing short of a miracle.

ABSTRACT

Claystone paleosols are common throughout the rock record (e.g., Pennington Fm., Upper Mississippian, TN) and formed in a variety of depositional environments. Studies of paleosols indicate that there is significant retention of primary soil features (i.e., slickensides, gilgai and oriented clay fabric) that are indicative of the Vertisol soil order. These clay-rich soils form from shrink-swell processes associated with seasonal moisture deficit and increased evapotranspiration. The high bulk density, abundance of fine clays, and low topographic position aids in the formation and preservation of Vertisols in the rock record. Most soils form on stable surfaces where pedogenic processes, such as translocation of mobile constituents, structural development of the soil matrix, and accumulation of pedogenic carbonate and Fe-Mn nodules, continue through time to alter the soil profile.

This study utilizes trends in macro- and micromorphology and bulk chemistry to: 1) address rates of Vertisol pedogenesis and 2) identify the characteristics associated with time steps within the pedogenic process. Pedogenic processes are driven by interrelationships between soil forming factors: climate, topography, time, biota, and parent material. A chronosequence analyzes time-dependent variations in soil profile characteristics while constraining the other soil-forming factors. Soils formed on terraces of the Brazos River, on the Coastal Prairie of Texas represent various stages (~400 yrs to 35,000 yrs) of landscape stability and pedogenesis. This chronosequence

study illustrates predictable variations in profile thickness, lack of preservation of relict primary sedimentary bedding, depth of leaching, and degree of development of pedogenic carbonate, slickensides, and clay fabric. These properties are least developed in the Ships Series representing short-term pedogenesis (~400 yrs). Conversely, maximum expression of these properties occurs in the Lake Charles Series, which represents ~35,000 years of pedogenesis. The Pledger and Burleson Series, two intermediate-aged profiles, represent ~3,500 and ~18,000 years of soil formation, respectively.

Application of time-dependent morphologic and geochemical trends derived from the modern chronosequence has resulted in two significant conclusions. PaleoVertisols form on stable landscape surfaces occurring at sequence boundaries. The modern chronosequence aids in interpreting the frequency, extent and timing of marine and nonmarine cycles (~400 ka Milankovitch-scale sea-level fluctuations) during the late Mississippian in Tennessee. Based on the modern Vertisol analogs, paleoVertisols represent 2-3 orders of magnitude shorter time than initially estimated for the Pennington Fm. As such, there may be significantly more time not represented by rock than previously thought in cyclic marine/nonmarine intervals containing paleoVertisols. The chronosequence study also highights an important problem regarding paleoclimate research utilizing paleosols. The results from this study suggest that time-dependent morphological and chemical features may mimic those that are climate-dependent. Soils formed in drier climates may display similar characteristics to those seen in younger profiles (Ships Series) whereas soils formed in wetter climates may exhibit features comparable to older profiles (Burleson Series), thus obscuring paleoclimate interpretations obtained from analysis of paleoVertisols.

TABLE OF CONTENTS

LIST OF FIGURES

FIGURE PAGE

LIST OF FIGURES (continued)

FIGURE PAGE

LIST OF TABLES

LIST OF PLATES

Chapter I.

Introduction

Vertisols are clay-rich soils with high shrink/swell potential (Soil Taxonomy, 1994). Modern Vertisols occur in many regions of the world, including the United States. Eastern Texas contains a broad range of Vertisols and those formed from alluvial type deposits are of particular interest for this study. Research conducted by the Paleopedology Group, University of Tennessee, has shown that the climatic regime indicated from measured records in eastern Texas may be very similar to what existed in Tennessee during the Late Mississippian based on paleoclimatic (paleoprecipitation) indicators such as estimated depth to pedogenic carbonate (Caudill, 1996; Caudill et al., 1996) and Fe-Mn occurrence (Stiles et al., 2001). The interest in modern Vertisols as analogs stems from the great abundance of paleoVertisols preserved in the rock record, particularly those that occur in the Paleozoic rocks of the Appalachian basin. Distinctive morphological features of Vertisols facilitate their recognition, and their abundance may be a result of the preservational bias of the clay-rich soil (Mora and Driese, 1999; Harding, 1995). Distinctive features include gilgai (soil microhighs and microlows), arcuate pedogenic slickenside surfaces, deep cracks associated with seasonal precipitation (Ahmad, 1983), and pedogenic carbonate accumulation. As such, the interest in developing a modern Vertisol chronosequence is pertinent to an understanding of the time required to develop such distinctive, commonly-preserved paleosols in the rock record (Mora and Driese, 1999; Caudill, 1996; Harding, 1995).

The goal of this thesis is to develop a conceptual model relating macromorphologic and micromorphologic features, bulk chemistry trends, and translocation in modern Vertisols as a function of time. Preservation potential of the age-related criteria developed in the modern will be tested for viability in the rock record, thereby developing guidelines for analysis of pedologic and geologic features. Soil development requires stable landscape conditions whereby parent material (alluvium) can be deposited and developed into a soil profile. A chronosequence analyzes time-dependent variations in soils formed from similar parent material, while constraining other soil forming factors (i.e., climate, topography, and biota). The crux of this study is: 1) the development of a chronosequence model (time required to develop and/or preserve features) using a set of modern Vertisol analogs (Ships, Pledger, Burleson, and Lake Charles Series, Texas) and 2) applying this model to paleoVertisols in the rock record (i.e., Pennington Formation, Tennessee). McCarthy and Plint (1998) discussed the application of interfluve paleosol expression to interpretation of sequence boundaries in terrestrial stratigraphic sections. Understanding the pedology, micromorphology and the depositional environment may help delineate the length of stability (time lapsed while at surface conditions) required for formation of a Vertisol profile, thereby enhancing the resolution of the depositional history and geomorphic stability prior to aggradation and burial. The Pennington Formation, in particular, consists of transgressive-regressive sequences indicated by limestone units truncated by paleosols. The fluctuations in sea level are considered to be of Milankovitch scale (100,000-400,000 yr cycles). As such, the paleosols should exhibit features and extent of development comparable to that portion of the total length of time (10,000yrs). Evaluation of the current amount of time represented by the paleosol units should indicate whether sea level fluctuations were occurring at a consistent rate through Mississippian time. Vail (1959) suggested that an increase in the thickness of the redbed units upward in the late Mississippian stratigraphic section should be indicative of longer duration of the cycles, as represented by the clastic deposits. This study may provide greater time resolution related to landscape stability at sequence boundaries. Identification and application of paleosols to the understanding of sequence boundaries have been cursory to broad-scale studies of environmental evolution. The significance of time-related criteria requisite to profile development may be an indicator of processes acting between major sequence deposition. Essentially, the cyclicity of Mississippian sea-level rise and fall may have occurred, at least regionally, on scales different than currently recognized.

Chapter II.

A Modern Vertisol Chronosequence:
Soils derived from alluvium deposited on terraces of the Brazos River, TX

Introduction

Vertisols are soils that exhibit distinct macromorphologic features (i.e., slickensides, gilgai microrelief and chimney tongues) that distinguish these soils from other soil orders. Formation of Vertisols occurs in geographic regions with seasonal or periodic moisture deficits. The intensity and periodicity of evapotranspiration affects the formation of chemical and physical characteristics of Vertisols.

Shrink-swell processes within smectite-rich soils occur when void space between clay platelets (rather than inner layer sites) fills with water (Coulombe et al., 1996; Wilding and Tessier, 1988). Swelling pressure may then exceed the strength of the soil and result in shear failure. The angle of shear failure is a function of overburden pressure and lateral swelling resistance (Coulombe et al., 1996; Wilding and Tessier, 1988). The resultant is movement along a corrugated and polished failure surface, or slickenside. Vertisols typically exhibit angular blocky structure and/or pressure cutans in the upper horizons, contain pedogenic carbonate and Fe/Mn nodules, and display surface expression of microtopographic or gilgai (microhigh and microlow) features (Coulombe et al., 1996; Wilding and Tessier, 1988; Ahmad, 1983). During the periods of increased rainfall, the microlow accumulates and translocates soluble cations downward within the profile. Eh conditions within the microlow further enhance mobility of redox-sensitive cations (Lin et al., 1998; Golden et al., 1997; White and Dixon, 1996). Translocation of cations preferentially upward along slickenside surfaces may occur by evaporative wicking in the microhigh (Miller, 2000; Ahmad, 1983; Yaalon and Kalmar, 1978).

Vertisol climosequence studies (Stiles et al., 2001; Miller, 2000) along the Gulf Coastal Prairie, Texas analyze the variation of Vertisol characteristics that may be associated with a moisture gradient occurring along the eastern and southern areas of the state. General trends in pedogenic development, associated with the moisture status of the soil (i.e., depth of leaching, Fe/Mn masses, and Bk horizon), are reflected in the macromorphology, micromorphology and bulk chemistry (based on mass balance calculations) of the soil pedons (Stiles, 2001). Leaching of mobile constituents, gilgai relief, slickenside development, and abundance of Fe/Mn and carbonate segregations (nodules or masses) may be considered a function of climatic factors, particularly precipitation (Stiles, 2001; Wilding and Tessier, 1988). Depth of leaching and to Bk horizons is most pronounced in areas that receive higher annual rainfall. Translocation of mobile constituents (Ca, Mg, Sr, and P) can vary from less than 30 cm in drier conditions, to greater than 60 cm in wetter conditions. A slight increase in these elements, particularly Ca, may occur in gypsiferous or calcrete horizons (Bk). Although the relationship is less clear, propagation of pedogenic processes and development of gilgai features may be a result of translocation and slickenside development (Wilding and Tessier, 1988). As precipitation increases, the spacing and relief of slickensides show an inverse relationship where common, intermediate spaced slickensides of moderate relief (10-30 cm) occur in drier conditions and abundant, closely-spaced slickensides with higher relief (30-50cm) occur in wetter climates (Stiles, 2001). Mukkara structures tend to be accentuated or more steeply inclined in wetter climatic conditions and may be a function of slickenside spacing. The combination of mukkara structures, slickenside spacing and relief creates distinct microclimates within the soil profile. Moisture accumulation and translocation occurs in the microlow; the microhigh acts as a moisture wick and precipitation front for many mobile constituents (carbonate nodules) (Wilding and Tessier, 1988). Redox conditions and the occurrence of Fe/Mn masses within the profile may also be used as a proxy for climate (Stiles et al., 2001). Fe/Mn masses and redoximorphic features are more abundant in the wetter climates or areas with less moisture deficit. Staining by Fe/Mn masses are more abundant in subsoil along slickensides, fractures and roots. Macromorphologic characterization of soils formed in drier climates have fewer Fe/Mn masses while redoximorphic features are rare to moderately abundant.

This chronosequence study addresses pedogenic processes where the main soil-forming factor that varies is time, while constraining other factors (i.e., parent material, vegetation, climate, and slope). Soils formed on stable terrace surfaces of increasing elevation from the current floodplain may exhibit different stages of development with increasing age. Soil macromorphology, micromorphology, and bulk chemistry indicate trends associated with duration of landscape stability whereby soil development may provide a proxy for rates of pedogenesis. The trends in pedogenic processes are remarkably similar for time and climate variation of the soil-forming factors (Stiles et al., 2001; this study). For example, soils formed in areas with a wetter climate may have characteristics (advanced pedogenesis) very similar to those developed from much older profiles. Similarly, soils that form in drier climates exhibit limited pedogenesis and are similar to those of juvenile or early stages of soil development. In soils formed on younger terraces, there is typically minimal translocation of mobile constituents (i.e., Ca and Mg), bedded sedimentary alluvium parent material, and pressure faces or slickenside surfaces within a limited depth range. With time, the amount of translocation increases; there are more abundant, widely-spaced and higher amplitude slickensides; occurrence of pedogenic carbonate nodules increases; and the microhigh and microlow profiles become more distinct.

The focus of this Vertisol chronosequence study was to: 1) characterize macromorphology, micromorphology and bulk chemistry of soil pedons on multiple terraces along the Brazos River; 2) determine whether there were characteristics of the profiles that indicate trends in pedogenesis with time; 3) construct a pedogenesis model for Vertisols as a function of time; and 4) determine whether there is a profile development maximum that is reached.

State Factors in Soil Formation

Soil formation occurs when parent material, derived from in situ weathering or deposition of sediment, undergoes various biological, chemical and physical processes. Several authors (e.g., Jenny, 1941, 1961; Simonson, 1959; Runge, 1973) attempted to understand the components of the soil formation/evolution processes. These components are very similar in nature, in that each tends to be interrelated and somewhat difficult to quantify. The soil formation model developed by Hans Jenny (1941) is the most widely used to explain the various "state factors" or components that affect pedogenic processes:

$$S = f\,(cl, o, r, p, t)$$

Where the soil (S) is a function of climate (cl), organisms (o), relief (r), parent material (p), and time (t). Studies to address changes in a state factor must attempt to constrain the others; this may be by accomplished by careful selection of study areas.

A soil chronosequence addresses various pedogenic processes that are associated with time and attempts to constrain: parent material, climate, vegetation/biota and relief. Vertisol chronosequence studies are rare, particularly those that recognize the current accepted pedogenic mechanism (soil mechanics model) (Wilding and Tessier, 1988). The role of time in the formation of Vertisols is not well understood and is dependent on the parent material. Weathering rate and profile development are variable and requires the presence or formation of clay with high surface area and base status (Coulombe et al., 1996; Wilding and

Tessier, 1988; Ahmad, 1983). Vertisol genesis requires a seasonal or periodic moisture deficit and therefore, climate is considered a significant soil-forming factor of this soil order. Topography and vegetation are of lesser importance to Vertisol formation. The following will address each state factor relative to Vertisol formation and discuss how this study attempted to constrain each factor.

Parent Material

Vertisols form from a wide variety of parent materials (igneous, sedimentary or metamorphic) (Coulombe et al., 1996; Wilding and Tessier, 1988; Ahmad, 1983). Igneous and metamorphic parent materials require a significant amount of time to weather enough solum for pedogenic processes to occur (Dudal and Eswaran, 1988). Basalt and volcanic ash are parent materials in Arizona and Utah, respectively. Sedimentary origins include alluvium, marl, limestone, and chalk (Coulombe et al., 1996). Vertisol formation in sedimentary units may require less time for profile genesis because of weathering and accumulation potential of these deposits. Coastal terrace or deltaic materials (>30% clay content) provide flat inland areas conducive to pedogenesis.

The backbasin (floodbasin) facies along the Brazos River consist mainly of smectite-rich, calcareous alluvium derived from Permian redbeds of north central Texas. The parent material fines-upward and typically forms Vertisols or vertic intergrades within the fluvio-deltaic setting of the Coastal Prairie. The Brazos River has historically had a variable flow regime resulting in several sets of terraces. These terraces are particularly incised further inland. This study will address two of the major terrace sets correlated with the Deweyville? And Beaumont Formations (Nordt, 1996) as well as two younger, minor terraces that complete the chronosequence study. The Beaumont Formation, which is Late Pleistocene in age, was deposited in a fluvio-deltaic setting and contains a relatively uniform mineralogy and texture (Kunze et al., 1963). Terrace deposits derived from the Brazos River are composed of sediment with comparable mineralogy and particle size favorable to Vertisol pedogenesis.

Sediment mineralogy associated with the pedons of this study consists primarily of montmorillonite, kaolinite and calcite (Appendix D). Secondary minerals include quartz, mica and montmorillonite-chlorite or montmorillonite-illite mixed clays. Clay abundance ranges from 45 to 72%, with slightly higher amounts occurring in the microlow profiles. Sand and coarse fraction size separates range from less than 10%, but may range from 10-15% in the older profiles. Textural classification throughout most of the profiles is clay and in the Ships pedon, silty clay and silty clay loam.

Climate

Vertisols may form in a variety of climates and precipitation regimes (ustic or udic). Seasonal or periodic (4 to 8 months each year) moisture deficits, with high evapotranspiration, are required for morphological development of Vertisols (Ahmad, 1983). The physical properties, characteristic of Vertisols (i.e., wedge-shaped peds, slickensides and gilgai), form due to wetting and drying of the solum. The resultant of the soil moisture status includes: 1) base cation translocation and accumulation, 2) redoximorphic concentrations and depletions, 3) slickenside occurrence and development, and 4) carbonate nodule precipitation and dissolution. These morphologic features are variable and a function of the intensity, duration and periodicity of rainfall (Coulombe et al., 1996; Bouma and Loveday, 1988). Vertisols occur in a broad range of precipitation regimes (250-3000 mm), and rainfall is usually in the range of 500-1000 mm (Coulombe et al., 1996). Average annual temperatures may exhibit similar variation (9-25°C), but typically range from 15.5° to 16.5°C (Ahmad, 1983).

Annual precipitation within the study area varies from 96 to 110 cm and 110 to 120 cm in Burleson County and Brazoria and Fort Bend Counties, Texas, respectively (www.ncdc.noaa.gov/ol/climate/climatedata.html). Temperatures range from approximately 35°C (July) to lows of 15°C (January). The climate on the Gulf Coastal Plain is somewhat regulated by warm ocean currents circulating in the Gulf of Mexico and major wind patterns that approach from the Gulf moving inland, perpendicular to the Coastal Plain (Crowley and North, 1991; http://encarta.msn.com)

Organic carbon stable isotope studies (based on estimated C4 composition) conducted by Nordt et al. (1992) and Nordt (1996) indicated climate change in Central Texas, from cooler/wetter to transitional conditions from 14,000 to 6,500 yr BP. A study by Blum and Valastro (1994) of climate and environmental change from the Edwards Plateau, Texas suggested that cool/wet conditions may have extended to 20,000 yr BP. According to Nordt (1996), an increase in C4 (80-85%) composition indicates a short, warmer and drier period to 5000 yr BP. From 5,000 to 2,000 yr BP, cooler and wetter conditions were established with modern climate being reached at the end of this period. A short period of drying may have occurred at the boundary between modern and cooler/wetter conditions. Cooler/wetter climatic conditions during the depositional and pedogenic history of the Ships, Pledger and Burleson pedons help to constrain the climate contribution to soil formation.

Vegetation

The Vertisol soil order differs from other orders based on the role of biota and vegetation on pedogenesis (Coulombe et al., 1996; Ahmad, 1983). Vegetation may have a minor impact on Vertisol formation by affecting the magnitude of soil-water extraction (surface cracking patterns) and evapotranspiration (Coulombe et al., 1996; Ahmad, 1983). Vertic soil properties such as clay content, structure, and shrink-swell limit or modify the vegetation population that may establish on the surface. Microtopographic variation (ML and MH) has an impact on drainage characteristics and subsequently the type of vegetation that occurs within the microenvironments. In general, prairie and savanna grasses are indigenous to Vertisols, as these species tend to thrive well in moisture-stressed conditions (Dudal, 1965; Probert et al., 1987). Trees must be deep-rooting, drought-resistant species such as mesquite and some bottomland hardwoods (i.e., oak and hickory). Species that establish on

Vertisols must be able to withstand root damage that may occur due to structural mobility along slickenside surfaces (Coulombe et al., 1996; Ahmad, 1983).

The vegetation composition of the Coastal Plain of Texas varies broadly with the precipitation gradient. The vegetation depends on the vegetation and land use of the soil surface (i.e., native grasses, farming and grazing). Grasslands are ubiquitous along the Coastal Prairie, with minor amounts of heat/drought-tolerant bottomland trees occurring closer to the coast. Although rainfall estimates indicate a high amount of precipitation, the rate of evapotranspiration becomes the major factor controlling soil moisture status and subsequent vegetation composition (Coulombe et al., 1996; Bouma and Loveday, 1988).

Topography

Surface topography is highly variable and dependent on the type of parent material or depositional environment in which the surface occurs. For example, Vertisols that form as a weathering product from basalt, may exhibit a different surface topography than those formed on alluvial terraces or coastal plains (Dudal and Eswaran, 1988; Ahmad, 1983). Vertisols may form on surfaces of slopes up to 30°, however, the most common occurrence is on slopes less than 5°. In areas with only slight variation in slope, there can be significant change in the type of drainage conditions and subsequently, the type of Vertisol that forms (Dudal and Eswaran, 1988; Wilding and Tessier, 1988; Ahmad, 1983). Gilgai are pedomorphic features in Vertisols that form due to shrink-swell processes and associated lateral and vertical swelling pressures of clay matrix, due to seasonal moisture deficit (Hallsworth et al., 1965). There are several types of Vertisol surface morphologies identified (e.g., round, mushroom and lattice), the most common being round and linear or tiger stripe gilgai (Dudal and Eswaran, 1988; Ahmad, 1983; Hallsworth et al, 1965). According to a study of Uruguayan Vertisols (Puentes et al., 1988), flat and undulating (convex) surfaces affect drainage such that normal (round) and linear gilgai form, respectively. Several references discuss gilgai formation in greater detail than is discussed here (Joeckel, 1999; Wilding and Tessier, 1988; Coulombe et al., 1996; Ahmad, 1983; Hallsworth et al., 1965).

Although macro-scale topography determines whether erosion by run-off or infiltration occurs, both micro and macro-scale surface topography greatly affect the drainage conditions, and ultimately the chemistry of the profile. Concave and flat macro- and micro-scale topography increases water storage resulting in: 1) the accumulation or retention of base cations and soluble silica and, 2) mobility of reduced iron (lower Eh conditions). This type of (confining) drainage favors the formation of smectite mineralogy (Coulombe et al., 1996), whereas convex or sloping surfaces favor different conditions. Domed or convex surfaces may enhance drainage resulting in: 1) increased leaching of base cations and soluble silica, 2) accumulation of iron oxides and oxyhydroxides, and 3) formation of kaolinite development. Similar trends associated with increased drainage due to topography may become more advanced as profiles age.

Time

A soil chronosequence addresses the systematic development of soil properties with increasing duration of pedogenesis. Most chronosequence studies focus on soil orders other than Vertisols for two reasons: 1) Vertisols have a less complex morphology and pedogenic history (polygenesis?), and 2) occurrence and formation of Vertisols are restricted to a particular climate regime. Bockheim (1980) utilized a suite of 32 chronosequences out of more than 70 represented in pedological, ecological, and geological literature, ranging in age from 500 years to 1 million years. A portion of the 70 soil chronosequence studies is reviewed in Steven and Walker (1970). Table 2.1 describes a variety of chronosequence studies and what properties were used as a duration-of-pedogenesis proxy. Applications of chronosequence studies include estimation of pedogenic duration on terraces of unknown age, correlation of geologic units based on paleosols (Busacca, 1987), and approximation of the minimum ages of surficial deposits by evaluating the pedomorphic maturity of relict soils formed on them (Busacca, 1987; Birkeland, 1984).

Pedogenic processes refer to the cumulative alteration of parent material as expressed in morphologic and bulk chemical characteristics. These processes begin upon initial subaerial exposure and may not remain constant through time. Busacca (1987) addresses a chronosequence of alluvially-derived soils formed on terraces, where a reduction in heterogeneity of parent material occurs with increasing duration of pedogenesis. Some studies (e.g., Busacca,

Table 2.1 Soil Chronosequence Studies			
Author	**Location**	**Description**	**Properties Used**
Markewich and Pavich (1989)	Coastal Plain of eastern US	Applicability of chronosequence study to Spodosol and Ultisol soil orders	Mobility and formation of clay, Fe, al oxyhydroxides; intense leaching and vertical flow
Vidic et al. (1991)	Upper Sava River Valley, Slovenia, Yugoslavia	Quaternary terrace sequence (Günz, Mindel, Riss and Würm terraces)	Soil thickness, thickness of Bt horizons, clay coatings, Fe-Mn concretions correlated with soil age
Busacca and Singer (1989)	Honcut Creek, Sacramento Valley, California	Soil development index; six soils (600 years to 1.6 my); xeric-thermic soil climatic regime	Elemental chemistry of silt fractions; type of mass balance approach
Marsan et al. (1988)	Agogna Valley, Northwestern Italy	Fluvial terraces used to determine morphological, chemical, and physical characteristics	CEC; clay content and aggregation;
Busacca (1987)	Honcut Creek, Sacramento Valley, California	Soil development index; six soils (600 years to 1.6 my); xeric-thermic soil climatic regime	Clay films, texture plus wet consistence, structure, and rubification correlated with soil age
Knight (1980)	Boorook, Victoria, Australia	Theoretical model from current features	Gilgai microrelief; surface and subsurface structural patterns
Bockheim (1980)	Multiple locations; variety of climatic conditions and parent material	Summary of chronosequences; various climatic regimes, parent materials and range of ages; application of chronofunctions	Clay content, pH, solum thickness, oxidation depth, and soluble salts associated with pedogenesis through time

1987) suggested that soil formation does not occur as a time continuum, but, occurs rather in a step-wise fashion once pedogenic thresholds are reached. Re-establishment of structural aggregates and gilgai microtopography post-disturbance (plowing) in a very short period of time (L. Wilding, pers. comm.,1999) may be indicative of more complex pedogenic processes related to Vertisol formation. Bockheim (1980) suggested that many properties continue to change through time and therefore, a dynamic equilibrium with the environment cannot be reached. Profile development is reflected in soil morphologic features and may be described quantitatively by a soil development index. These indices are developed by scoring soil properties compared to the parent material characteristics (Marsan et al., 1988; Busacca, 1987; Harden, 1982; Bockheim, 1980; Bilzi and Ciolkosz, 1977). Semi-logarithmic and log-log models (Y or log Y = a + b log X: where Y is soil property and X is soil age) are applicable to most soil morphological features within a variety of climatic regimes (Harden and Taylor, 1983; Bockheim, 1980; Birkeland, 1974; Yaalon, 1971). The main source of variability between solum and parent material is base leaching and acidification of soils, which increases with profile age (Vidic et al., 1991). Leaching of carbonate, accumulation of aluminosilicates, aluminimum hydroxides, and Fe-Mn sesquioxides, soil thickness, thickness of Bt horizons and the amount and continuity of clay coatings typically increase with soil age (Vidic et al., 1991; Markewich and Pavitch, 1991; Aniku and Singer, 1990). These trends in morphology and bulk chemistry are applicable to soils with normal genetic horizonation; Vertisols, however, exhibit microscale topography and hydrologic conditions conducive to differential accumulation and depletion within the microhigh and microlow profiles. As such, the role of time in Vertisol pedogenic processes is not well understood and will be addressed in this study.

The Gulf Coastal Plain contains fluvio-deltaic deposits that develop soils with very little tread (<1% slope). The geomorphic position of the profiles incorporated in this study is the backbasin portion of the floodplain. Macro-scale topography and geomorphic position, in addition to parent material, have supported pedogenesis of calcareous soils (Vertisols) with high base status, smectite mineralogy, and round gilgai microtopography. The selection of pedons that exhibit very similar macro- and micro-topographic characteristics has allowed the role played by topography in the formation of the soil pedons to be constrained across the chronosequence study area.

Soil-forming factors are inherently interdependent. In order to address the time aspect of pedogenesis, the other soil-forming factors (parent material, climate, vegetation and topography) must be constrained. In order to constrain the soil forming factors, careful site selection was based on source of parent material, reasonable profile correlation, and similarity of soil properties (clay mineral content, texture, drainage, and structure).

Study Area

This study includes four modern soil profiles from the Coastal Prairie of Texas (Figure 2.1): Ships (~400 yrs BP), Pledger (~3500 yrs BP), Burleson (18,000 yrs BP) and Lake Charles (~35,000 yrs BP). The Ships pedon (Terrace

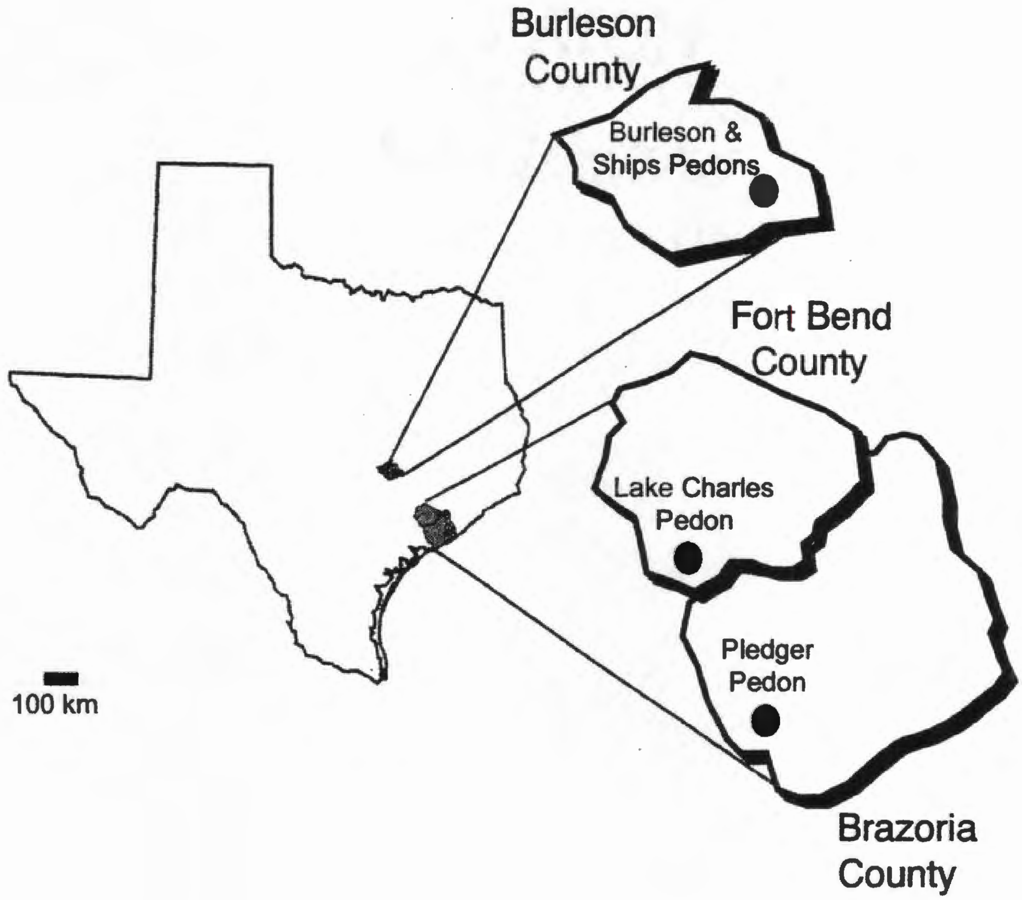

Figure 2.1: Ships and Burleson pedons were sampled in Burleson County; Lake Charles pedons were sampled in Fort Bend County; and Pledger Pedons were sampled in Brazoria County. All locations are contained within the Coastal Prairie of Texas.

1) was sampled on land managed by the Texas A & M University Agricultural Experiment Station, Burleson County (Figure 2.2). Burleson samples (Terrace 3) were collected adjacent to the Ervin See property (40m south of Highway 60) in Burleson County, near Snook, Texas. Dr. Larry Wilding (Department of Crop and Soil Science, Texas A & M University) assisted in the site location and preparation for the Texas portion of this study. Field reconnaissance (pit study) of the Pledger Series (Terrace 2) was not incorporated as part of this study. Samples from the Pledger pedons were collected by the NRCS from near Dance Bayou, Brazoria County, Texas. Detailed field photographs, bulk soil samples, and oriented soil thin-section samples were made available through Dr. Warren Lynn, NRCS through the NSSC Laboratory in Lincoln, Nebraska. Lake Charles (Terrace 4) samples were collected as part of an NSF-sponsored climosequence study concurrently conducted by the Paleopedology Group (S.G. Driese and C.I. Mora) at the University of Tennessee, Texas A & M University (L.P. Wilding), and Baylor University (L.C. Nordt). This pedon was sampled in Fort Bend County, Texas located to the northwest of Brazoria County (Stiles, 2001).

The Ships and Burleson pedons are developed from alluvial deposits on laterally adjacent terraces (T1 and T3, Figure 2.2, Table 2.2) of the Brazos River and have been radiocarbon dated to less than 400 years BP (personal communication, Dr. Larry Wilding, Texas A & M University) and 18,000 years BP (Nordt et al., 1992), respectively. A soil profile was buried beneath the Ships pedon between 500 and 2500 yrs BP (radiocarbon dating of hearth charcoal). The stacked profiles suggest that there were two phases of landscape

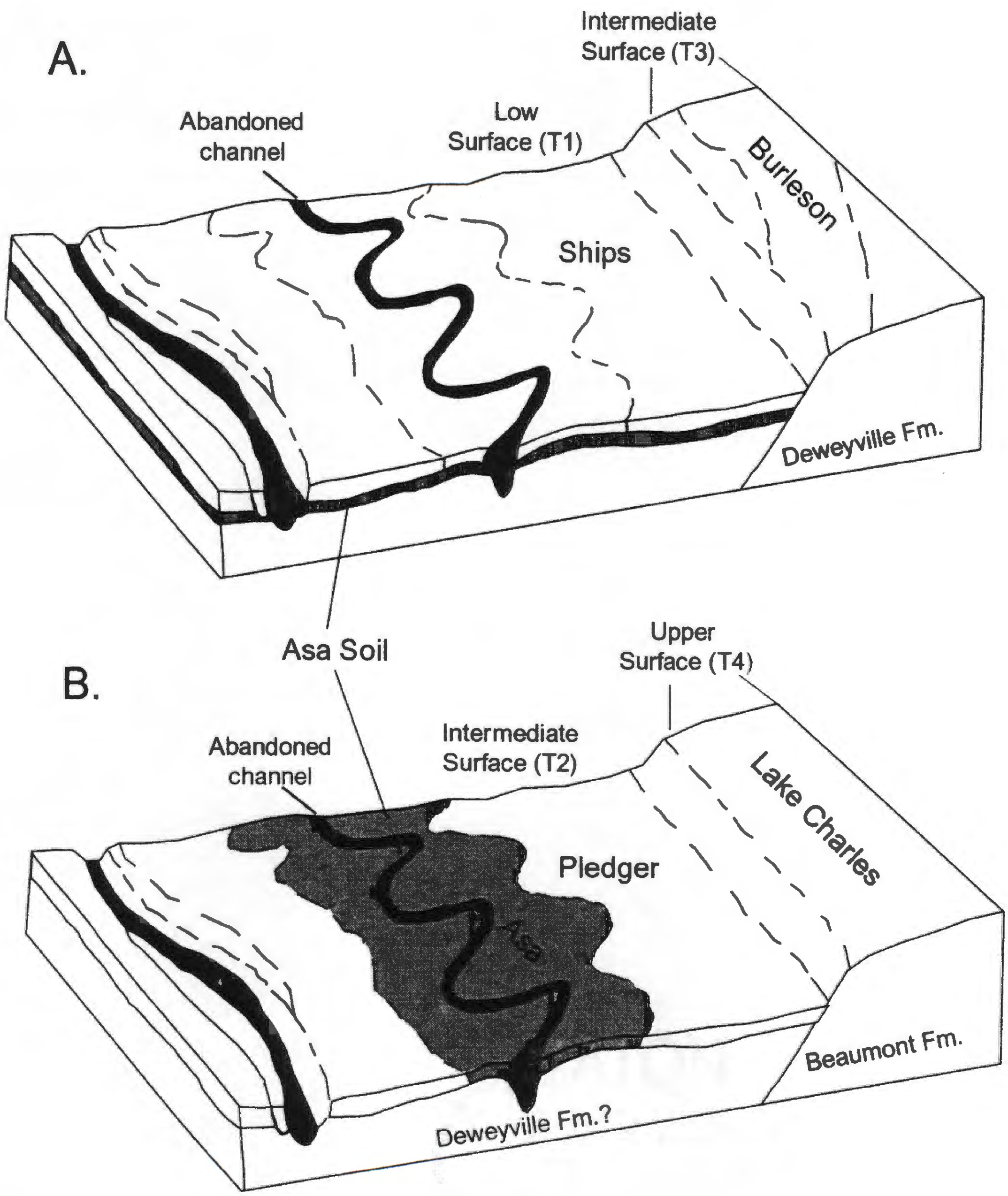

Figure 2.2: Schematic of terraces (T1-T4) and pedons associated with stable surfaces: A) representative cross section of terraces near Burleson Co., TX. B) representative cross section of terraces from Brazoria Co., TX.

Table 2.2 Terrace and soil series correlation				
TERRACE	**SOIL SERIES**	**AGE RANGE**	**METHOD**	**LOCATION**
T1	Ships	<400 yr BP	Radiocarbon dating (Wilding, pers. comm., 1999)	Burleson Co., TX
T2	Pledger	~3500 yr BP	Geomorphic correlation (Lynn, pers. comm., 2000)	Brazoria Co., TX
T3	Burleson	18,000 yr BP	Radiocarbon dating (Nordt et al., 1992)	Burleson Co., TX
T4	Lake Charles	35,000 yr BP	Radiocarbon dating (Birdseye and Aronow, 1991)	Fort Bend Co., TX

stability associated with the Ships surface. This buried profile is described as Asa or Asa-like in pedologic characteristics and provides a means of correlation to the Pledger surface. According to the Soil Survey for Brazoria County, Texas, the Asa Series is mapped as a lateral equivalent (facies) to the Pledger Series along the San Bernard and Brazos Rivers (Brazoria County, TX). Silty and sandy sediments deposited on a meander ridge, proximal to the river, comprise the parent material of the Asa series. Pledger pedons (T2, Figure 2) are derived from clay-rich sediments deposited within a flood basin, distal from the river channel.

The Lake Charles Series represents the uppermost and oldest terrace (T4, Figure 2) included in this study. Although Lake Charles samples from this study were sampled in Fort Bend County, the series also occurs within Brazoria County and adjacent to and elevated from the Pledger Series. The Lake Charles Series formed from sediment derived from the upper, fluvio-deltaic facies of the Beaumont Formation (Birdseye and Aronow, 1991). The geomorphic relationship between Burleson (T3) and Lake Charles (T4) Series is less clear but differing ages are supported by radiocarbon dates.

Methods

Methodology for this study followed that utilized by the National Resource Conservation Service (NRCS) and the Paleopedology Group at the University of Tennessee, Knoxville. Macromorphological descriptions (Appendix A) were completed according to methods outlined in the Field Book for Describing and

Sampling Soils (Schoeneberger et al., 1998) and incorporated terminology from Retallack (1988). The Ships and Burleson profiles were described and sampled by Phillip Owens (TAMU) and the author. John Wiedenfeld (USDA, NRCS, Rosenburg, TX) described the Pledger and Lake Charles profiles. Edward Griffin, Larry Wilding, and Lee Nordt also assisted with the Lake Charles description. Driese, Mora, Stiles, and Miller sampled the Lake Charles. The Ships, Burleson and Lake Charles pedons were sampled and analyzed according to the following methodology.

Sampling of soil profiles occurred as follows: 10cm interval samples were collected for whole-soil chemistry and bulk density (Appendix C), and by horizon (delineated by field description) for thin section (Appendix B), particle-size analysis and clay mineralogy (Appendix D). Bulk-density measurements were performed using the paraffin-coated clod method (Blake and Hartge, 1986). This method requires air-dried samples be weighed, coated with paraffin, and re-weighed. Each paraffin-coated clod was suspended in a water column and weighed to obtain volumetric displacement, with the known density of water and paraffin used as correction factors in bulk-density calculations.

Whole-soil bulk chemistry samples (from 10 cm intervals) were measured into metal tins and allowed to oven dry at approximately 60°C. Each sample was powdered in a shatterbox, followed by standard preparation of pressed pellets and run on the EG & G Ortec X-Ray Fluorescence Analyzer housed at the Department of Geological Sciences, University of Tennessee, Knoxville. Each run utilized appropriate shale and clay soil standards. Higher temperature

(~100°C) heating prior to grinding the sample in shatter box was attempted in order to minimize pellet degradation during storage and sample analysis. This degradation occurred when the pellet was under vacuum in the XRF and, in some samples, while stored in a desiccator. The combination of vacuum and heating likely removed structural water that was found stable at lower temperatures. Bulk chemical data are included in Appendix C.

Oriented samples taken from each horizon were coated with boat resin to enhance durability and maintain the physical properties during transport and treatment. Thin section preparation by water-free methods (Mora et al., 1993) required that void space be filled with epoxy (isotropic in crossed polarized light) to minimize plucking during slide preparation. Each soil thin section, prepared to 30 μm thickness, was analyzed under doubly-polarized light using standard petrographic microscopes. Brewer (1964, 1976) and Fitzpatrick (1993) were used as a guide to micromorphological descriptions (see Appendix B) for terminology). Appendix B contains micromorphological descriptions.

Sampling of the Pledger Series was not included as part of the field reconnaissance of this study. Field descriptions and bulk samples were obtained courtesy of Warren Lynn (NRCS). The NRCS collected bulk soil samples on a by-horizon basis only. Thin section preparation and whole-soil bulk chemistry studies were conducted by the author, utilizing methods similar to those listed above.

Particle size analysis and selected clay mineralogical analysis was completed at the Department of Crop and Soil Science, Texas A & M University

(Ships and Burleson) and at the National Soil Survey Lab of the NRCS in Lincoln, Nebraska (Pledger and Lake Charles).

Selection of Parent Material and Immobile Element

Mass-balance calculations require that a representative sample of the parent material be identified and chosen. These calculations are based on the relative difference (translocation) in elemental composition in the solum compared to the same elemental composition of the parent material, corrected for volumetric changes during weathering. Typically the best-preserved parent material occurs well below the zone of pedogenesis. In the Ships Pedon, bedded alluvium is denoted by horizons Ck1, Ck2 and Ck3 (131 to 170+cm) (see later presentation of results). An average composition of the three horizons was used to minimize local variation due to sedimentary layering. Inflection points in the clay- and silt-size fractions suggest the occurrence of bedded sediments and further support the choice of parent material composition.

Particle size analyses were particularly important for parent material selection for the Pledger Pedon. The basal portion of the profile exhibits a significant increase in sand content, from less than 10% to near 60%, below 250cm (see later presentation of results). The occurrence of bedded alluvium helped to further constrain the depth range incorporated into the mass-balance calculations. The C1 horizon (220-265 cm) represents the lowermost, bedded alluvium that maintains similar grain-size characteristics and hydrology as the other profiles included in the chronosequence study. A major break in the Ti/Zr ratio (Appendix C) also constrains the lower depth included as part of the parent material.

Parent material selection for the Burleson included the deepest portion of the pedon that could be sampled. The parent material in the Burleson no longer contains evidence of primary bedding, inflections in grain size at depth, or major fluctuations in bulk chemical analysis (see later results). Although the parent material portion of the profile appears fairly homogeneous, there are some variations in bulk chemistry that suggest that soil formation may still be occurring (i.e., Zr, Mn and Cr). Similarly, the Lake Charles Pedon contains minimal variation in grain-size with a marked decrease in sand and an increase in clay content (see later results). The B'ss4 horizon was used in the mass balance calculations and represents the lower most horizon described and sampled as part of the study.

Testing for parent material uniformity is significant not only for correlation between terraces, but also to identify any discontinuities (stratigraphic breaks) in the soil profile. Two different plots (Figure 2.3) are used to assess and compare parent material uniformity: TiO_2 vs. TiO_2/Zr and Zr vs. Zr/TiO_2. Figure 2.3A illustrates a general decrease in the amount of Zr relative to Ti as depth increases within a profile. Higher weight percents of Zr (relative to TiO_2) in older profiles and lower weight percents of Zr in younger profiles suggests that: 1) there was lesser abundance of TiO_2 in the older profiles originally or 2) an increase in Zr occurred due to translocation processes, such as influx of detrital zircon grains. The preservation of a similar trend between pedons suggests that

A

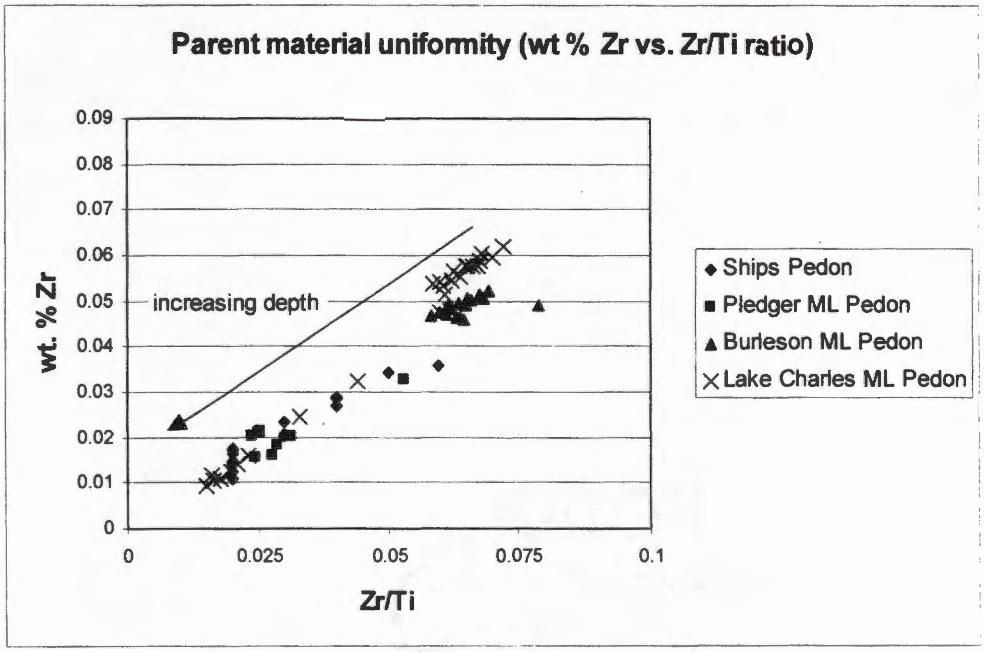

B

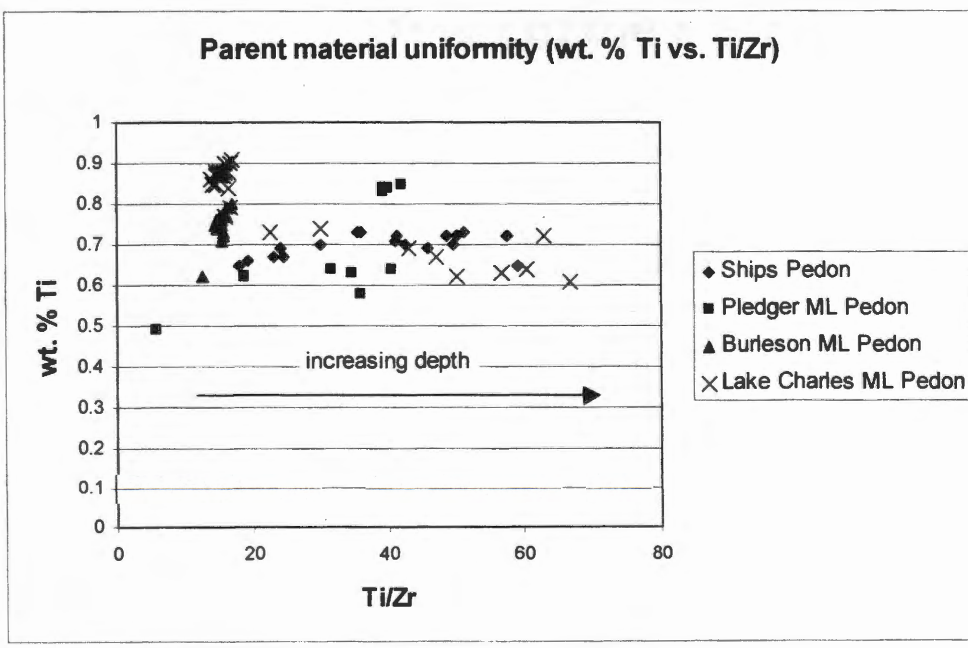

Figure 2.3 Parent material uniformity plots indicate a similar sedimentary source for each of the terrace deposits. Arrows indicate a general increasing depth trend.

the alluvium sediment source has remained the same across the chronosequence. The fact that there is a depth function for Zr indicates non-uniformity of Zr with depth and thus it is less suitable as an immobile index element for mass balance. There is no variation in TiO_2 with depth, thus TiO_2 shows greater uniformity within the soils and is more suitable for use as an immobile index element for mass balance.

Figure 2.3B illustrates no increase in TiO_2 relative to Zr with depth. Lower portions of the profile, particularly for the Lake Charles and Burleson microlows, have more conservative TiO_2/Zr ratios. Although there are Lake Charles and Burleson data points at a wide variety of TiO_2/Zr values, the increase (TiO_2/Zr) cannot be solely attributed to an increase in TiO_2. Variation in Zr content is likely the cause of the range in TiO_2/Zr values. This may be a result of mobility of Zr by a process similar to wetting-front phenomena, pushing grains along by shrink-swell processes. In general, there is agreement across the profiles, that the parent material has remained fairly uniform.

Strain calculations are utilized for determination of the relatively immobile element (Ti, Zr and Cr) required for complete mass-balance calculations. Strain may be used to describe volume loss or gain within the soil profile, which may be associated with the duration of pedogenesis. Titanium oxide-based strain values (Figure 2.4) are typically less than 25%, whereas values based on immobile Cr and Zr range from 100% to 25%, respectively. Titanium oxide will therefore be used as the immobile trace element in the mass-balance calculations present in this thesis. Zirconium exhibits fairly conservative trends, but does tend to over

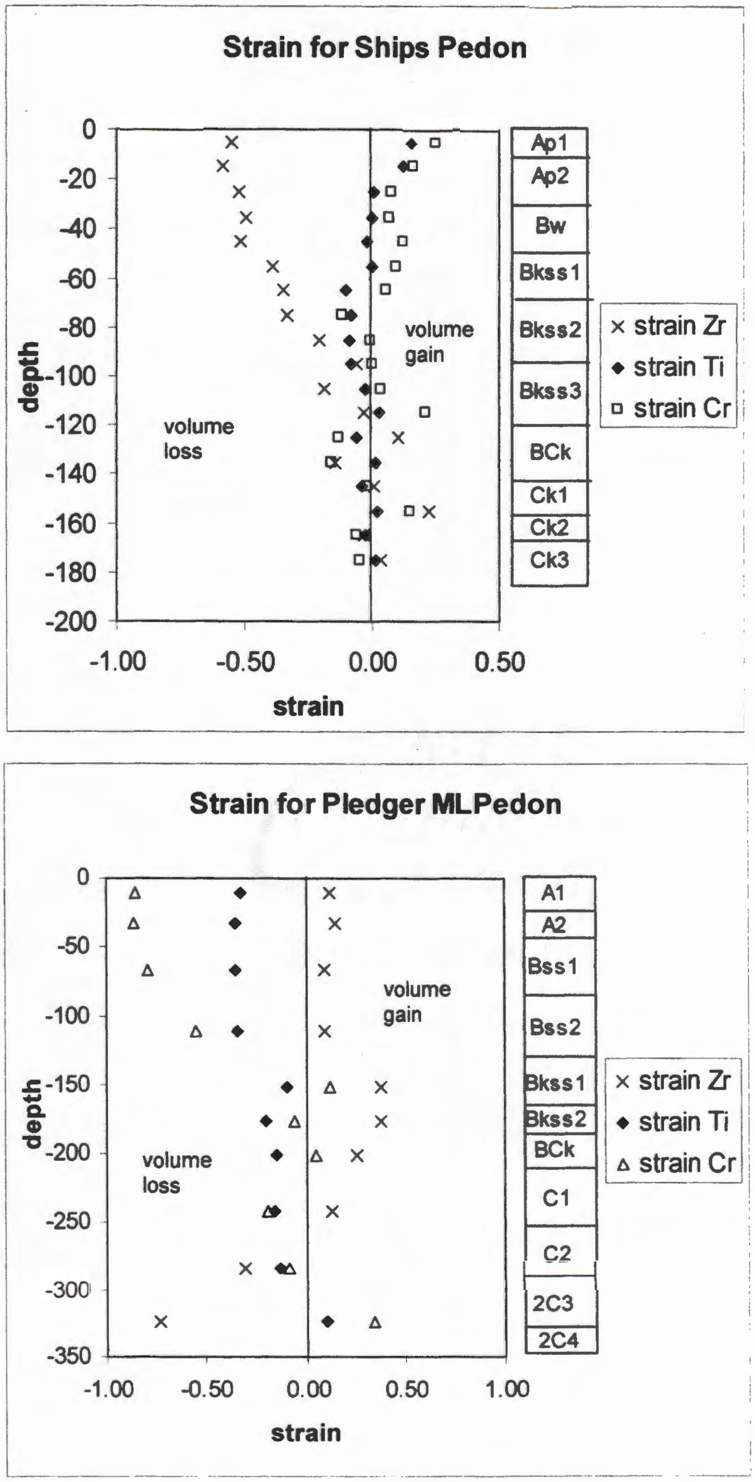

Figure 2.4 Strain values for the Ships (~400 yr) and Pledger (~3,500 yr) calculated for different assumed immobile index elements. Pedons are indicative of soil volume loss or gain.

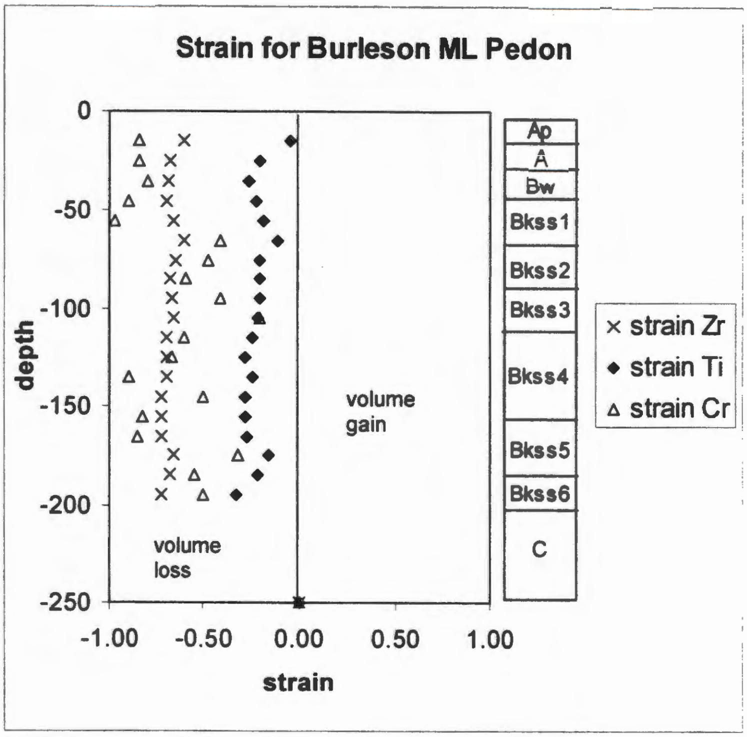

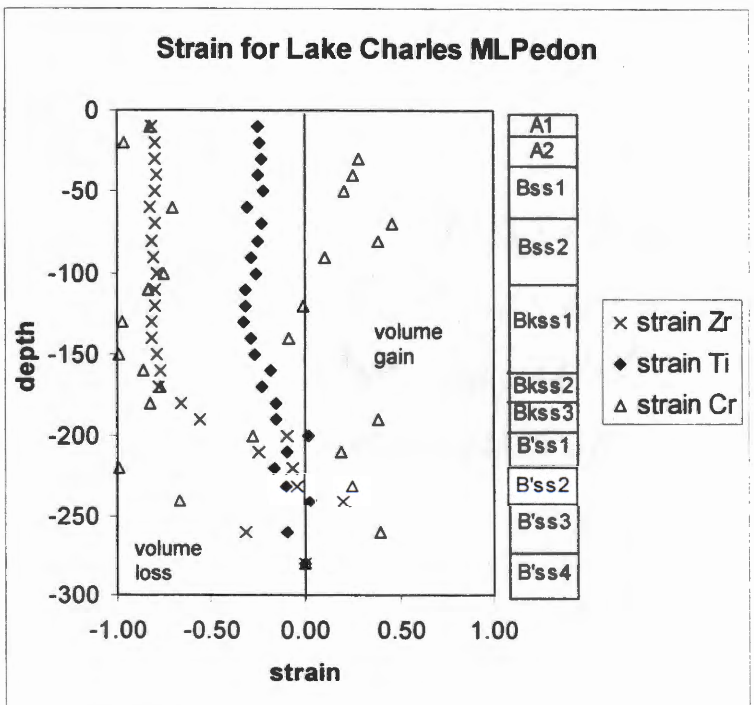

Figure 2.4 (continued) Strain values for the Burleson (~18,000 yr) and Lake Charles (~35,000 yr) calculated for different assumed immobile index elements. Pedons are indicative of soil volume loss or gain.

estimate volume loss particularly in the upper portion of the solum. Chromium shows comparable volume gains as Ti, for the Ships, but is much more variable in the other pedons. Redox conditions within the Vertisol profiles may be conducive to Cr mobility and/or complexation. However, across the chronosequence, there is a general trend of increased volume loss with increasing duration of pedogenesis (discussed in later results section).

Results

Each pedon (Ships, Pledger, Burleson and Lake Charles) will be discussed in order of profile age or length of time of pedogenesis. The macromorphology, micromorphology and bulk chemistry of respective pedons will emphasize 'within profile' variation. Clay mineralogy and particle size analyses will be included when data were available. The feature most characteristic of Vertisols is the occurrence of gilgai or microtopography. The microhigh (MH) and microlow (ML) profiles are characterized as mounds and bowls, respectively. Macromorphology tables, included in each section, describe microlow characteristics, except in the case of the Ships Pedon, for which gilgai microhigh and microlow features do not occur. This approach is similar to that of the NRCS, which uses the microlow profile to define the soil series and the geographic extent of each. The rationale for utilizing the microlow is based on the idea that the ML functions as a more or less closed system whereas the MH may be much more variable from site to site (Driese et al., 2000; Wilding and Tessier, 1988; Knight, 1980).

Pedon 1: Ships Series (~400 yr BP)

Macromorphology

The Ships Pedon represents the youngest of the terrace deposits of this chronosequence. Table 2.3 and Figure 2.5 (A-E) provide a general macromophologic characterization of the Ships profile. Original bedded calcareous, brown to red alluvium (10YR 3/2 and 2.5YR4/6) is preserved in the basal portion of the profile at a depth of 130-180 cm. The contact between the advancing front of pedogenesis (~110-131cm) and bedded parent material is gradual and is characterized by a transition from 50% bedding structure and 50% weak, fine angular blocky structure to bedding structure (bedded sedimentary alluvium) and change in color from brown (7.5YR 3/4) to layers of light and dark brown (5YR 4/4, 2.5YR 4/6 and 10YR 3/2). Mixing of parent material is identified by incorporation of lithorelicts and crack infill by sediment (calcareous silt) from the horizon above(Figure 2.5E). Pedogenic processes within the Ships profile are most expressed in the upper portion of the profile (solum). The occurrence of slickensides (Figure 2.5B) and associated pressure faces ranges from 44 to 131 cm, with Bkss1-Bkss3 horizons occurring from 44-110 cm. The slickenside surface inclination generally increases with depth from 25°-35° to 25°-45° within the Bkss1 and Bkss3 horizons, respectively. Structural development within the solum ranges from moderate, medium subangular blocky (Ap2) to strong, fine angular blocky (Bkss1 and Bkss2). Bedding structure dominates below the

Table 2.3 Ships Pedon- Characteristic Summary

Horizon	Depth	Slickensides	$CaCO_3$ nodules	Roots/pores & redox	Structure	Matrix
Ap1	0-9	---	---	Common fine and few very fine	Moderate, fine SBK	Brown (7.5YR3/3) clay
Ap2	9-26	---	---	Worm casts; few fine and very fine roots and pores	Moderate, medium SBK	Brown (7.5 YR3/4) clay
Bw	26-44	Few pressure faces	---	Few very fine and few fine roots; few very fine pores	Moderate, medium ABK	Brown (7.5 YR3/4); 2-5mm highly weathered shells
Bkss1	44-62	Slickensides (25-35°) discrete discontinuous, random orientation	Few weakly cemented nodules with septarian voids	Few fine and few very fine roots; few very fine pores	Strong, fine ABK	Brown (7.5 YR3/4) clay
Bkss2	62-86	Common intersecting slickensides (33-35°) continuous master slick at 35°	2% weakly cemented, 2 to 5mm nodules containing septarian voids	Few very fine roots and pores	Strong, fine ABK	Brown (7.5 YR3/4) clay
Bkss3	86-110	Common and continuous (25-40°)	1% weakly cemented (2-5mm) nodules with septarian voids	Few very fine roots and pores	Moderate, medium ABK	Brown to light brown (15%-2.5YR3/6 and 85%-7.5 YR3/4) clay
BCk	110-131	Many pressure faces; few 5 cm slickensides (long axis)	Few weakly cemented nodules	Few very fine roots; few fine pores	50% bedding (rock) structure; 50% weak, fine ABK	Brown to dark brown (50%-2.5YR3/6 and 50%-10YR3/2) clay

Table 2.3 Ships Pedon- Characteristic Summary (continued)

Horizon	Depth	Slickensides	$CaCO_3$ nodules	Roots/pores & redox	Structure	Matrix
Ck1	131-145	---	Few , weakly cemented nodules	Few very fine roots; few fine pores; Fe depletions along pores and nodules; few fine Mn masses along pores	Bedding structure; 1 to 2 mm silt loam strata	Brown (5YR4/4) clay; 5YR4/6 silt loam strata and crack infill; few very fine 10YR6/2 Fe depletions
Ck2	145-151	---	Few 2-5mm weakly cemented nodules (no voids)	Few very fine pores; few Mn masses lining pores	Bedding structure; 5% material from below mixed in (lithorelicts?)	Dark brown (10YR3/2) clay; 2.5YR4/6 material from lower strata
Ck3	151-170	---	Nodules and discrete pore fill	Few fine roots and pores; few Mn masses lining pores	Bedding structure;	Brown (2.5YR4/6) clay; 10% 10YR3/2 from above as crack infill

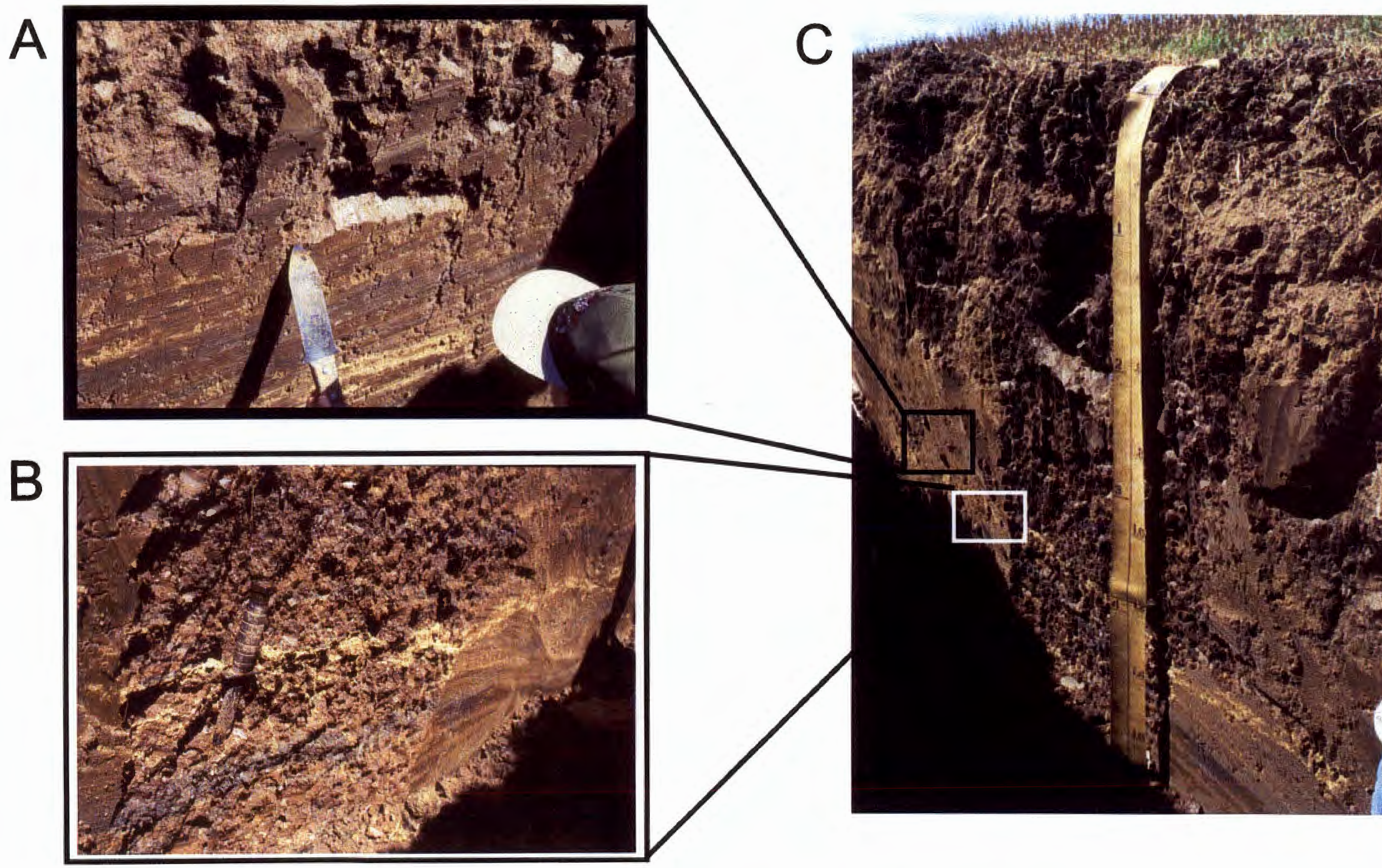

Figure 2.5 Ships Pedon macromorphology. A) The Ships profile has a limited depth range of slickensides; B) Excavated slickenside surface indicated by the soil knife; C) Preserved bedded alluvium at the base of the profile. Also note the light-colored band of powdery carbonate visible near the soil knife.

D

E

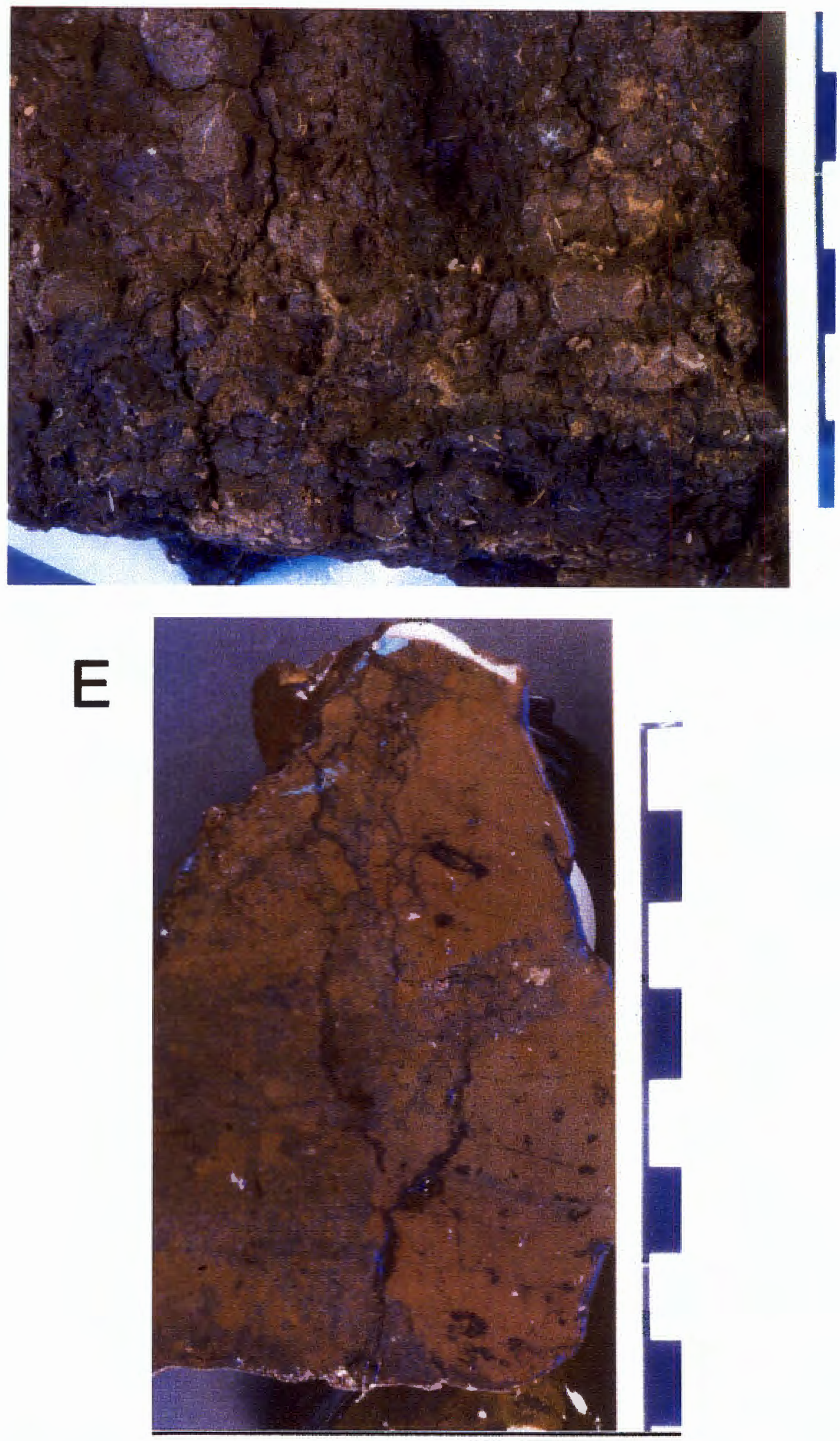

Figure 2.5 (continued) Ships Pedon macromorphology. D) Bedded alluvium with dark charcoal-like layer overlain by haploidized matrix material; E) Hand-sample illustrating the mixing of matrix and translocation, particularly along ped surfaces and in soil shrinkage cracks. Bar scale is in cm.

maximum depth of pedogenesis. The Ships pedon contains no gilgai microtopography or mukkara, with master slickenside topography having very low relief (~10cm) and very closely spaced peaks (~10-20 cm).

Few weakly cemented carbonate nodules, ranging in size from 2 to 5 mm, typically contain septarian voids (shrinkage of nodules). The Ck1 (131-145 cm) horizon contains a 1 to 2 mm calcareous, silt loam layer (Figure 2.5C) that follows bedding, with some variation associated with structural development and hydrology of slickenside surfaces. Powder carbonate and nodules not containing septaria increase in abundance within the parent material. Figures 2.5D and 2.5E illustrate where redoximorphic conditions within the Ships have resulted in variegation of color (within the parent strata) as a result of Mn masses and concentrations. Fe depletions along pores and nodules and Mn masses lining pores are indicative of (reduced) conditions conducive to mobility for these redox-sensitive elements.

Micromorphology

The Ships Pedon is characterized as having a calcareous matrix with rounded to subangular silt to fine sand-sized detrital quartz grains. Structural characteristics visible in thin section include granular texture (Ap1 and Ap2), and asepic-plasmic grades into sepic-plasmic fabrics with depth. This increase in structural development (i.e., pressure faces, slickenside fibers, and clay strings) is indicative of shrink-swell processes occurring within the profile (Figure2.6A), beginning at 44 cm (Bkss1) and extending to 110 cm (Bkss3). The transition to non-slickensided zones is marked by sepic-plasmic fabric and illuviated clay,

A

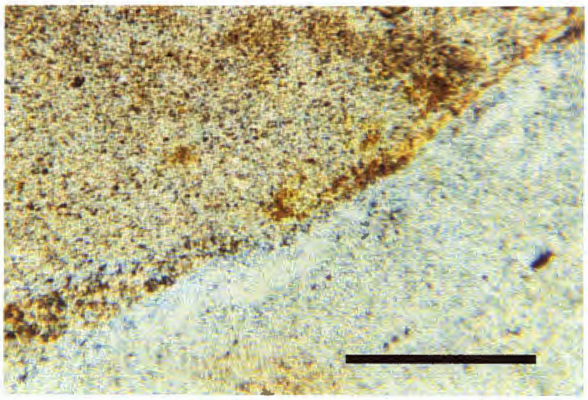

no gilgai; 57-70 cm; XPL

B

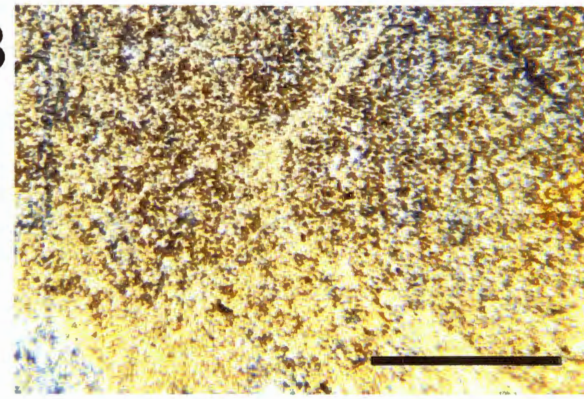

no gilgai; 86-110 cm; XPL

C

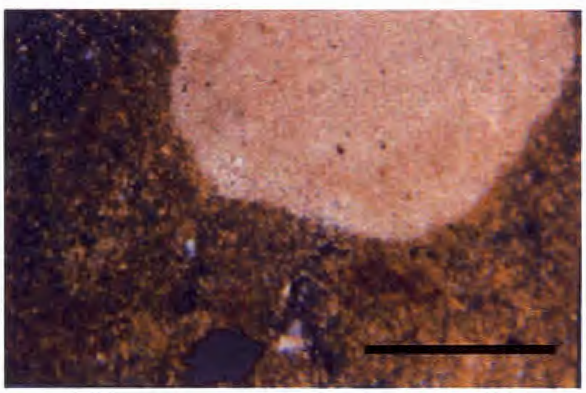

no gilgai; 62-86 cm; XPL

D

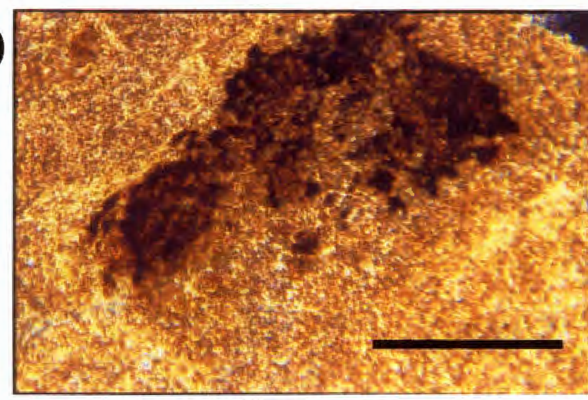

no gilgai; 110-131 cm; XPL

Figure 2.6 Ships Pedon micromorphology. A) Slickenside fibers oriented at 45 degrees to photomicrograph; B) Clay fabric oriented along perimeter of subangular to angular blocky ped; C) carbonate nodule has distinct boundary with surrounding matrix; D) weakly cemented Fe-Mn segregations. Bar scale is 0.5 mm. (XPL=crossed polarized light; PPL=plain polarized light) where sedimentary layering is disturbed. Illuviated clays typically line pores and are oriented adjacent to ped surfaces (Figure 2.6B). Mixing or haploidization of the bedded alluvium occurs through: 1) infill of vertical cracks (BCk and Ck1 horizons), 2) bioturbation from burrowing organisms and roots of vegetation (Bkss3 to Ck1), and 3) shrink-swell processes of overlying horizons. Evidence of advancement of pedogenesis downward in the profile is supported by redoximorphic concentrations and depletions on ped surfaces. Grain-size variation, associated with sedimentary bedding (Figure 2.5B-C) of the BCk to Ck3 horizons, is very minimal and may play a role where redoximorphic depletion or concentration occurs. Ped surfaces, within the BCk and Ck1 horizons, provide stable surfaces for concentration or depletion of iron and manganese.

Iron-manganese nodules or concentrations (Figure 2.6C) occur throughout the Ships profile. Dendritic and concentrically laminated nodules are two primary morphologies identified, with the former being most common. Dendritic or patchy Fe-Mn concentrations are found within the entire profile and engulf varying amounts of matrix or carbonate material. Concentrically laminated Fe-Mn nodules will delaminate or dissolve by removal of reactive surface material (outer rings); this process may be enhanced where calcareous matrix has been incorporated within sequential layers.

The Ships profile formed from calcareous bedded alluvium, which is preserved at depths greater than 131 cm (Ck1-Ck3). Finely disseminated carbonate is present throughout the profile. This powder carbonate coalesced forming a calcareous silt loam layer (Figure 2.5C) and also tends to be found as crack infillings. Powder carbonate, which is a finely disseminated carbonate, forms by a combination of dissolution of carbonate nodules, and precipitation from matrix of parent material-derived carbonate. Carbonate nodules (Figure 2.6D) range in size from 2 to 5 mm; some may contain septarian cracks or voids that may or may not be infilled with secondary carbonate cement. Homogeneous nodules with (Bkss1 to Ck3) or without (Bkss2 to Ck3) septarian cracks tend to have very distinct boundaries with the surrounding soil matrix. Some carbonate segregations (Ap2 to Ck3), weakly cemented carbonate nodules with diffuse boundaries, formed by dissolving other pedogenic nodules or from matrix carbonate.

Bulk Chemistry

Several processes contribute to variations in bulk chemistry within a soil profile: topography, drainage, soil moisture status (frequency and duration of rainfall events), and clay content (weight percent and composition). The extent of soil development may be indicated by translocation of mobile constituents (element or oxide), relative to an immobile element or oxide (Zr, TiO_2 or Cr), downward in the soil profile. Appendix C provides primary geochemical data and translocation values from mass-balance calculations. Table C4.1 provides a glossary of symbols and formulas utilized in mass-balance calculations. Retallack (1991) used molecular ratios, which relate the concentration of a constituent in the weathered portion of the profile (Cw) to the concentration of that same constituent in the parent material (Cp), in addition to strain and translocations of Brimhall and Dietrich (1986) and Brimhall et al. (1991). To establish the most conservative of the three immobile elements, strain calculations (Brimhall and Dietrich, 1986; Brimhall et al., 1991) were completed and compared between each of the elements. Positive strain values indicate dilation; negative strain is indicative of collapse. From Figure 2.4, TiO_2 appears to be most conservative of the three elements with dilation ranging form 5-25% to depths less than 120 cm (Ships and Burleson) and collapse of 5-35% in portions of each pedon (Ships, Pledger, Burleson and Lake Charles) in the study (Figure 2.4). Zr is conservative for the Pledger pedon (10-40%), but appears to overestimate collapse in the Burleson (60-72%), Ships (3-59%) and Lake Charles (5-82%) (Figure 2.4). Cr strain values are highly variable, but consistently overestimate collapse from as little as 0 to nearly 100% collapse of the soil (Figure 2.4). As such, Ti is used as the immobile element to calculate the translocation results (tau-Ti) in the following bulk chemistry sections. Unless otherwise stated, positive tau values indicate a gain or accumulation at depth; negative tau values suggest a loss or translocation of a constituent relative to the parent material. Each section will begin with a general discussion of translocation indices (i.e., calcification, base loss, oxidation and salinization) followed by more detailed discussion of key constituents (elemental and oxides) within the profile.

The Ships Pedon is variable through the profile (Figure 2.7A-D) with overall gains and losses of less than 30%, suggesting that most of the cations and oxides are conserved through the profile. Exceptions to the moderate loss

A

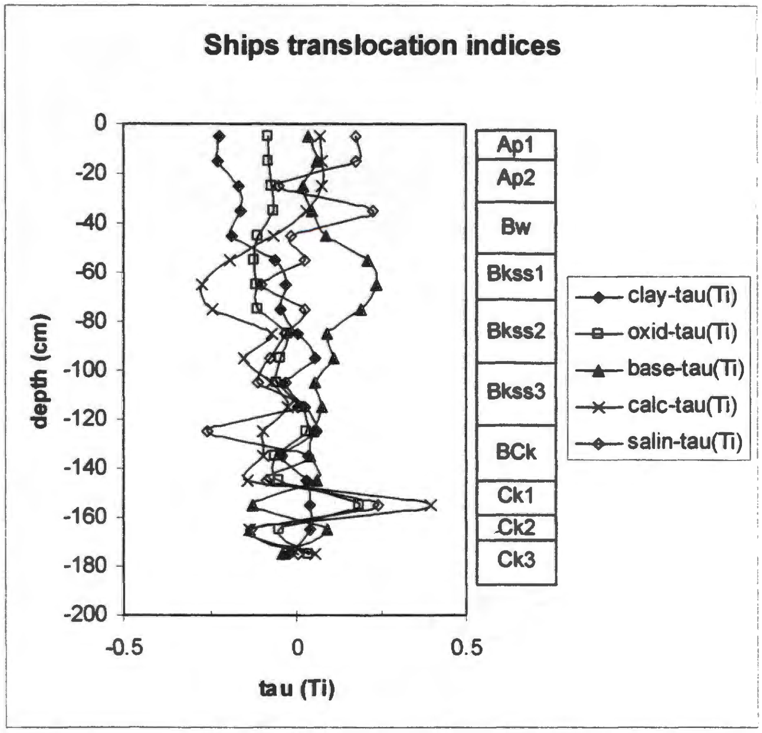

B

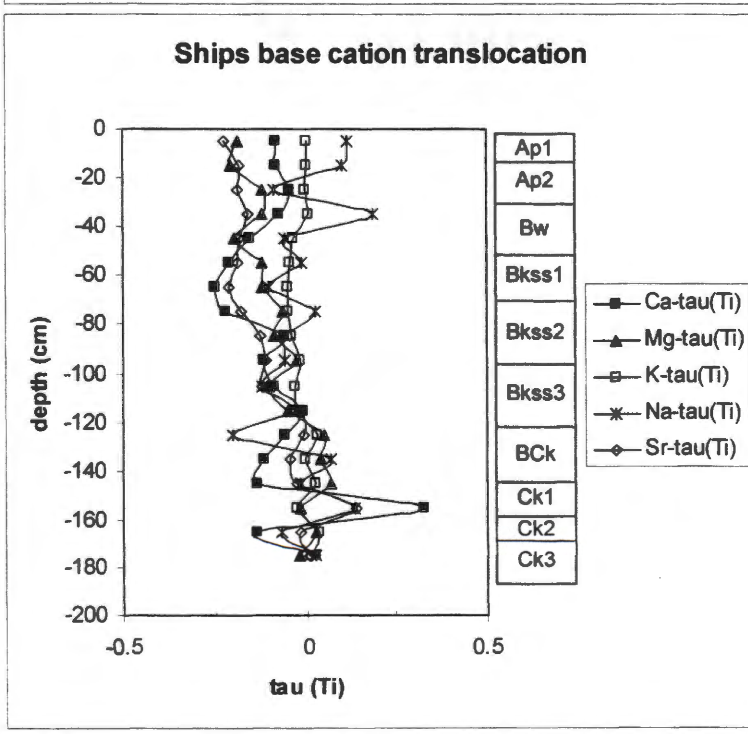

Figure 2.7 Ships Pedon molecular ratios and element translocations calculated using TiO_2 as immobile trace index: A) clay (clayeyness), oxid (oxidation), base (base loss), calc (clacification), and salin (salinization) are translocation indices, and B) translocation of base cations within the soil profile.

C

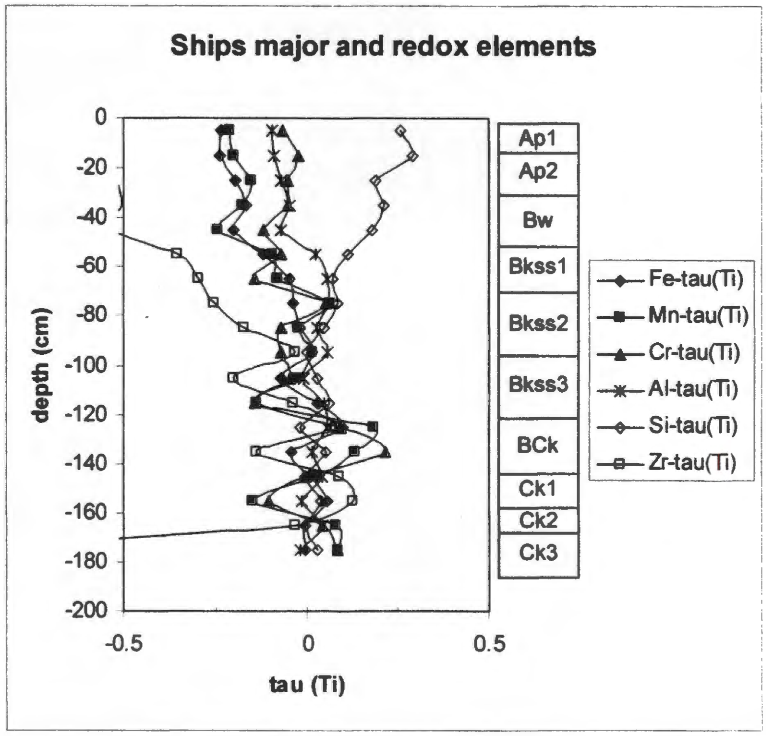

D

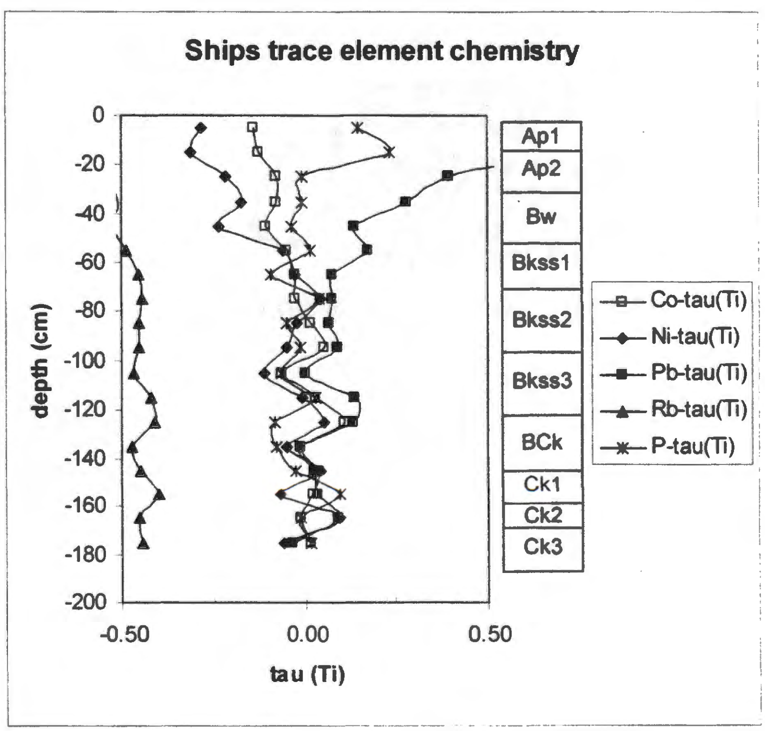

Figure 2.7 (continued) Ships Pedon element translocations calculated using Ti as immobile trace index: C) major and redox element translocation trends, and D) trace element trends within the soil profile.

trend occur in several places. In particular, at 160cm depth the calcification index reached nearly 45% within the Ships profile. This depth corresponds to a calcareous silt layer just above the original, bedded parent material. Exchangeable bases are another index used to interpret translocation of base cations (Na, K, Ca, and Mg) relative to Al (see Table C4.2). Positive tau-Ti values for this index are associated with a gain in the exchangeable base ratio relative to the parent composition ratio; negative tau-Ti values suggests a loss relative to parent. When the ratio is greater than +1, this suggests that there is a greater increase in the amount of aluminum (and clays) than the base cations in the profile. The Ships profile has a minor to moderate increase of 10-25% exchangeable base index in the Bkss1 and Bkss2 horizons (50-80cm); a decrease of the calcification index (5-10%) is reflected at the same depth. Salinization, in addition to the calcification and exchangeable base indices, reflects the relative mobility of Na compared to K. Within the Ships profile Na and K are conserved, except where relative gains of 25 to 30% and loss of 25% occur at depths of 40 and 160cm and 130 cm, respectively. The oxidation index (Fe/Al) remains very close to parent material composition suggesting redoximorphic features (Fe mobility) may be limited in this profile.

Divalent cations (Figure 2.7B) such as Ca, Mg and Sr have very similar trends with depth, with minor losses occurring from 40 to 80 cm (Bw to Bkss2). Calcium is slightly more erratic in the lower portions of the profile (BCk to Ck3) and may reflect variations within the original parent alluvium. Sodium and K, although both are monovalent, have different translocation patterns with depth.

There is essentially very little deviation of K from the parent material composition, possibly suggesting the occurrence of a minor K-rich mineral phase (e.g., illite). Clay-rich soils such as Vertisols may exhibit a variety of hydrologic conditions conducive to mobility of redoximorphic (redox)-sensitive elements (i.e., Fe, Mn and Cr).

Moderate loss of Fe, Mn and Cr (5-25%) down to the Bkss2/Bkss3 contact suggests very limited saturation of the profile for extended periods of time; high Eh conditions are not conducive to wholesale mobility of reduced cations. Interestingly, the redox-sensitive elements (Figure 2.7C) closely follow the variation in Al with depth. Aluminum trends with depth may be used as a generic indicator of clay content and mobility. As such, there may be a correlation between clay content and Fe and Mn mobility. Similarly, Si trends show moderate gains from 2 to 30% to 180m, but are more pronounced from the surface to the base of the Bkss2 horizon. Zirconium and Si commonly occur in the silt- to sand-size fraction, however in the Ships profile, there appears to be an inverse relationship in their occurrence. Losses of Zr ranging from greater than 50% within the Ap1 and Ap2 horizons to variable amounts of 5-15% below the Bkss2 horizon indicate that a direct correlation between grain size composition and elemental analyses may not be plausible.

Trace element chemistry (Figure 2.7D) includes trends for Co, Ni, Pb, Rb, and P. Fertilizer applications will enrich the soil with nutrients such as N, P and K. Phosphorus depletion in the profile is typically a function of plant uptake. Each elemental trend is very similar below a depth of 70cm; upper horizons have similar inflection points with Pb showing a significant gain of 25 to 75% to the Bkss1 horizon. Lead additions may be attributed to lead aerosols from gasoline or from pesticides/herbicides. Rubidium and Co have very similar translocation trends throughout the profile, however, this relationship is not well understood.

The Ships Pedon thus has experienced minimal to moderate translocation with some variation possibly related to original composition at the time of deposition. This is not to say that there has been no pedogenic processes acting, as this is clearly stated elsewhere in the Ships results, rather, there is some limit to the depth to which these processes have occurred.

Clay mineralogy and particle-size analysis

Clay mineral analysis was not completed on the Ships profile, however, utilizing petrographic descriptions, there is an abundance of clays responsible for shrink-swell processes (Montmorillonite). Calcite is also very common, as identified through finely disseminated, weakly cemented segregations, and nodular carbonate morphologies. Detrital quartz grains typically occurred in a slightly coarser fraction, but are likely to occur in the clay-size fraction as well. The clay fraction (Figure 2.8) ranges from 60 to 70% at depth and declines to nearly 40% at the soil surface. An inverse relationship occurs between the clay and silt fraction, where silt composition at depth is 30 to 40% and increases toward the surface to 55%. Very little variation occurs within the sand fraction, remaining less than 2% through most of the profile. The Ap horizon is characterized by an increase in sand and silt relative to clay content,

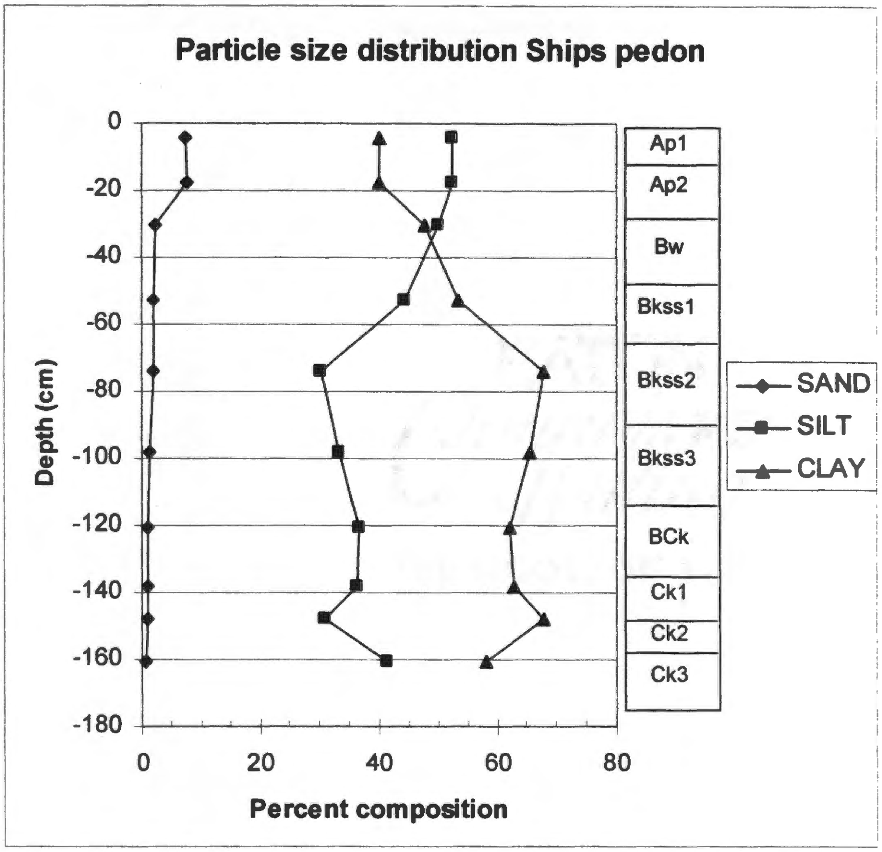

Figure 2.8 Ships particle size analysis. Note the decrease in clay relative to silt in the upper portions of the profile.

suggesting surficial mixing associated with plowing. An increase in clay content functions as a hydrologic barrier at 150cm and has resulted in deposition of the powder calcite layer.

Pedon 2: Pledger Series (~3,500 yr BP)

Macromorphology

The Pledger Pedon (Table 2.4; Figure 2.9) represents the youngest profile examined with gilgai or microtopographic features. The surface expression of the microhigh (MH) and microlow (ML) is limited due to drainage and organic content of the upper A horizon, but nonetheless it is distinct in macromorphologic expression. Gilgai topography has moderate relief (10 cm) and spacing between microhigh mounds of 2-3 m. Mukkara or chimney-like features do not penetrate to the soil surface in all microhighs. Slickensides are abundant and closely spaced, with thickness of slickensided horizons ranging from 124 and 138 cm in the MH and ML, respectively. The angular inclination of wedge-shaped aggregates increases with depth from 35-45°(Bss1) to 50-60° (Bkss2). Structural aggregates in the MH range from moderate, fine subangular blocky in the surface horizons to moderate, fine (Bk and Bkss1) to moderate, medium angular blocky (Bkss2 to BC3). The ML contains moderate, fine subangular blocky (A1 to Bss1), moderate (Bss2 to Bkss1) to weak (Bkss2 to BCk), medium angular blocky, and massive (parent material) structure. The depth of pedogenesis reaches 179-182 cm (MH) and 182-220 cm (ML) with bedded, brown to red calcareous silty clay alluvium (parent material) occurring between

Table 2.4 Pledger ML Pedon- Characteristic Summary

Horizon	Depth	Slickensides	$CaCO_3$ nodules	Roots/pores & redox	Structure	Matrix
A1	0-20	---	---	Many very fine and few fine pores; common fine and few medium roots; 1% fine, Fe concentrations in pore linings	Moderate fine SBK	Black (10YR2/1) clay; 1% (7.5YR5/6) Fe concentrations
A2	20-44	---	---	Common fine and few medium roots; many very fine and few fine pores; <1%fine, strong brown Fe concentrations in pore linings	Moderate, fine SBK	Black (10YR2/1) clay; <1% (7.5YR5/6) Fe concentrations
Bss1	44-88	Common prominent slickensides; common wedge-shaped peds (35-45°)	---	Common fine and few medium roots; many very fine and few fine pores; <1% fine, strong brown Fe concentrations in pore linings	Moderate, fine SBK	Black (10YR2/1) clay; <1% (7.5YR5/6) Fe concentrations
Bss2	88-133	Common prominent slickensides; many distinct pressure faces; common wedge-shaped peds (40-45°)	---	Few fine and medium roots; common very fine and few fine pores; <1% fine, strong brown Fe concentrations in pore linings and ped interiors	Moderate, medium ABK	Black (10YR2/1) clay; <1% (7.5YR5/6) Fe concentrations

Table 2.4 Pledger ML Pedon- Characteristic Summary (continued)

Horizon	Depth	Slickensides	$CaCO_3$ nodules	Roots/pores & redox	Structure	Matrix
Bkss1	133-171	Common prominent slickensides; many prominent pressure faces; common wedge-shaped peds (50-60°)	2% hard-pitted (1-5mm) nodules	Few fine roots; common very fine and few fine pores; 2% grayish brown and Fe-depletions on ped surfaces and lining pores; <1% fine and medium distinct, strong brown Fe concentrations in pore linings and ped surfaces	Moderate medium ABK	Yellowish red (5YR4/6) clay; 2% grayish brown (10YR5/2) Fe-depletions; <1% fine and medium distinct, strong brown 7.5YR5/8) Fe concentrations
Bkss2	171-182	Common prominent slickensides; few prominent pressure faces; common wedge-shaped peds (50-60°)	2% hard-pitted nodules (1-5mm)	Few fine roots; common very fine and few fine pores; 1% fine and medium gray Fe-depletions on surfaces of peds; 1% fine and medium weakly cemented Fe-Mn nodules	Weak, medium ABK	Yellowish red (5YR4/6) silty clay; 1% fine and medium gray (10YR6/1) Fe-depletions; 1% fine and medium weakly cemented Fe-Mn nodules
BCk	182-220	Few pressure faces	1% hard-pitted (1-5mm) nodules	Few fine roots; common very fine and few fine pores; 3% fine and medium gray Fe-depletions on ped surfaces and pore linings; 1% fine weakly cemented Fe-Mn; 1% black masses of Mn lining pores	Weak, medium ABK	Red (2.5YR4/6) clay; 3% fine and medium gray (10YR6/1) Fe-depletions; 1% black (10YR2/1) masses of Mn
C1	220-265	---	Few fine threads of $CaCO_3$ lining pores	Common very fine and few fine pores; few fine weakly cemented Fe-Mn nodules; 1% fine black masses of Mn and 3% fine and 1% medium brown Fe-depletions lining pores	Massive	Red (2.5YR4/6) silty clay; few crayfish krotovina; 1% fine prominent black (10YR2/1) masses of Mn; 3% fine and 1% medium brown (7.5YR5/2) Fe-depletions

Table 2.4 Pledger ML Pedon- Characteristic Summary (continued)

Horizon	Depth	Slickensides	$CaCO_3$ nodules	Roots/pores & redox	Structure	Matrix
C2	265-304	---	---	Common very fine and few fine pores; 1% weakly cemented Fe-Mn nodules; 1% fine black masses of Mn lining pores; 1% fine and 1% medium brown Fe-depletions lining pores	Massive	Yellowish red (5YR4/6) silty clay; 1% fine black (10YR2/1) masses of Mn; 1% fine and 1% medium prominent brown (7.5YR5/2) Fe-depletions
2C3	304-345	---	---	Common, very fine and few fine pores; 1% fine weakly cemented Fe-Mn nodules; 1%fine prominent black masses of Mn pore linings; 3% fine and 1% medium light brownish gray Fe- depletions within the matrix and pore linings	Massive	Brown (7.5YR5/4) loam; 1% fine prominent black (10YR2/1) masses of Mn; 3% fine and 1% medium light brownish gray (10YR6/2) Fe-depletions
2C4	345-365	---	---	Common very fine and few fine pores; few weakly cemented Fe-Mn nodules; 1% fine, black masses of Mn lining pores; 5% and 1% medium light brownish gray Fe-depletions within the matrix and lining pores	massive	Brown (7.5YR5/4) sandy loam; 1% fine, black (10YR2/1) masses of Mn; 5% and 1% medium distinct light brownish gray (10YR6/2) Fe-depletions

A

B

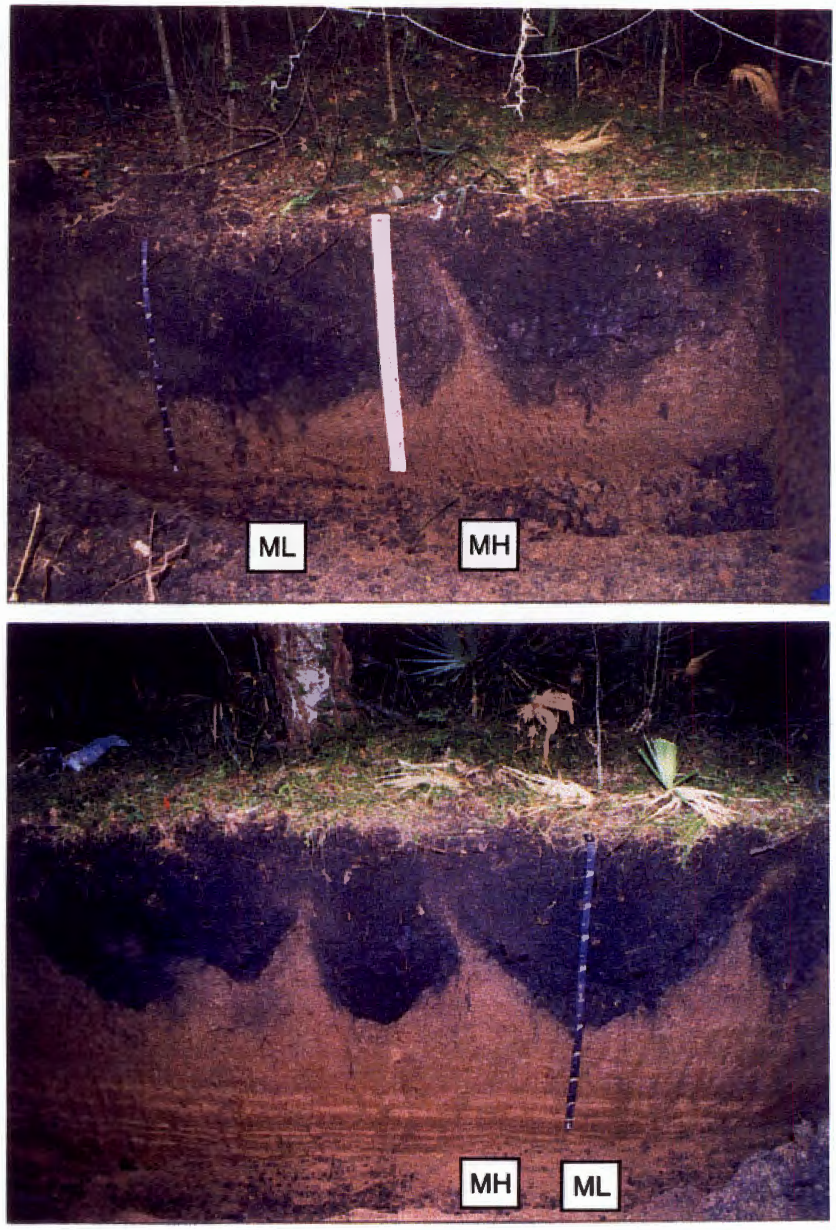

Figure 2.9 Pledger Pedon macromorphology. The microlow (ML) profile is the very dark, bowl-shaped region; the microhigh (MH) profile is the bright red-brown chimney protruding toward the soil surface. A) and B) are close in proximity in the field. Note that the spacing between the microhighs is variable. Preservation of bedded alluvium is illustrated in B. Tape is 200-210 cm in length.

220-265cm. The depth to the top of the Bk horizon occurs much closer to the soil surface in the MH, where depths range from 33-55 cm (MH) and 133-171 cm (ML). In the MH hard, pitted carbonate nodules range in size from 1 to 5 m with composition ranging from 1 (Bk to Bkss2) to 3% (B'ss to BC3). The parent material contains fine carbonate threads lining pores. The ML carbonate nodules of similar size and abundance occur beginning at the Bkss1 horizon (133-171 cm). Nodule morphology is variable in the MH with gray, white, and buff coloration of the carbonate. Matrix colors are also variable, characterized by dark brown (7.5YR 4/3-4) in the Bk and Bkss2 horizons, bright red (5YR 4/4) in B'ss and BC2 horizons, and yellowish-red (2.5YR 4/6) occurring deeper within the solum (BC1, BC3 and C1 horizons). Lower, bedded strata contain variegations of yellowish red (5YR 4/6, 7.5YR 5/4) and brown (7.5YR5/4). Redox depletions and concentrations further add to the color variability as well as assist in recognition of redoximorphic conditions. Fine- and medium-sized Fe concentrations occur throughout the profile (pore linings and ped interiors), representing approximately 1% of the grain composition. Mn (10YR 2/1) concentrations or masses also contribute roughly 1% to the coloration, particularly in pore linings. Within the ML, Fe-Mn are coalesced into weakly-cemented, fine and medium-sized nodules. Fine and medium, gray Fe depletions are identified on ped surfaces and lining pores of the B'ss to C1 (MH) and Bkss1 to 2C4 (ML).

Micromorphology

The micromorphology (Figure 2.10A-E) of the Pledger Pedons is divided into three main areas: 1) Fe-Mn nodules, concentrations or depletions, 2) segregations, nodules and matrix carbonate, and 3) matrix characteristics (i.e., clay fabrics, bioturbation features, and lithorelicts). There are two end-member morphologies of Fe-Mn concentrations exhibited within the Pledger profiles. Dendritic concentrations (and nodules) are typically moderately to weakly cemented and are found branching within the calcareous matrix and detrital quartz, throughout most of the MH and ML profiles. Degree of nodule cementation is indicated by the distinction between using concentration versus nodule terminology. The ML contains numerous examples of concentrically laminated Fe-Mn nodules. This morphology is further characterized by detrital quartz silt and pedogenic clays that were engulfed during nodule formation. Both dendritic and concentrically (Figure 2.10C-E) laminated Fe-Mn nodules occur within the ML profile, particularly in the Bss2 horizon. In lower portions of the ML profile (e.g., Bkss2) Fe-Mn oxides and oxyhydroxides appear to be weathering out of pedorelicts within the soil matrix. Mobility of the various Fe-Mn species results in the redoximorphic concentrations and depletions along ped surfaces and bedding boundaries. Bkss2 and B'ss horizons in the MH, and Bkss2 to BC2 in the ML, are examples of these redoximorphic features. Dendritic Mn and Fe staining of carbonate nodules is very common within this profile, suggesting complex hydrologic conditions.

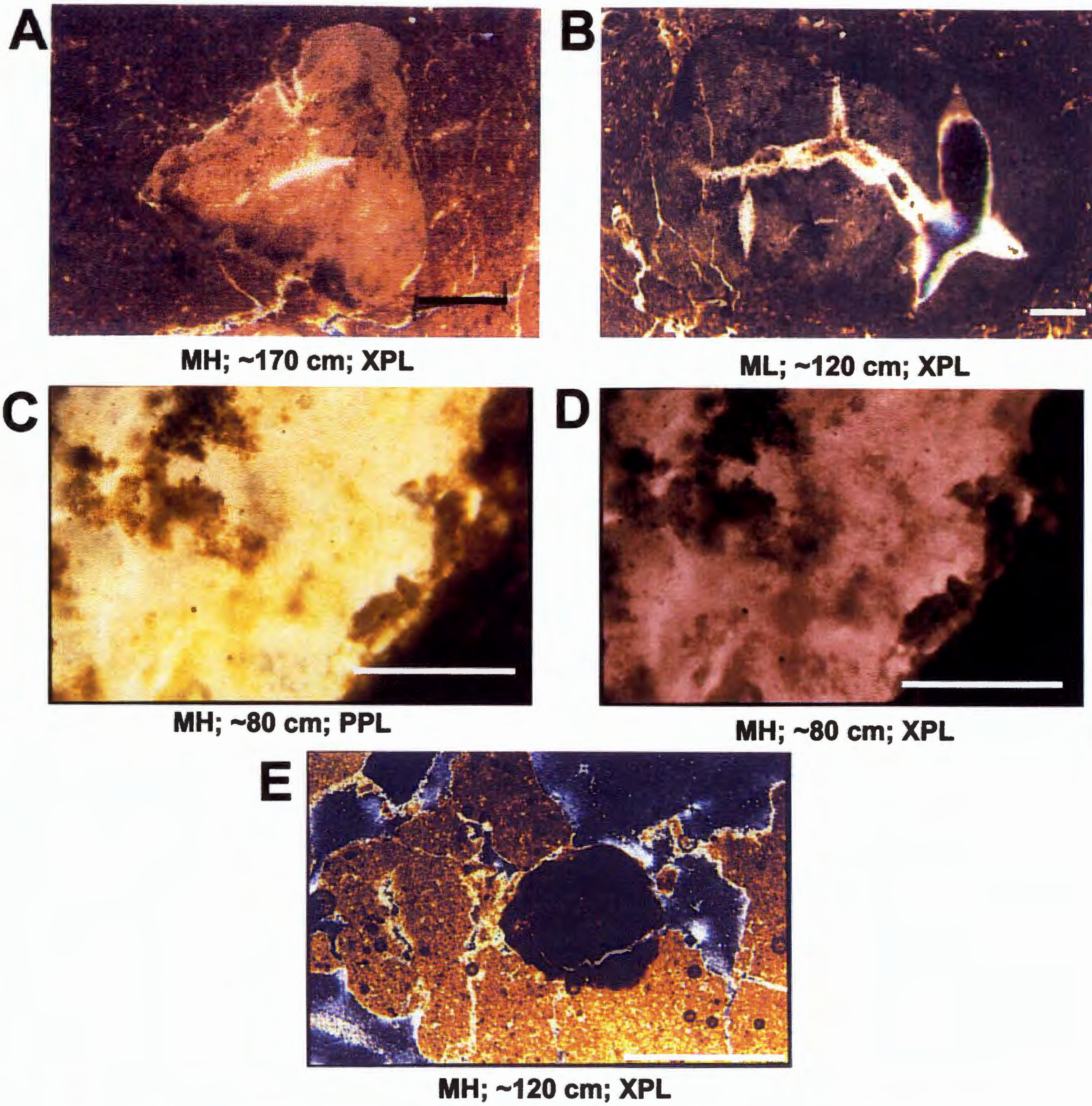

Figure 2.10 Pledger Pedon micromorphology. A) Triangular shaped carbonate nodule with infilled septarian voids and distinct boundary with matrix; B) carbonate nodule with large septarian void, partially infilled with spar cement; C-D) carbonate nodule with dendritic Fe-Mn concentrations and distinct boundary with matrix; E) well-cemented Fe-Mn nodule. A and B have scale bars of 0.5 mm; C-E have scale bars of 1mm. (XPL=crossed polarized light; PPL=plane polarized light)

Coloration of carbonate nodules is an obvious characteristic when viewing these soils in thin section. Some nodules (Figure 2.10A-B) are buff to light brown (Fe stained), whereas others are distinctly gray (Mn incorporation into nodule) and bright white. Dendritic Mn (Figure 2.10C-D) was commonly found in nodules in lower portions of both the ML and MH profiles. Recrystallized carbonate nodules have a tendency to have diffuse boundaries with the surrounding matrix; some of these may contain more distinct boundaries and have septarian voids (Figure 2.10B). Most of the pore space within the nodules containing septaria was not completely occluded. Finely disseminated matrix carbonate was present within all horizons of the MH and increasing with depth (below Bss2) in the ML.

Matrix material is composed of finely disseminated carbonate (through most horizons), detrital mono- and polycrystalline quartz, and lithorelicts. Bioturbation (arcuate burrow backfill) and vertical cracks (original bedding perpendicular) incorporate coarser sediments into the fine matrix and disrupt any sedimentary layering preserved in lowermost horizons. In general, slickensided horizons (both MH and ML) exhibit sepic-plasmic and lattice-sepic fabrics; pedo- or lithorelicts have experienced extensive mixing and differential redoximorphic staining.

Bulk Chemistry

The Pledger ML profile was sampled to greater depth than the other profiles incorporated into this study, but was sampled by the NRCS only by genetic horizons, rather than in 10cm depth increments. Parent material used in

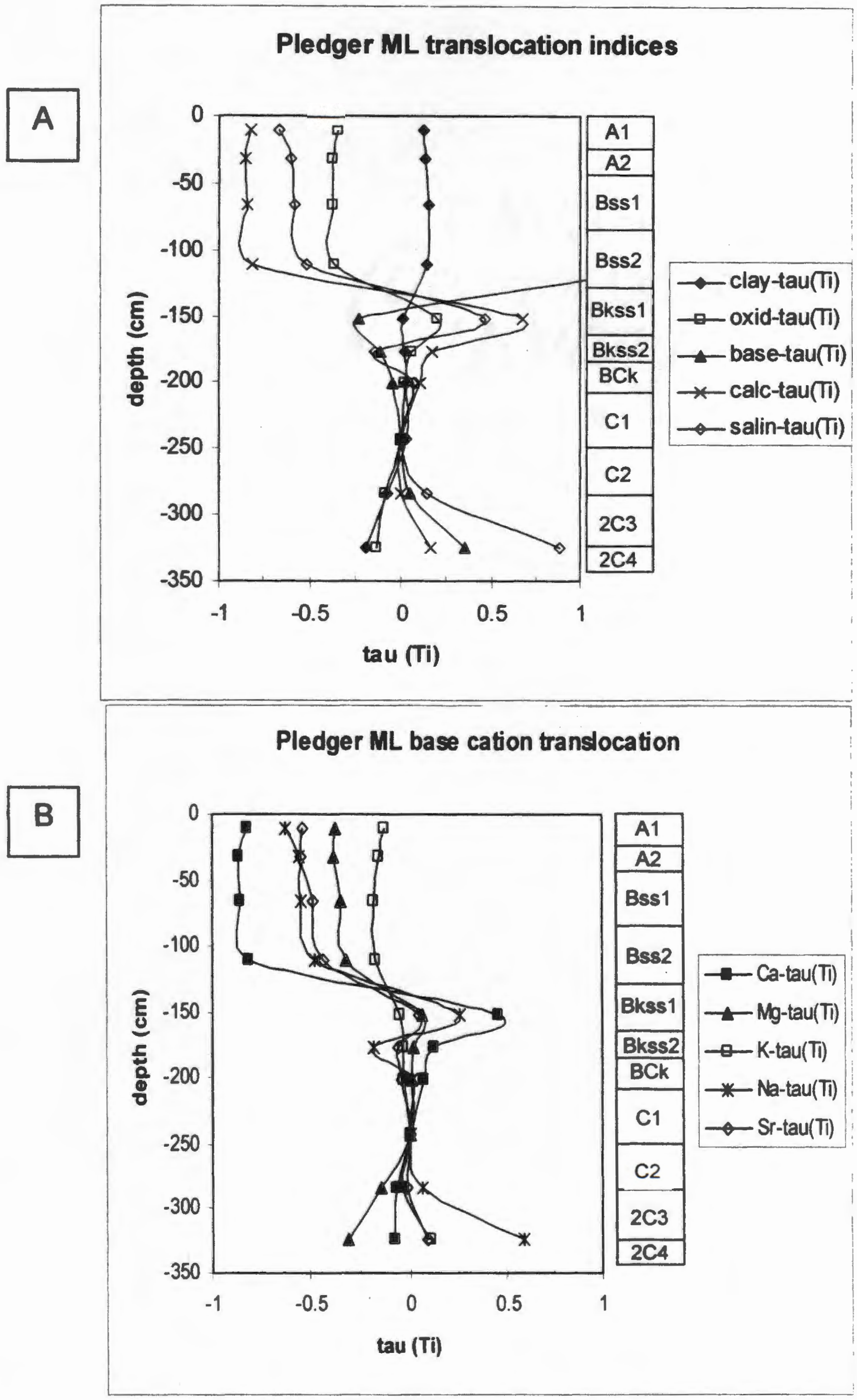

Figure 2.11 Pledger ML profile molecular ratios and element translocations calculated using Ti as immobile index element. A) clay (clayeyness), oxid (oxidation), base (base loss), calc (calcification), and salin (salinization) are translocation indices. B) translocation of base cations within soil profile.

C

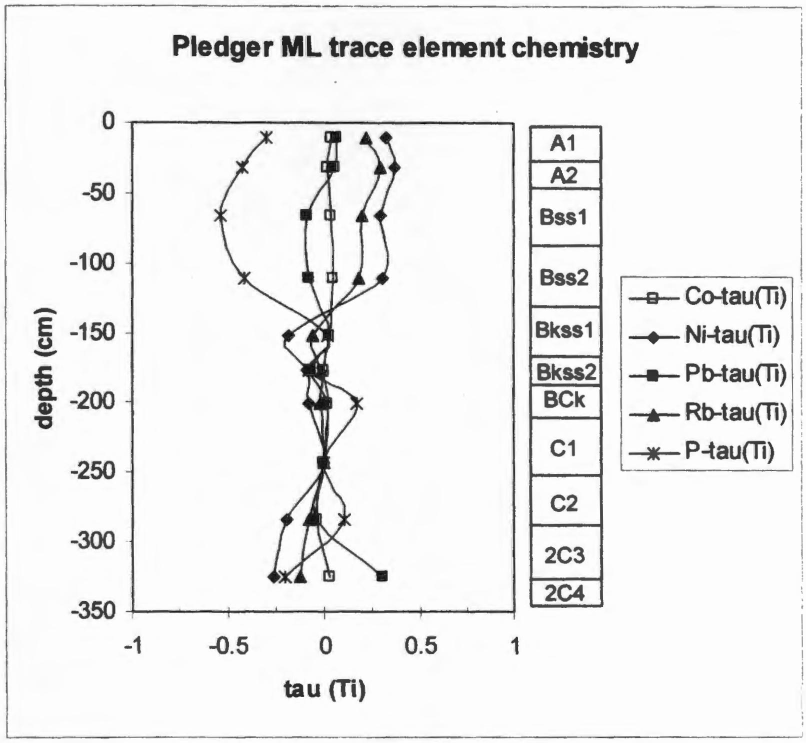

D

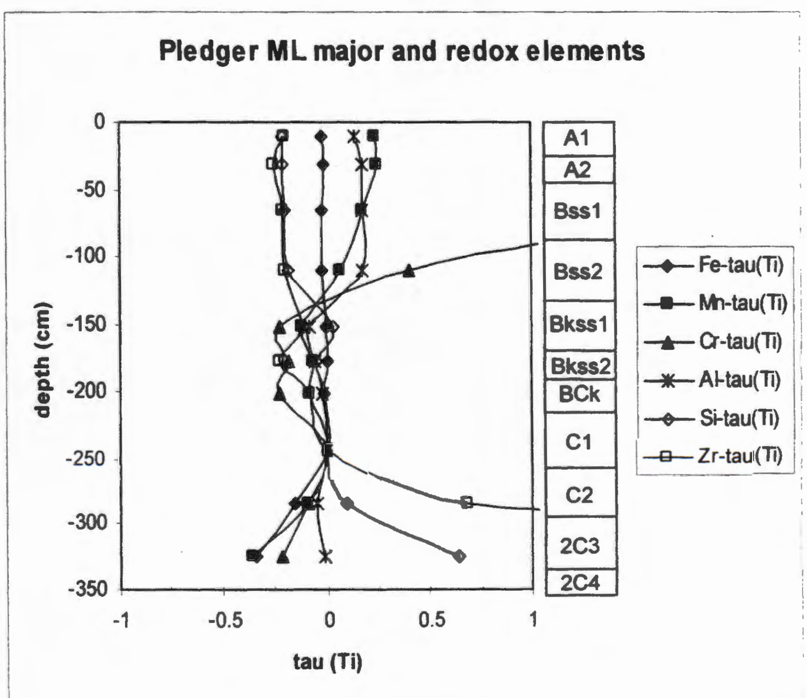

Figure 2.11 (continued) Pledger ML profile element translocations calculated using Ti as immobile trace index element: C) major and redox element translocation trends, and D) trace element trends within the soil profile.

the mass-balance calculations employed the C1 horizon (220-265 cm) bulk chemistry values; this is indicated on the plot as the intersection of the various indices (Figure 2.11A). The translocation indices illustrate a very pronounced variation with depth. Calcification, salinization and oxidation exhibit incrementally greater translocation in the upper 130 cm (A1 to Bss2) of 80%, 50% and 30%, respectively. A sharp increase in these indices within the Bkss1 horizon suggests that this depth interval represents a significant zone of accumulation relative to parent material. Exchangeable bases have an inverse trend in which there is greater than 100% gain in the upper part of the solum and a marked decrease at 150cm (Bkss1). If clay content can be generally modeled by Al content, then the increase in the ratio (Al to base cations) should correlate with an increase in clay content. Although the next section goes into more detail, it is important to note that the upper part of the solum (surface to 150cm) has an increase in clay content of 55 to ~80%. Overall variation in oxidation, exchangeable bases, calcification, and salinization below the Bkss2 horizon is variable but typically ranges +/-10% relative to the parent composition.

Base cation translocations (Figure 2.11B) are very similar to those exhibited by the various indices, which is expected given that the ratio includes the weight percent of the base cation. However, if a particular cation or cations exhibited different behavior than the remaining ones, then the translocation indices trends may look substantially different. A second scenario, related to the translocation indices trends, may be a result of a change in the amount of Al due to an increase or decrease in clay content. Potassium, Mg, Sr, Na and Ca trends express increasingly more loss from the upper solum and gain in the Bkss1 horizon, respectively. Within the BCk and C1, the base cations approach parent material compositions with gains/losses of less than 10%.

The redox-sensitive cations (Figure 2.11C) within the Pledger exhibit different behavior than in the Ships. Fe and Mn show general gain (~30%) or conservation in the profile, whereas Cr is very erratic in the upper solum (to Bkss1). Chromium and Zr are considered relatively immobile, however, Cr shows greater than 100% increase; in addition, approximately 50% Zr has been lost in the profile. Aluminum and Si are inversely related to each other; Al increases (25%) toward the soil surface, while a loss of 25% Si occurs in the upper solum. This may be suggestive a change in grain size, if Al is used to model clay content and Si is analogous to silt and sand content. If the relative gain/loss of Al and Si are similar, this may also indicate that the coarse (sand) fraction of the soil has changed very little or has changed at a ratio consistent with the ratio constituents. Particle-size analyses in the next section appear to support the general increase of clay and decrease of silt, with no major change in sand content in the upper solum. Zirconium appears to have a consistent loss of 35% throughout most of the profile and changes to major increase at depths greater than C1 (250cm). The increase in Si and Zr may correspond to a change in parent subsoil lithology (clay to sand), and were instrumental in selection of a more appropriate parent material.

Trace element chemistry (Figure 2.11D) aids in identification of change in source area of parent material. Phosphorus and Pb have similar trends as Si; Ni and Rb trends are comparable to Al. Phosphorus depletion, however, is very pronounced in the upper solum, with some enrichment in the BCk horizon. Although the exact relationship is not clear, there may be some correlation between the cation and grain-size fraction (clay surface complexation). The source area for the alluvium appears to have been the same throughout the history of the profile. Cobalt shows very little translocation and is conserved through out the profile.

In summary, the Pledger ML profile exhibits interesting trends in bulk chemistry that may be associated not only with pedogenesis, but also original grain size variation inherent to alluvium-derived deposits. These trends are also consistent with more advanced pedogenesis as compared with the Ships Pedon.

Clay mineralogy and particle-size analysis

Clay mineral analyses conducted on the Pledger Series included only the ML profile (Appendix D). Montmorillonite is the most abundant mineral of the soil matrix and remains fairly consistent in ranked abundance through the entire profile. Kaolinite, calcite and mica comprise the secondary mineral assemblage. Calcite is missing in the A2 and Bss1 horizons, but reaches concentrations similar to kaolinite and mica below these horizons. An increase in mica occurs in the 2C4 horizon, thereby obtaining a similar rank as montmorillonite. Quartz decreases from the A2 to Bss1 horizon, and maintains a rank of 1 throughout the remainder of the profile. Smectite is recognized as the dominant descriptive mineral component for the Pledger ML and MH profiles.

The particle-size distribution (Figure 2.12) for the Pledger Pedon (ML) was very instrumental in parent material selection and identification of what appears to be a lithologic and stratigraphic break between 300 and 350 cm. Sand content (in the ML) above this break is minimal (<3%). A major decline in both silt and clay occurs at 300 cm, which falls within the zone of major increase in sand content. Sand content within the MH increases from 1% to 6% between 185-198 cm and 18-33 cm, respectively. There is general increase in clay content (45 to ~70%) upward in the (ML) profile; a major increase occurs between the Bss2 (72%) and Bkss1 (53%). The silt percent composition trend of the MH and ML profiles mirrors the clay fraction, possibly suggesting decomposition of silt-sized minerals to the clay fraction. Based on these observations, it seemed prudent to select C1 horizon sediment at 250cm depth as the most probable parent material fro the Pledger Pedon.

Pedon 3: Burleson Series (~18,000 yr BP)

Macromorphology

The Burleson Pedon contains several features (see Table 2.5) not yet formed within the younger Ships and Pledger Pedons. The main characteristic that delineates the Burleson is the occurrence of moderately weathered parent material (at ~250+ cm depth) that is a relatively homogeneous (rather than bedded), red, silty clay alluvium. Pedogenic processes have occurred to a more significant depth, with a minimum of 190 cm, and have modified, to some degree, what is characterized here as parent material.

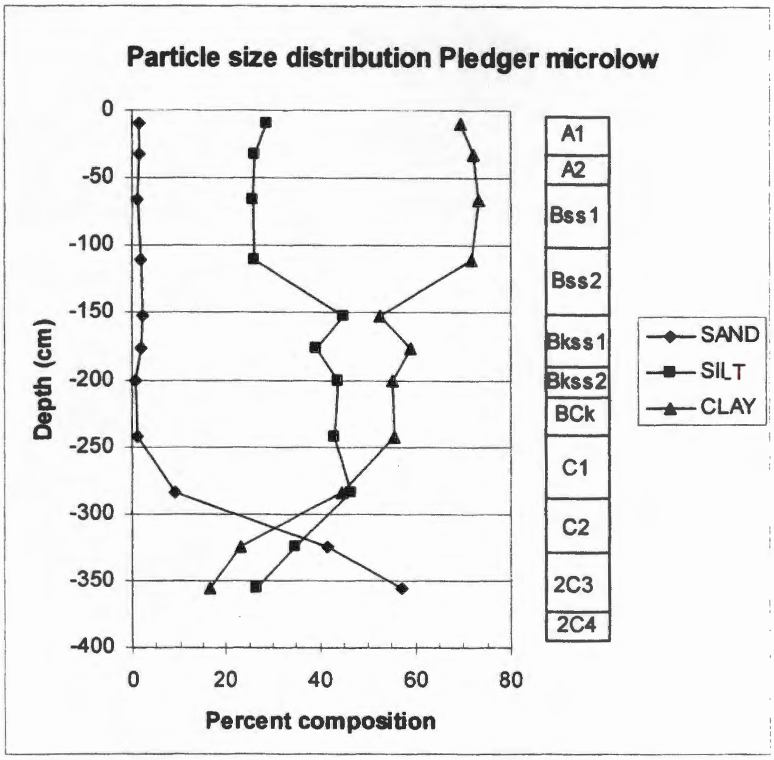

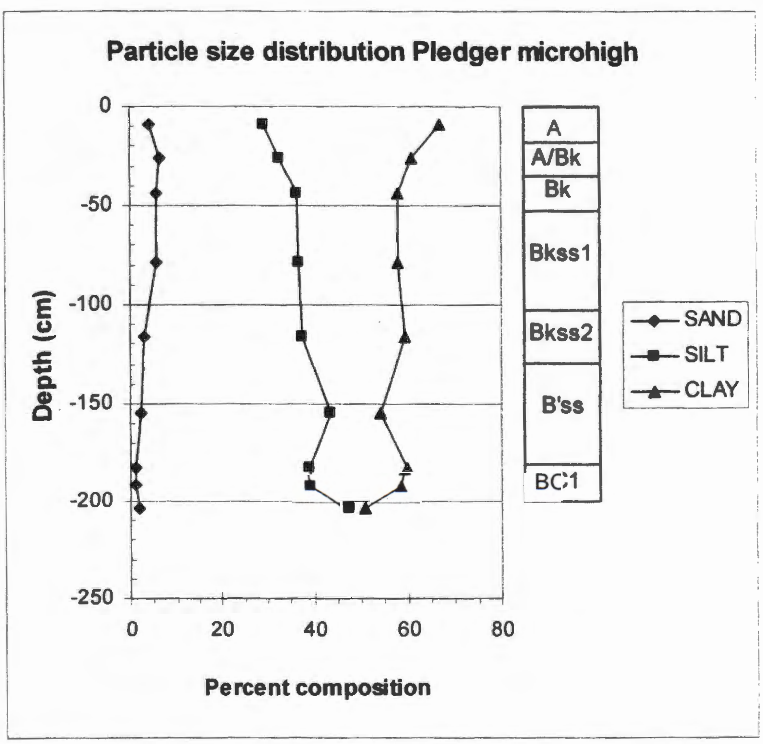

Figure 2.12 Pledger MH and ML particle size distribution. An abrupt change in sand content necessitated an alternative choice of parent material. The parent material chosen for mass-balance calculations ranged from 220 to 265 cm.

Macromorphological development (Table 2.5; Figure 2.13) within the Burleson Pedon is best identified by the establishment of surficial expression of microtopography or gilgai. Gilgai form as a response to shrink-swell processes within the soil matrix and may be related to the thickness of the horizons containing slickensides. The Bkss horizons of the MH and ML profiles have thicknesses of 156 cm and 161 cm, respectively. The slickensides are abundant and closely-spaced; the gilgai have moderate relief (from 10-20 cm) and adjacent MH are 4 to 6 m apart. Burleson Series soils often exhibit greater relief (30 cm; pers. comm., Driese, 2001) than indicated in this study; plowing has resulted in removal of MH material and mixing of the upper ~10-15 cm of the MH and ML. Sharp mukkara and associated chimney tongues are pronounced in the Burleson pedon and penetrate (nearly) to the soil surface.

Slickensides increase in abundance with depth; the Bkss1 (39-65 cm) horizon contains a few slickensides with a dip of 30-45°, and the Bkss2 through Bkss5 horizons have common slickensides dipping at 25-54° (generally increasing with depth). Strong, fine and medium angular blocky structure is associated with the Bw and Bkss1 through Bkss5 horizons for both MH and ML profiles. The surface horizons of the ML profile differ where the Ap horizon is characterized as strong, fine granular and the A horizon is weak, medium subangular blocky. The parent material structure is characterized as massive.

Parent material plays a significant role in the red (5YR 4/6) color of the Bk through Bkss2 horizons of the MH profile; Bkss3 and Bkss4 vary in color, with 5YR 4/6 becoming more abundant than 7.5YR 4/3 with depth. The black

Table 2.5 Burleson ML Pedon- Characteristic Summary

Horizon	Depth	Slickensides	$CaCO_3$ nodules	Roots/pores & redox	Structure	Matrix
Ap	0-11	---	---	Common very fine pores; many fine roots	Strong, fine granular	Black (10YR2/1) clay
A	11-23	---	---	Common fine roots; common very fine pores; reduction around root traces	Weak, medium SBK	Black (10YR3/1) clay
Bw	23-39	Many prominent pressure faces	---	Common very fine roots with reduction rinds; few fine pores	Strong fine ABK	Black (10YR3/1) clay
Bkss1	39-65	Few slickensides (30-45°)	Few fine nodules	Few very fine roots, few fine pores	Strong, fine ABK	Black (N2/0) clay
Bkss2	65-86	Slickensides common (20-37°)	---	Few very fine roots; few very fine pores	Strong, fine ABK	Black (N2/0) clay
Bkss3	86-109	Many slickensides 925-33°)	Few fine nodules	Few very fine roots; few very fine pores	Strong, medium ABK	Black (N2/0) clay
Bkss4	109-156	Common slickensides (25-48°)	Red $CaCO_3$ from parent material; few fine nodules	Few very fine roots; few very fine pores	Strong, medium ABK	Black (N2/0) clay
Bkss5	156-185	Common slickensides (30-35°)	Fine $CaCO_3$ nodules	Few very fine roots; 2% black organics filling pores and root channels	Moderate , medium ABK	Black (10YR4/1) clay; 5 cm wide 5YR4/6 vertical inclusion (crayfish krotovina): 2% black (10YR2/1) organics
Bkss6	186-200	Few slickensides	Common fine and medium nodules	Few very fine roots	Weak coarse ABK	(60% 10YR4/1; 30% 5YR4/6; and 10% 10YR2/1) clay

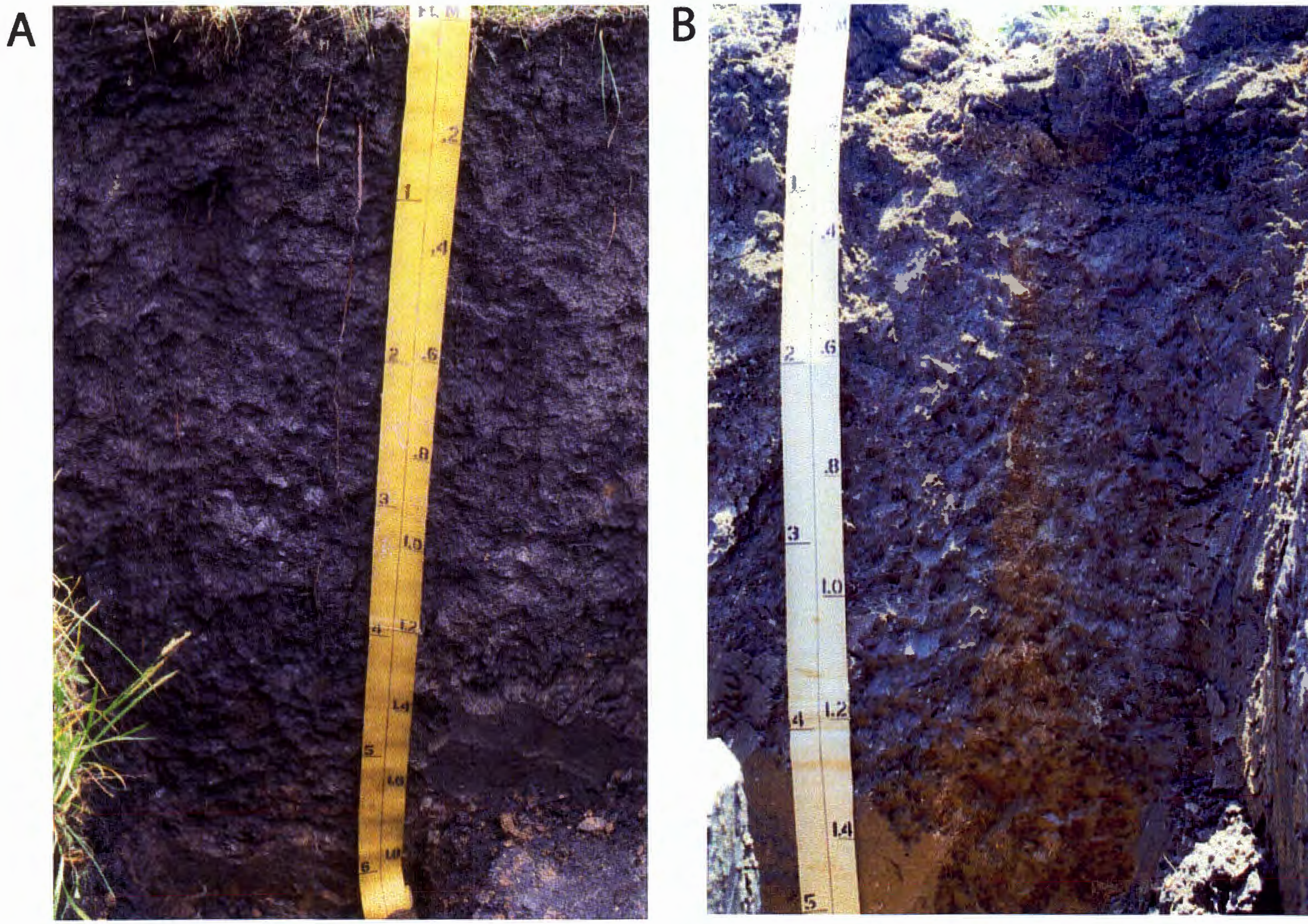

Figure 2.13 Burleson macromorphology: A) microlow profile and B) microhigh profile. Note the red parent material chimney and well-developed slickensides (basal portion) in the MH.

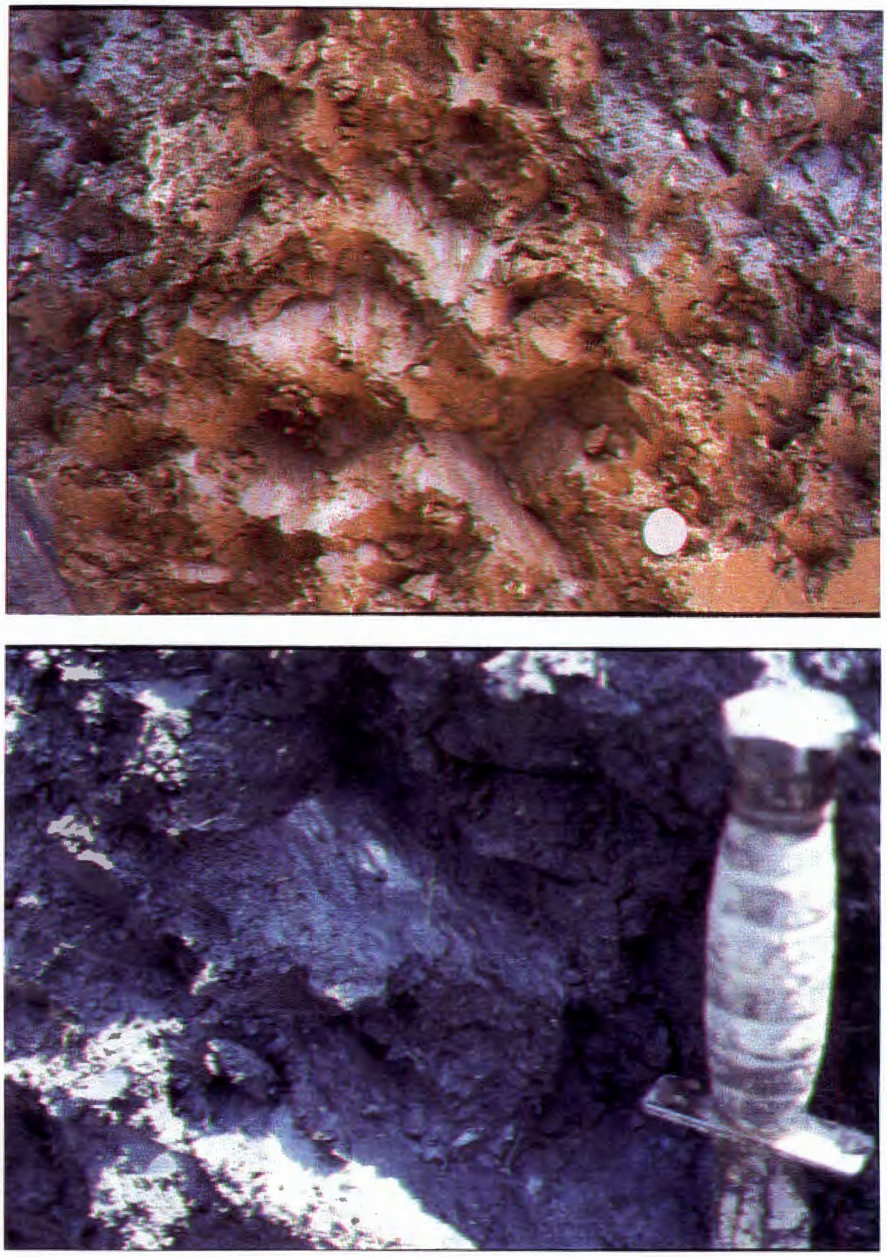

Figure 2.13 (continued) Burleson Pedon macromorphology. A) Stacked corrugated slickensides ~160 cm in the microhigh profile; B) Corrugated and polished slickenside with fine roots and Fe-Mn nodules at a depth of ~100 cm in the ML profile. Quarter dollar used for scale in A; soil knife for scale in B.

(10YR3/1 and N2/0) coloration of the ML profile contrasts greatly from the red MH. The Bkss6 horizon of the ML profile contains a mixture of black, dark gray, and red colors, suggesting incorporation of the red parent alluvium (C horizon, MH profile). Although Fe-Mn concentrations/segregations surely affect the coloration of the profile and are abundant within the ML, specific identification of masses, nodules, or depletions will be included as part of the micromorphology. Whereas Mn is very strong clay -staining agent, organic complexes also promote the very dark color associated with the ML.

Carbonate nodules vary significantly between the MH and ML profiles, which may be a byproduct of the contrasting hydrologic conditions between the two microenvironments. The ML contains few fine nodules from the Bkss1 horizon and lower in the profile. Two types of carbonate morphology occur within the MH: powder and nodular carbonate. Nine percent powder and 2% nodular (with some septaria) carbonate within the Bk and Bkss1 horizons marks an inflection point where there is an increase in nodular and concomitant decrease in powder morphologies with depth.

Micromorphology

Petrographically, the Burleson MH and ML profiles support the macro-scale evidence of variation in carbonate morphology (Figure 2.14A). Finely disseminated carbonate is present ubiquitously in the matrix of both profiles. Silt-sized, coarsely recrystallized (microspar) carbonate nodules appear in the Bkss4 horizon (ML); larger nodules (Figure 2.14A) containing septarian voids lined with

A

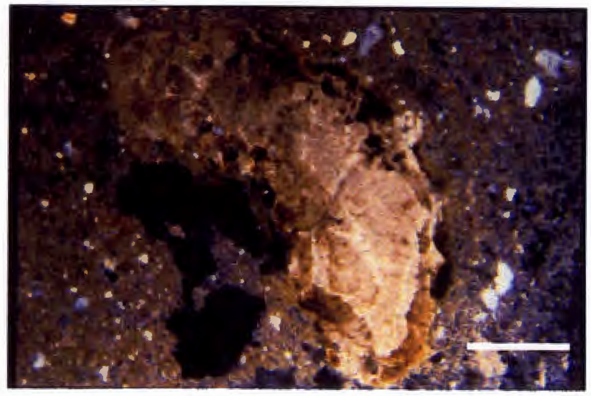

MH; 65-80 cm; XPL

B

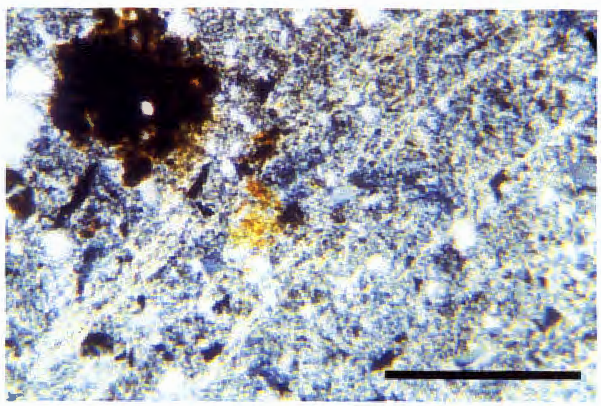

ML; 115-145 cm; XPL

C

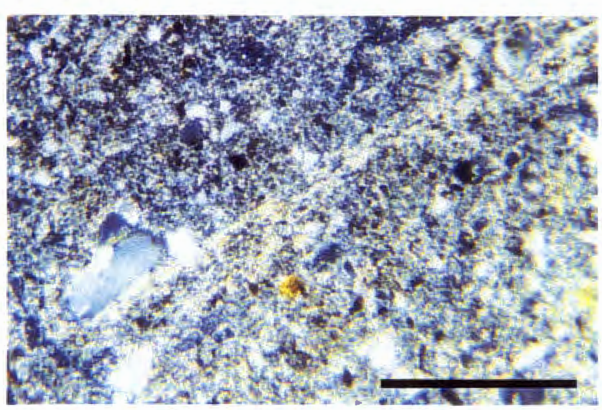

ML; 115-145 cm; XPL

Figure 2.14 Burleson Pedon micromorphology. A) Carbonate nodule without large septarian cracks (infilled?) and Fe-Mn concentration on the upper surface; B) Fe-Mn nodule with detrital quartz is dissolving on the outer edges; C) sepic-plasmic oriented clay fabric due to shrink-swell processes. Bar scale in A is 1 mm; B and C bar scale is 0.5 mm. (XPL=crossed polarized light; PPL=plane polarized light).

coarse crystals (not occluded) occur within the Bkss4 and Bkss5 horizons (ML). Carbonate morphology in the MH profile suggests active precipitation and/or dissolution of nodules. Nodules are present to the soil surface with a trend of increasing size with depth. Similar to the ML, there is a variety of carbonate nodule sizes that are recrystallized to coarse microspar and that may or may not contain septarian cracks. Some nodules appear to engulf detrital quartz and fine matrix material within the carbonate fabric (of the nodule). Nodule boundaries may provide information related to carbonate dynamics (dissolving or precipitating), for nodules that have distinct boundaries and are surrounded by secondary precipitation (from matrix?), and for others that are rounded segregations and have diffuse boundaries with the calcareous matrix material (Bkss5, MH profile).

Distinction between the Burleson MH and ML matrix material is related to the coloration, whereby parent material imparts bright red calcareous material and organic or Mn oxide complexes stains clay mineral surfaces to very dark gray to black. Concentrically laminated nodules (Figure 2.14A) contain inclusions of detrital quartz and calcareous matrix material and morphologies may vary from well cemented to those undergoing delamination or dissolution of outer Fe-Mn layers. The MH profile is particularly prone to nodule delamination. Mn-dendrites and weakly cemented segregations (Figure 2.14B) are more common within the MH profile than in the ML. Redoximorphic depletions and concentrations may be associated with mobilization of Fe from in situ weathering of Fe-Mn nodules. Drab areas occur within the matrix, particularly when associated with crayfish burrowing, but may not always correlate well with changes in grain size (Bkss5, ML).

The lack of occurrence of bedded alluvium at depth is strikingly different that observed in the two previous pedons (Ships and Pledger). The Bkss1 horizon of the MH profile represents the contact between the MH and ML microenvironments. Red calcareous parent material is mixed with the drab, gray matrix material from the ML; dark red pedorelicts incorporated into the drab matrix may be a result of plowing. Silt and fine sand-sized, subangular to rounded detrital quartz is present in minor quantities throughout the profile. Some recrystallized carbonate nodules are similar in size to the detrital (mono- and polycrystalline) quartz grains present. Grain-size variability is particularly pronounced in areas that have undergone significant bioturbation (crayfish krotovina). Identification of soil structure, other than that associated with major cracks and bioturbation, is complicated due to the intense staining of clay surfaces. One exception to this, however, was the lattice-sepic fabric visible in the Bkss4 thin section. Lattice-sepic and sepic-plasmic fabrics (Figure 2.14C), in general, are likely present within the horizons with slickensides.

Bulk Chemistry

The translocation indices appear to be less variable than the Ships and Pledger profiles. This is true but may be exaggerated because of the scale of the x-axis. The significant gain in the exchangeable base ratio required a broader scale. The 150 to 400% increase in exchangeable base index may be due to: 1) an increase in clay in the upper portions of the profile, 2) a decrease in base cations relative to Al, or 3) a significant increase in Al relative to the parent material. There does appear to be a consistent gain of ~15% Al (over the parent material composition) throughout the solum. Clay content shows a slight increase over parent material compositions, but may not be able to explain the major increase in the exchangeable base index. Oxidation, salinization and calcification (Figure 2.15A) exhibit increasing trends in translocation from 50-70%, respectively. Salinization shows some variability through the profile and can be seen more clearly in the Na-translocation graph (Figure 2.15B).

Base cation translocation within the Burleson ML profile ranges from 40 to ~100%. Calcium shows the most significant loss (75 to ~100%) relative to the parent material. According to the horizon notation and field reconnaissance, the profile is calcareous below approximately 40 cm. This attests to the very high carbonate content of the parent material. Strontium and Mg, two divalent species in addition to Ca, decrease in translocation with depth from 60% (A) to 50% (C). Chromium and Mn (Figure 2.15C) are highly variable in percent gain, whereas Fe is consistently lost to ~45% throughout the profile. This dichotomy in redoximorphic behavior suggests that Eh conditions conducive to Fe mobility or Mn complexes on the clay surface are more tightly held than those of Fe. The field coloration is very dark, which supports the Mn oxide complexation as an explanation, but does not clearly explain low Fe/high Mn content of the solum relative to the parent material. Silica and Al show very little variation with

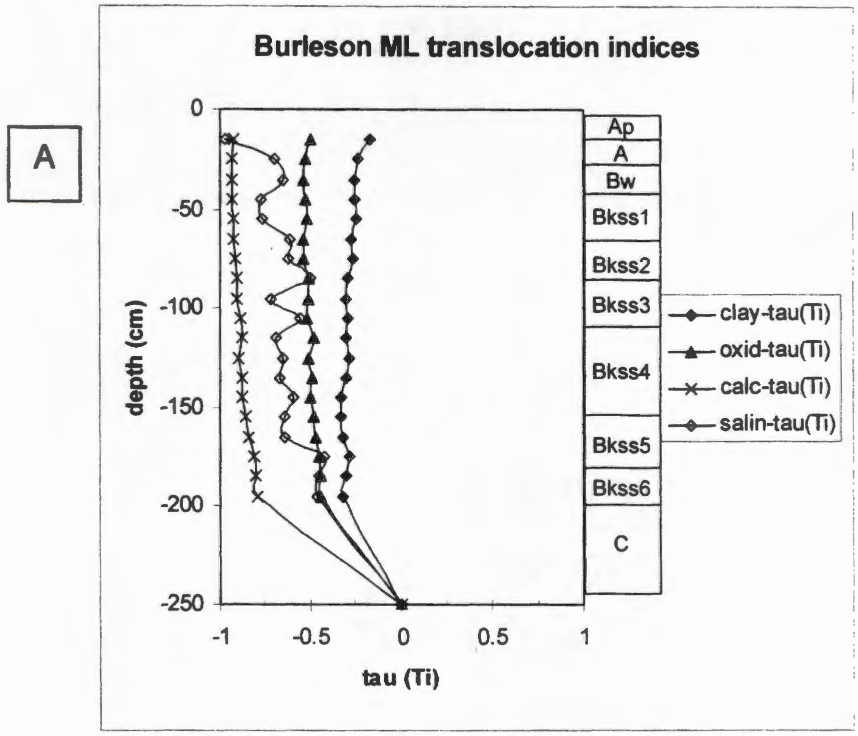

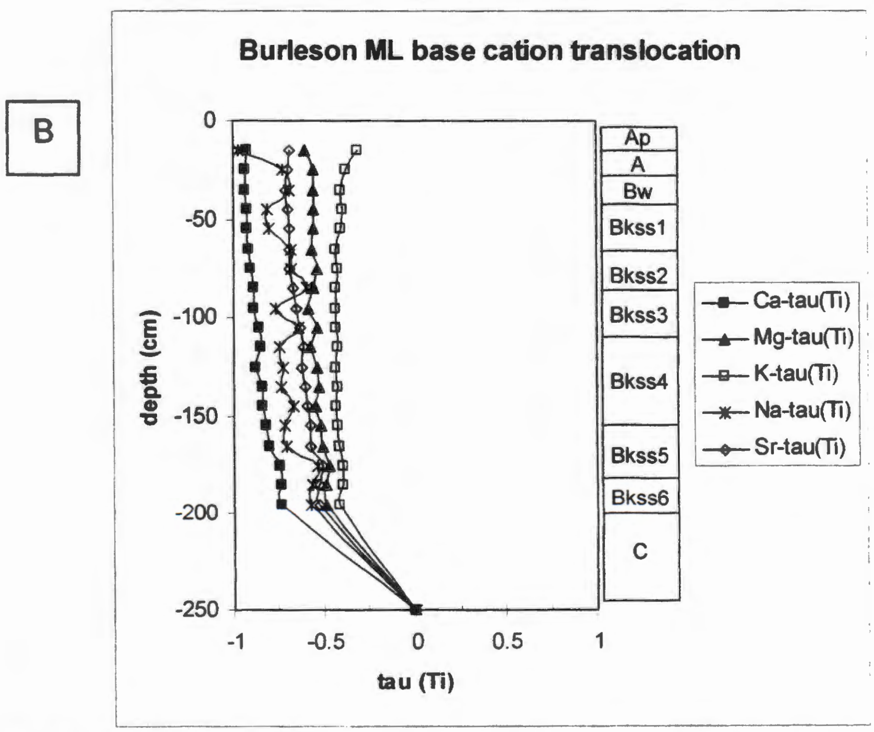

Figure 2.15 Burleson ML profile molecular ratios and element translocations calculated using Ti as immobile index element. A) clay (clayeyness), oxid (oxidation), base (base loss), calc (calcification), and salin (salinization) are translocation indices. Note the change in the x-axis scale. B) translocation of base cations within soil profile.

C

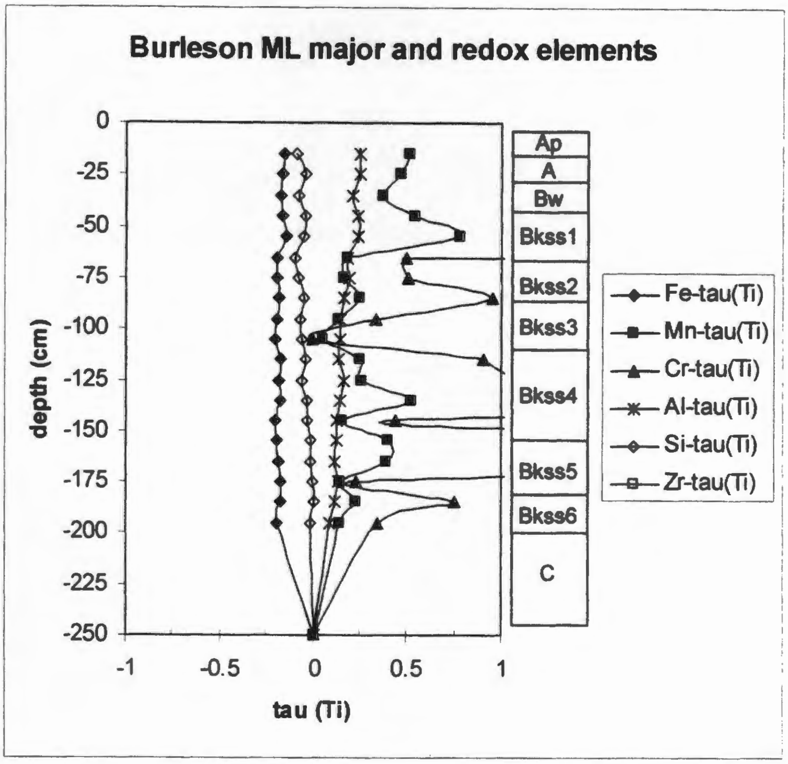

D

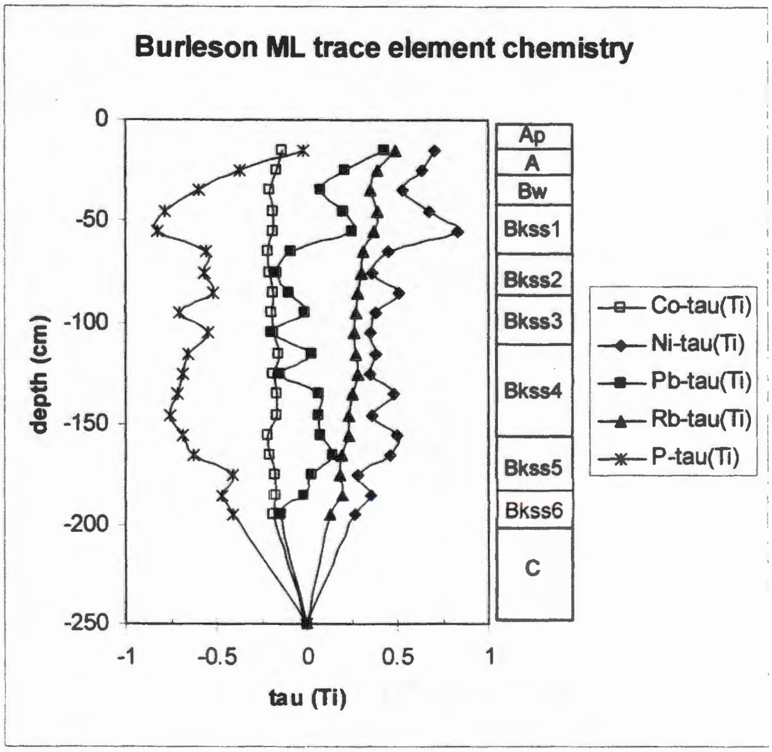

Figure 2.15 (continued) Burleson ML profile bulk chemistry with Ti as immobile trace element: C) major and redox element translocation trends, and D) trace element trends within the soil profile.

depth; Si declines very slightly near the surface and Al increases gradually from the C horizon to the surface.

The Burleson ML profile contains variable trends (Figure 2.15D) in trace elements. Co and Rb are conservative with depth, with loss of ~20% and gain of ~20%, respectively. A general decrease (with depth) and similar depth trends in Ni and Pb suggest that pedogenic processes have affected the mobility of these two trace elements in a congruent fashion. Phosphorus translocation ranges from a loss of 50-75%, with the A horizon approaching parent compositions. Although purely speculative, this may be an artifact of plowing off the upper surface of the MH profile, which is filled with calcareous red alluvium from the parent material.

The Burleson ML profile illustrates the impact of advanced pedogenic processes. The primary record of this is the consistent depth profiles, showing trends with very little variation. Little variation in grain size rules out the variation in trace elements occurring in a particular size fraction.

Clay mineralogy and particle-size analysis

Clay mineral analyses (Figure 2.16) were not available for the Burleson MH and ML profiles. Based on petrographic descriptions and the general descriptive mineralogy, major mineral compositions can be determined. Montmorillonite is likely the dominant mineralogy within the matrix, based on the presence of slickensides within some horizons. Detrital quartz grains were visible either as skeletal matrix grains or as inclusions within Fe-Mn nodules.

A

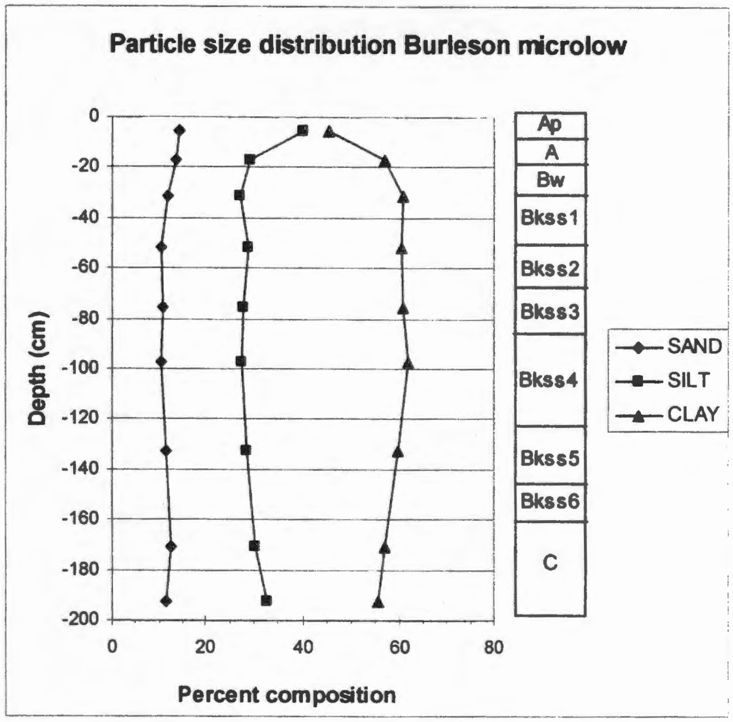

B

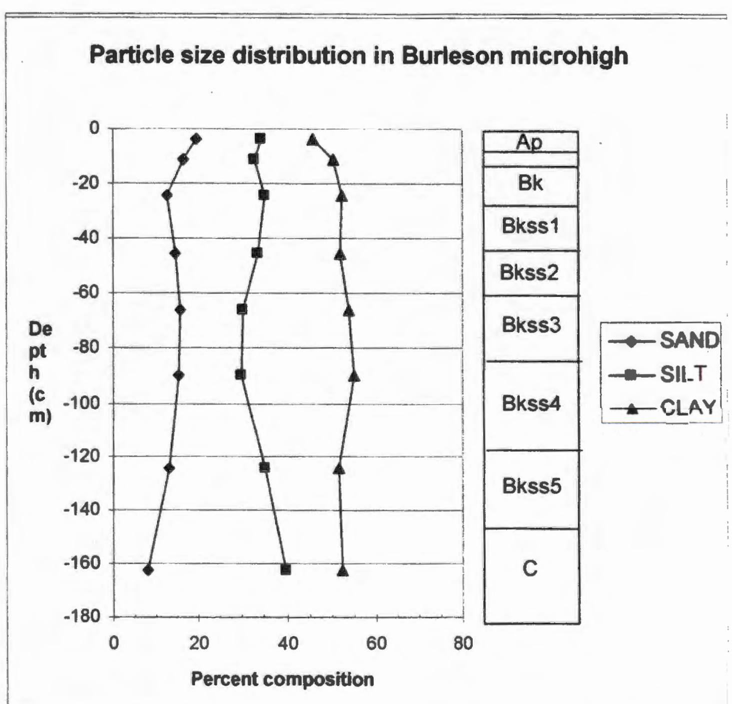

Figure 2.16 Burleson MH and ML particle size distribution. There is very little variation in grain size with depth. A slight increase (5%) in clay content occurs gradually from depth to 100cm in the ML.

Weight percent of calcite in the ML is very low (<2%) through most of the profile. There is an increase in weight percent calcite to 10.4% in the Bkss6 horizon (adjacent to parent material). The Burleson MH profile is significantly more calcareous with minimum values at the soil surface of 7.5% and reaching a maximum of 23.6% in the Bkss5 horizon.

Particle-size analysis trends are interesting because there is very little change in weight percent of the sand (~12%), silt (~29%) and clay (~59%) within the homogeneous profile. The microhigh profile is somewhat homogenous, however, there is a general increasing trend in sand to ~20%. A very minor inflection in grain size (51.9 to 54%) occurs between the Bkss3 and Bkss4 horizons. Both silt and clay size fractions decrease slightly moving upward in the profile.

Pedon 4: Lake Charles Series (~35,000 yr BP)

Macromorphology

The Lake Charles Pedon represents the oldest profile utilized for the chronosequence study. Advancement of pedogenesis downward within the profile reaches a range of 176 to 212 cm (Table 2.6; Figure 2.17). Homogenized red, calcareous silty clay alluvium occurs at 200 cm, with the upper portion of the profile undergoing intense shrink-swell processes. The thickness of the slickensided region is 212 cm and 271 cm in the microhigh and microlow, respectively. Gilgai topography is accentuated in the Lake Charles profiles and

Table 2.6 Lake Charles ML Pedon- Characteristic Summary

Horizon	Depth	Slickensides	CO3 nodules	Roots/pores & redox	Structure	Matrix
A1	0-10	Few faint pressure surfaces	----	Common very fine and fine roots; common fine interstitial pores	Moderate fine and medium SBK parting to moderate medium granular	Black (2.5Y2/1) clay
A2	10-29	Common distinct pressure surfaces	---	Common fine and medium roots; common fine tubular pores	Moderate fine and medium SBK	Black (2.5Y2/1) clay
Bss1	29-61	Common distinct intersecting slickensides (50-65°)	---	Common fine roots; common fine tubular pores	Weak medium wedge-shaped structure parting to moderate medium SBK	Black (2.5Y2/1) clay
Bss2	61-103	Many prominent intersecting slickensides (30-40°)	---	Common fine roots; common fine tubular pores	Strong medium and coarse wedge shaped structure parting to moderate medium ABK	Very dark gray (2.5Y3/1) clay; very few crayfish krotovina filled with yellowish red (5YR5/6) and very dark gray clay (2.5Y3/1)
Bss3	103-135	Many prominent intersecting slickensides (45-60°)	---	Common fine roots; few fine black Fe-Mn nodules	Strong medium and coarse wedge-shaped structure parting to moderate medium ABK	Very dark gray (2.5Y3/1) clay; very few crayfish krotovina filled with yellowish red (5YR5/6) and very dark gray clay (2.5Y3/1); few fine black (10YR2/1) Fe-Mn nodules

Table 2.6 Lake Charles ML Pedon- Characteristic Summary (continued)

Horizon	Depth	Slickensides	CO3 nodules	Roots/pores & redox	Structure	Matrix
Bkss1	135-158	Common prominent intersecting slickensides (35-45°)	1% fine uncoated nodules; 2% nodules coated with strong brown (7.5YR5/6)Fe	Common very fine and fine roots;	Moderate medium and coarse wedge-shaped structure parting to moderate medium and coarse ABK	Dark gray (2.5Y4/1) clay; very few crayfish krotovina filled with yellowish red (5YR5/6) and very dark gray (2.5Y3/1)clay
Bkss2	158-175	Common prominent intersecting slickensides (30-45°)	3% fine and medium nodules coated with brown (10YR4/3) iron; 2% uncoated nodules	Common very fine and fine roots	Weak coarse wedge-shaped structure partying to moderate medium and coarse ABK	60% gray (2.5Y5/1),; 20% light olive brown (2.5Y5/3); 20% light yellowish brown (2.5Y6/3) clay;
Bkss3	175-193	Common distinct intersecting slickensides (35-40°)	Few fine nodules	Common very fine and fine roots; 1% greenish gray (5GY7/1)Fe-depletions on slickenside surface	Moderate coarse prismatic structure parting to moderate medium and coarse SBK	yellowish red (5YR5/6) clay; 5 % crayfish krotovinas filled with yellowish red (5YR5/6) and very dark gray (10YR3/1) clay

Table 2.6 Lake Charles ML Pedon- Characteristic Summary (continued)

Horizon	Depth	Slickensides	CO3 nodules	Roots/pores & redox	Structure	Matrix
B'ss1	193-216	Common distinct dark gray (10YR4/1) intersecting slickensides (30-35°)	Few fine rounded concretions coated with yellow (10YR7/8) iron	7% fine and medium prominent light greenish gray (5GY7/1) iron depletions on surfaces of slickensides	Weak, coarse wedge-shaped structure parting to weak, medium and coarse SBK	yellowish red (5YR5/6)
B'ss2	216-240	Common prominent intersecting slickensides (25-35°)	---	Very few very fine roots between peds; 10% fine prominent light greenish gray (10GY 7/1, 8/1) iron depletions on slickenside surfaces	Moderate coarse wedge-shaped structure parting to moderate medium and coarse SBK	yellowish red (5YR4/6)
B'ss3	240-272	Few faint intersecting slickensides (15-25°)	---	Very few very fine roots between peds; 4% fine prominent light olive gray(5Y6/2) iron depletions along root traces, in interiors of peds, and on slickenside surfaces; few fine and medium black (10YR2/1) Fe-Mn masses on root traces	Weak coarse ABK parting to weak medium ABK	yellowish red (5YR5/6)
B'ss4	272-300	Few prominent intersecting slickensides (15-25°)	---	Very few very fine roots between peds; 6% fine and medium light gray (5Y7/2) iron depletions on root traces, in ped interiors, and on slickenside surfaces	---	yellowish red (5YR5/6)

A

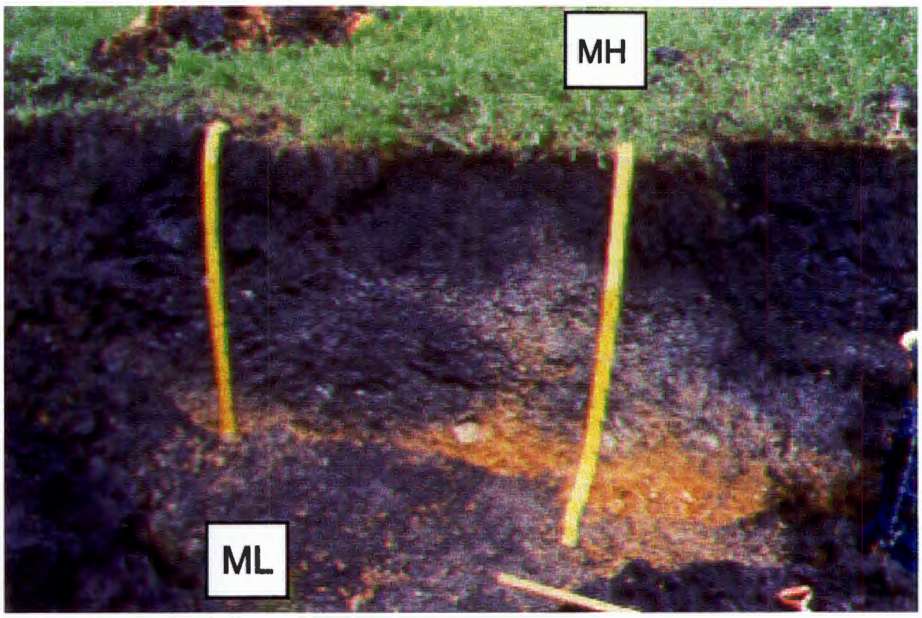

Figure 2.17 A) Lake Charles Pedon macromorphology. The darker areas are indentified as microlows (ML). The bright red-brown parent material is rising upward to the soil surface in the microhighs. Tape length is 2 m to the base of the exposed parent material.

B

C

Figure 2.17 (continued) Lake Charles macromorphology. B) Wedge-shaped aggregate formed by the intersection of slickenside surfaces; C) Dark soil matrix mixed with red, calcareous parent material. Drab areas represent redox deptions. Dark black segregations are Fe-Mn nodules. B and C are hand samples from the microhigh at ~250 cm and ~190cm depth, respectively. The bar scale is in cm.

is indicated by 30 to 50 cm relief and spacing between microhighs that ranges from 3 to 4 m. Sharp mukkara with chimney tongues may be associated with the shallow occurrence of the Bk horizon in the MH (28-70 cm). MH and ML profile distinctness is indicated by color, structure, carbonate accumulation, and crayfish krotovina.

Coloration of the ML profile is predominantly dark gray (2.5Y 3-4/1) to black (2.5Y 2/1) to the Bkss1 horizon, is mottled with gray and yellowish red (5YR 5/6) to light yellowish brown (2.5Y 5/3) through Bkss3, and incorporates yellowish red (5YR 5/6) parent material into the B'ss1 and B'ss2 horizons. Bioturbation of the mottled horizons is indicated by the incorporation of parent material in crayfish krotovina. The MH also exhibits variations in color with depth. Very dark gray (10YR 3/1) to dark grayish brown (2.5Y 4/2) color occurs from the surface to the Bkss3 horizon. The Bkss4 and Bkss5 horizons are highly variable, including dark gray (10YR 4/1), olive brown (2.5Y 4/3) and yellowish brown (10YR 5/6) colors within the matrix. Evidence for proximity to parent material is suggested by a color change (Bss1) to strong brown (7.5 YR 4/6) and yellowish red (5YR 4/6). In addition to bioturbation, structural aggregates and associated matrix hydrology may also affect matrix coloration.

Structural development (Figure 2.17B-C) within the MH and ML is similar, but may be slightly better in the MH at depth. The surface horizons (A1 to Bss1) of the ML are moderate, fine and medium subangular blocky. Aggregate size increases with depth from moderate, medium angular blocky (Bss2 and Bss3) to medium and coarse angular blocky (Bkss1 and Bkss2). B'ss1 and B'ss2 have weak to moderate, medium and coarse subangular blocky structure. The MH exhibits a similar trend in development from granular to weak, medium subangular blocky in surface horizons and transitioning to moderate fine and medium angular blocky (Bkss1 to Bkss3). Strong, medium and coarse angular blocky structure (Bkss4 and Bkss5) is indicated by very defined, sharp ped surface intersections. Below these horizons there is a return to moderate medium and coarse angular blocky structure.

Carbonate morphology and occurrence differs significantly between the MH and ML profiles. The ML profile has a lesser abundance of nodules, typically fine and to medium-sized, most of which are coated with strong brown (7.5YR 5/6) and brown (10YR 4/3) iron oxides. Carbonate nodules are much more abundant in the MH, ranging in size from fine to coarse. Nodule morphology (color) varies from brownish (10YR 6/2) in darker surface horizons to white (10YR 8/1) through most of the MH profile. Carbonate nodules appear to concentrate along the contact between Bkss5 and Bss1 horizons. The concentration of carbonate may be a result of soil hydrologic conditions similar to redoximorphic depletions and concentrations.

Iron depletions (5GY 6-7/1), in both the MH and ML profiles, occur predominantly along slickenside surfaces and root pore linings. Drab (reduced?) material is also associated with infill of the crayfish krotovina. Fine, black dendritic Fe-Mn masses (Figure 2.17C) also occur along slickenside surfaces within the Bss2 horizon in the MH; fine, black nodules are present within the Bss3 of the ML.

Micromorphology

Fe-Mn concentrations are present through much of the MH and ML profiles. A significant proportion of the nodules (Fe-Mn) present within the Lake Charles are concentrically laminated (Figure 2.18C-D). These types of nodules suggest multiple generations of formation and typically have matrix carbonate and detrital quartz grains engulfed within the lamina. The carbonate may serve as an area of dissolution, when hydrologic conditions change, resulting in the nodules delaminating. The red parent material (MH) is conducive for identification of redoximorphic depletions that would otherwise be masked by the dark matrix colors of the ML. The Bss1 and Bss2 horizons (MH) have redox depletions and enrichments within the red parent material, along fractures and slickenside surfaces.

The matrix of the Lake Charles Pedon differs slightly from the pedons discussed to this point. Micropeds and inclusion of dark soil matrix "balls" or pedorelicts (Figure 2.18F) are present in horizons of both the MH and ML. Haploidization or mixing of the dark soil matrix (Figure 2.18E) with the red parent material occurs within the full profile of the MH and is more common below the Bkss2 horizon (ML). Detrital quartz, twinned and untwinned feldspars and cubic sulphate crystals are grains incorporated into the calcareous matrix of both profiles.

Carbonate and gypsiferous(?) phases (Figure 2.18A-B) are found in the MH and ML profiles, with carbonate nodules and segregations being much more abundant. Bss3 (ML), for example, contains recrystallized carbonate nodules

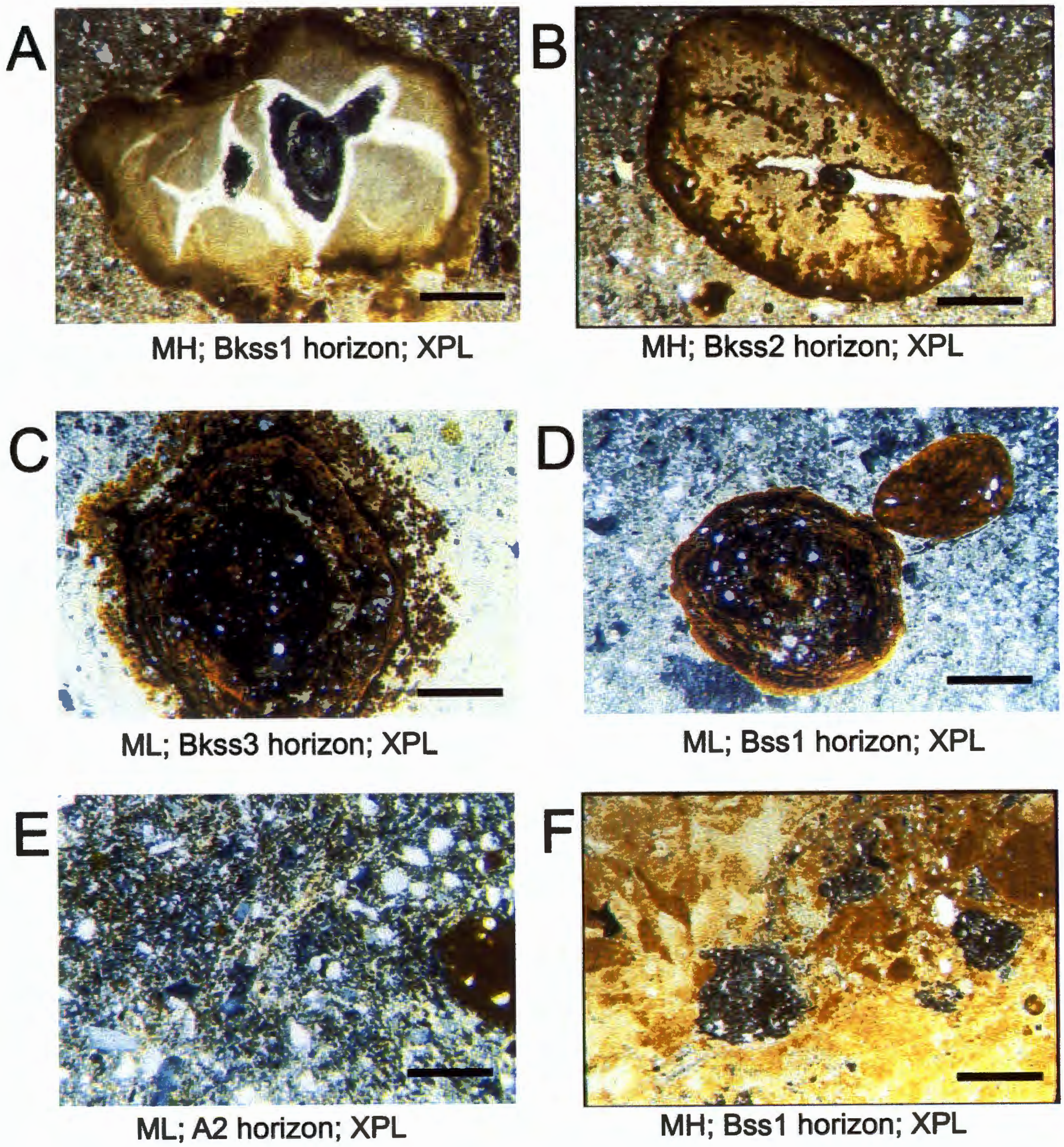

Figure 2.18 Lake Charles Pedon photomicrographs. A) Carbonate nodule with coarse calcite filling septarian voids; B) Carbonate nodule with Mn dendrites Fe-Mn concentrations at nodule perimeter; C) Fe-Mn nodule with both concentric and dendritic morphologies; D) Concentrically laminated Fe-Mn nodule with engulfed detrital quartz; E) Sepic plasmic clay fabric indicated by birefringent (yellow) clay: F) Redox depletions and dark soil matrix within red, calcareous alluvium. Bar scale is 1 mm. (XPL=crossed polarized light; PPL=plane polarized light).

with some smaller nodules appearing to have spalled off from larger ones. Sparry calcite fills septarian voids, when present, within the microspar nodules. The MH profile contains a powder carbonate phase in which segregations have diffuse boundaries with the adjacent matrix. Some nodules have been undergoing dissolution/precipitation as evidenced by a boundary rind around the nodule. Fe-Mn impregnation of some carbonate nodules have formed from variation of the hydrologic conditions in both the MH and ML profiles.

Bulk chemistry

The Lake Charles ML profile exhibits similar trends in translocation as the Burleson profile over a similar depth range (~200cm). Sampling for this profile is to a depth of 250+ cm, with mass balance calculations based on parent material at 270 cm.

Calcification and salinization (Figure 2.19A) have depleted to nearly 100%, with the latter being more erratic. Below 150 cm, the translocation indices become significantly more variable and approach parent material compositions at depth. The oxidation index shows a 50% reduction and exchangeable bases index reflects 0 to 300% increase relative to the parent material composition to 150 cm.

Base cation translocation (Figure 2.19B) trends are similar, as indicated by conservative translocation to 150 cm, which becomes more erratic to a depth of 270 cm. Strontium and K have maximum losses of approximately 50%, as contrasted with the maximum loss of Na and Ca to nearly 100% to 150 cm

A

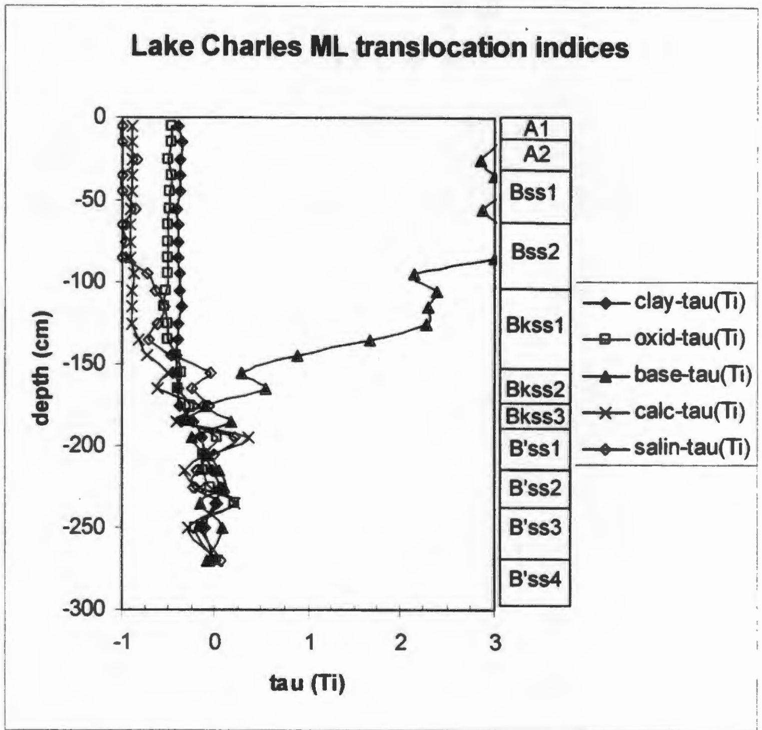

B

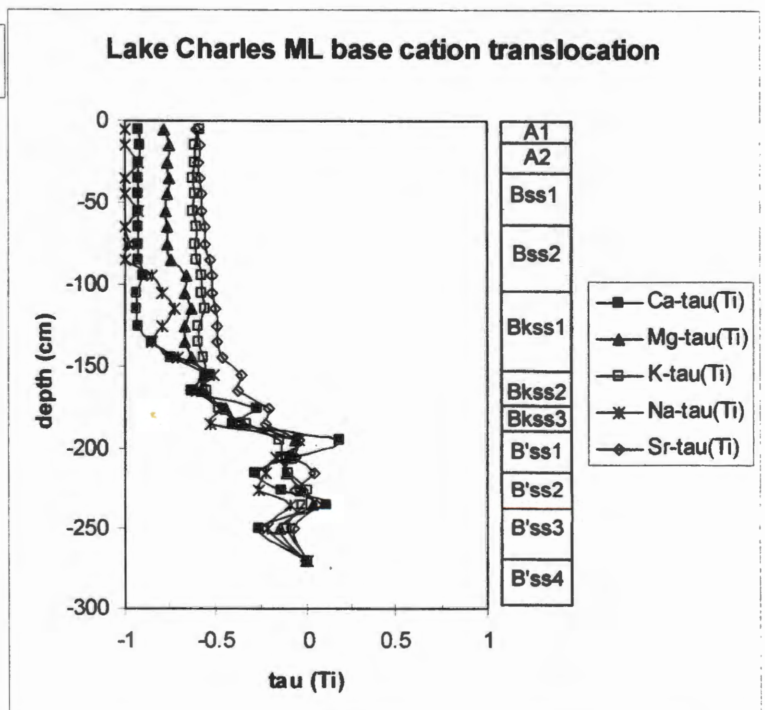

Figure 2.19 Lake Charles ML profile molecular ratios and element translocations calculated using Ti as immobile index element: A) clay (clayeyness), oxid (oxidation), base (base loss), calc (calcification), and salin (salinization) are translocation indices, and B) translocation of base cations within soil profile.

C

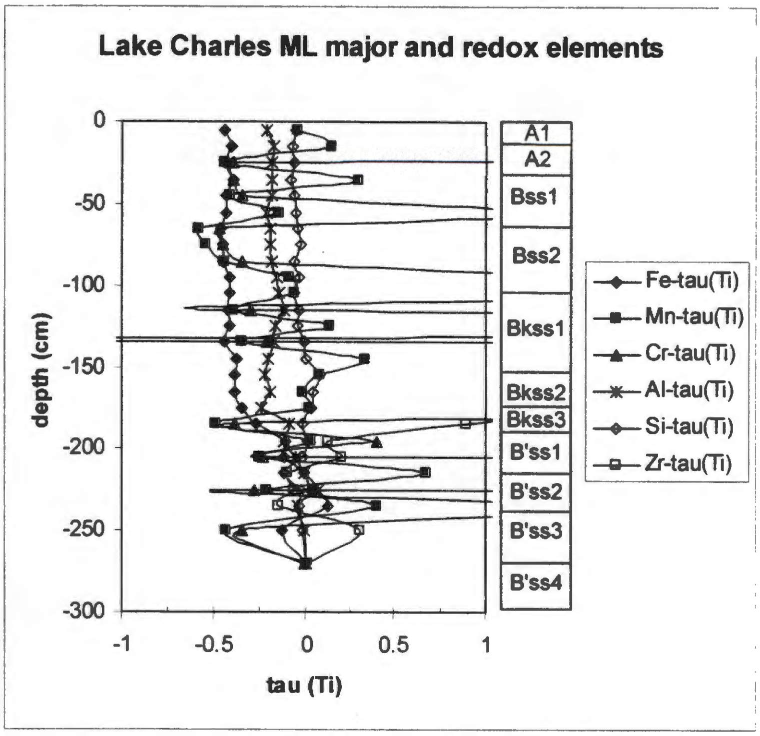

D

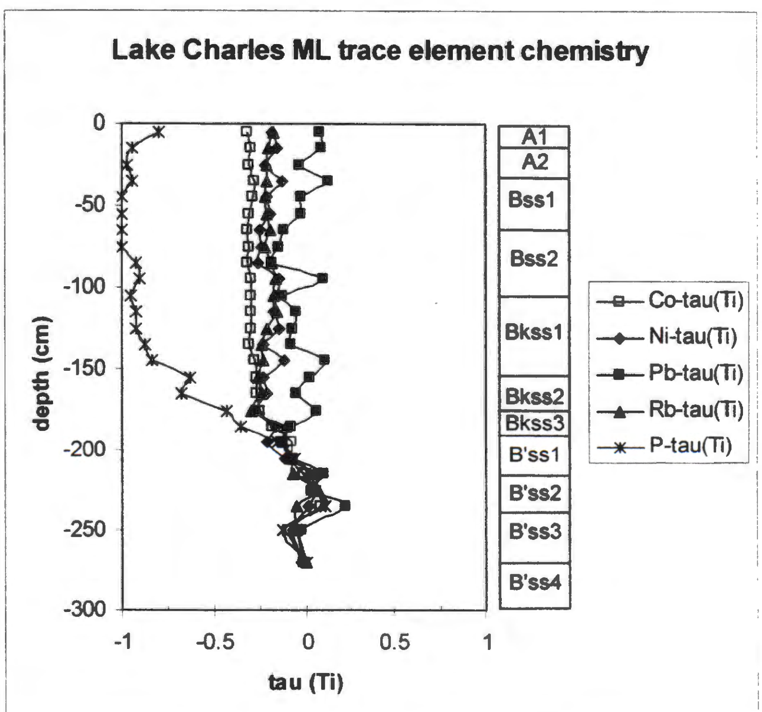

Figure 2.19 (continued) Lake Charles ML profile element translocations calculated using Ti as immobile index element: C) major and redox element translocation trends, and D) trace element trends within the soil profile.

(Bkss1). Magnesium is intermediate between the Sr-K and Ca-Na trendlines with 75% loss. Variation below 150cm may be a result of differential translocation associated with multiple sets of slickenside surfaces. Mn, Zr and Cr (Figure 2.19C) are very erratic throughout the profile. Whereas Zr and Cr may be a relict of selection of the immobile oxide (TiO_2), this is not as conclusive for Mn. Mn translocation is strongly a function of redoximorphic conditions and the tendency for Mn oxides to complex on clay mineral surfaces. Interestingly, Cr has inflections that correlate well with those of Mn translocation, indicating that Cr may be mobile under similar conditions. Iron, Al and Si have less variable trends and therefore suggest the less sporadic mobility and concentration of these constituents. Loss of Fe in the profile is most pronounced above 200 cm and reaches approximately 50%. The trend in iron loss follows Al (clay fraction) translocation, but Al has undergone approximately 25% loss. Silica is conserved through the profile and maintains compositions very similar to the parent material.

Trace element chemistry (Figure 2.19D) of the Lake Charles ML is divided into two major populations, those with minor to moderate translocation and P, which has significant loss of ~100% to 150cm. Cobalt is fairly consistent throughout the profile with a loss of approximately 25%, with an inflection around 170cm approaching parent material content. Nickel and Pb are variable within the profile and have very similar trends with depth, but occurring at slightly different scales, -10 to 25% and -10 to -5%, respectively. Translocation trends of Rb are variable, with very minimal fluctuations ranging from –10 to –20%.

The bulk chemistry trends of the Lake Charles suggest that pedogenesis has occurred to a depth of significantly more than 150 cm. The similarity of trace element analysis (no major fluctuations) indicates that if polygenesis were likely, then the source area of the sediment had not changed significantly.

Particle size analysis and clay mineralogy

Montmorillonite is the primary mineral component for both the ML and MH pedons. The Bkss3 and B'ss2 horizons have a decrease in the relative abundance of montmorillonite, which is likely associated with a major increase in the weight percent of calcite within those particular horizons. Kaolinite, quartz and montmorillonite-chlorite (Bss1 and Bss2) are secondary in the matrix composition. Mica compositions are consistent within the profile and are recognized as tertiary level in relative abundance. Depths of 216-240 cm (ML) and 144-176 cm (MH) have a mixed clay general descriptive mineralogy.

Weight percent clay (Figure2.20) has a generally decreasing trend upward in the MH profile and averages~55%, with a maximum of 72% at 210-240 cm depth. The silt size fraction exhibits an inverse trend with an increase upward in the profile. Sand content increases upward in the profile, but has a major inflection between Bkss4 and Bkss5; this inflection point is reflected as a 7.5% increase between the two horizons. The ML profile has a similar inflection point, a 5.5% increase, between the Bkss2 and Bkss3 horizons at 158-175 cm and 175-193 cm, respectively. Clay content reflects a decrease in composition, of

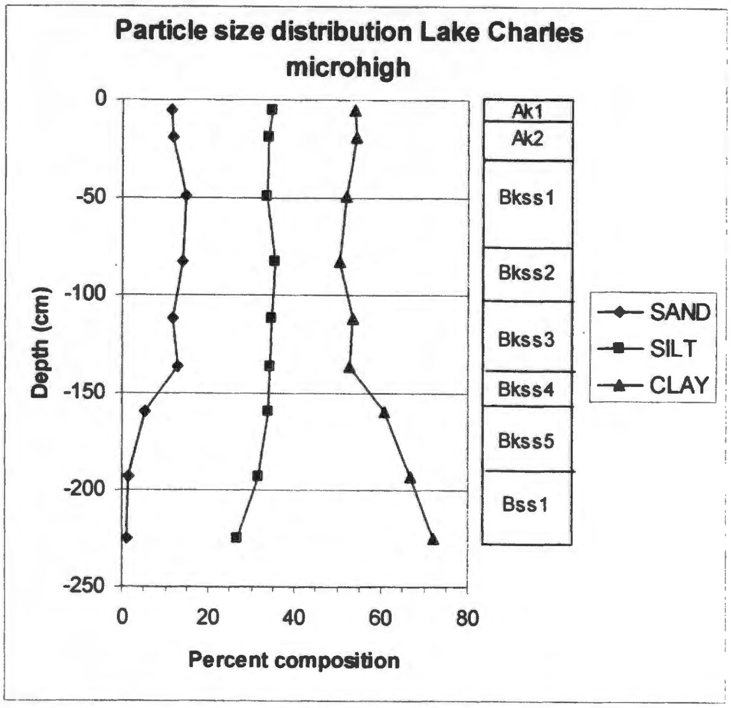

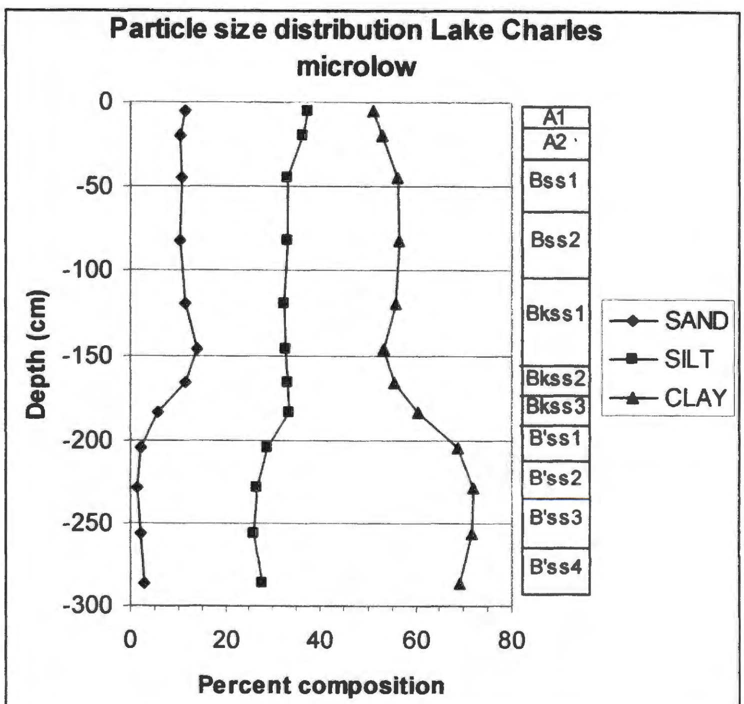

Figure 2.20 Lake Charles MH and ML particle size distribution. There is a decrease in clay content upward in the profile with an abrupt transition at 150cm. This change is also reflected in the sand and silt fractions.

similar magnitude (~5%), at the same depth as the sand inflection point. This may be associated with a lithologic break or may be evidence of polygenesis.

Discussion: Summary of chronosequence trends

The Ships (~400yrs), Pledger (3,500yrs), Burleson (~18,000yrs), and Lake Charles Series (35,000yrs) represent a chronosequence of pedons formed on stable landscape surfaces from sediment derived from the Brazos River drainage basin. The results of this study should help determine features that are characteristic on each terrace that correlate with soil age. Variations in macromorphology, micromorphology and bulk chemistry with time will be instrumental in attempting to decipher directions and rates of pedogenesis. Direction of pedogenesis, in this case, refers to features that are present in the younger, less well-developed soils and are either better-developed or obliterated in the older profiles. Rates of pedogenesis refer to how quickly the time-dependent features appear or are incorporated into the soil profile. From this point forward, profile age is defined as the length of time that a particular surface has been stable and undergoing pedogenic processes. This is roughly correlative to the terrace age, but for ease of discussion this terminology will be used.

The nature of this study is mostly descriptive, rather than quantitative, and limits estimations and interpolation of profile age. Soil chronofunctions are available (Vitousek et al., 1997; Chadwick et al., 1999; Chorover et al., 1999; Ciolkzi and Bilzi, 1977; Harden, 1982; Busacca, 1987), but each are for other soil orders. Chronosequence studies on the Vertisol soil order have been limited because of the formerly popular interpretation (Buol et al., 1989) of pedogenesis that implies pedoturbation and wholesale self-mulching. This process would result in removal of diagnostic horizonation. Most chronofunction studies rely on horizon distinctiveness and other properties that do not fit well with vertic characteristics. Macromorphologic features such as slickensides, angular blocky structure and gilgai are important indicators of the amount of development of a particular profile. As such, the current versions of chronofunctions are not applicable and must be adapted to this soil type. Future work may attempt to address this, however, with this qualitative study there are several characteristics that may be instrumental in the development of quantitative studies. There are three main areas, namely, macromorphology, micromorphology and bulk chemistry, where qualitative time-dependent variations can be determined.

Macromorphology

Macromorphology (Table 2.7) is the primary means to identify Vertisols and vertic intergrades. The Ships profile represents the youngest, least-developed end-member and the Lake Charles is the oldest, most developed end-member. The difference between stages of development between the Burleson and the Lake Charles are less clear than the other stages, and may represent a decline in the rate of pedogenesis (terminal stage?) after the profile reaches a certain age or maturity level. Chadwick and Chorover (2001) described this phenomenon as a pedogenic threshold where particular characteristics do not

Table 2.7 Comparison of Chronosequence Pedon Microlows

Characteristics	Ships	Pledger	Burleson	Lake Charles
Parent Material	bedded, brown to red calcareous silty clay alluvium	bedded, brown to red calcareous silty clay alluvium	red calcareous silty clay alluvium	red calcareous silty clay alluvium
Depth to Parent	130-180 cm	220-265 cm	250+ cm	270 cm
Depth to top of Bk	44-62 cm	33-55 (MH);133-171 cm	14-34 (MH); 39-65 cm	28-70 (MH);135-158cm
Depth of pedogenesis	110-131cm	179-182(MH); 182-220(ML)	190-250+cm	176-212cm
Slickenside dev.	abundant, closely-spaced (66cm)	abundant, closely spaced (124MH;138ML)	abundant, closely-spaced (156MH;161ML)	abundant, closely-spaced (212MH;271ML)
Gilgai topography	no surface expression of gilgai	moderate relief (10 cm); spacing 2-3m	moderate relief (10-20cm) due to plowing; spacing 4-6m	high relief (30-50cm); spacing 3-4m????
Mukkara	no mukkara developed	chimney tongues do not penetrate to surface in all MH	sharp mukkara with chimney tongues	sharp mukkara with chimney tongues
Sepic-plasmic fabrics	44-62 cm	44-88 cm	39-65 cm	29-61 cm
Fe/Mn masses	few masses in Ck1	common in ML	abundant in ML	abundant
Redox	rare to common in subsoil (Ck1) along pores and nodules	common in subsoil along ped surfaces, pores and fractures	abundant in subsoil, along slickensides, fractures and roots	abundant in subsoil, along slickensides, fractures and roots
Carbonate morphology	powder CO3 layer following master slickenside and sedimentary layering; nodules typically contain septarian voids; nodule interior similar to matrix	variable nodule morphology; multiple phases of ped. CO3 formation?; some contain dendritic Mn; powder CO3 less common	powder and nodule morphology along contact between MH/ML and within MH; limited occurrence in ML	variable nodule morphology (yellow, white, and brownish-gray) and size (fine to medium)

Table 2.7 (continued) Comparison of Chronosequence Pedon Microlows

Characteristics	Ships	Pledger	Burleson	Lake Charles
Calcification index	minor loss (10-15%) to 150cm; gain (45%) at 160cm	major loss (80%) to 120cm; major gain (75%) at 150cm	major loss (85%) to 200cm	major loss (90%) to 140cm; variable gain/loss (25%) to 70cm
Base loss index	base conservation through profile; minor gain (10%) at 60-70cm	major loss (90%) to 120cm; major gain (70%) at 150cm	major loss (90%) throughout profile	major loss (90%) to 150cm; variable gain/loss (25%) to 280cm
Oxidation	minor (5%) loss to 170cm	moderate loss (30%) to 120cm; moderate gain (25%) at 150cm	major loss through profile (50%)	major losses (50%) to 150cm; moderate losses (20-30%) to 240cm
Salinization	minor enrichment (10%) to 70cm; variable loss/gain to 180cm	major loss (50%) to 120cm; major gain (50%) at 150cm	Major loss (50-95%) loss to 200cm	Major loss (50-100%) to 150cm; variable loss (10-20%) to 270cm

continue to development after some amount of time. Several characteristics are particularly useful for estimating profile age, which include: occurrence of bedded alluvium, depth of pedogenesis, thickness and development of slickensided horizons, and expression of gilgai topography. Secondary features include redoximorphic and carbonate concentrations.

Original bedded alluvium should represent the most juvenile, end-member prior to soil formation. This assumes that there is a very short duration between deposition of alluvium (i.e., seasonal or annual) thereby limiting any intermediary pedogenesis. The profile age, however, includes deposition and/or any stages of pedogenesis prior to the formation and development of the entire soil profile. The Ships Pedon represents primary or stage one of soil development. This is indicated by the bedding structure in the basal portion of the profile and preservation of bedded, calcareous alluvium. The contact between horizons above and the parent material is relatively distinct (130-180 cm). The Pledger Pedon contains brown to red calcareous silty clay alluvium very similar in appearance to the Ships at a depth of 220 to 265 cm. In addition to crack infillings, at depth within the Pledger ML profile there are redoximorphic features that occur on the ped surfaces. This 3,500 yr Pedon represents the intermediate or stage 2 of development. Both the Burleson and Lake Charles Pedons are underlain by homogenized, calcareous red alluvium at depths of 250 and 270 cm, respectively. The bedded alluvium has been pedogenically modified to the extent that evidence of the original bedding is no longer visible. An age distinction between the Lake Charles and the Burleson cannot be made based on this criterion but this does allow separation between the secondary and tertiary levels of pedogenic development of Vertisols.

Depth of advancement of pedogenesis downward in the profile is indicated by the incorporation of lithorelicts into superposed horizons or pedorelicts transported downward from horizons above. Field recognition of advancement of pedogenesis also includes disruption of the alluvium by vertical cracks, infill of cracks with sediment from horizons above, and bioturbation. The Ships Pedon has a very distinct contact with overlying horizons, but does have a zone of disruption at depth range of 110-131cm. The Pledger, Burleson and Lake Charles Pedons each have experienced deeper pedogenesis typically ranging from 180 to 250cm. Homogenization (Burleson and Lake Charles) is not included in the estimation of depth of pedogenesis, because the process responsible is not clearly understood. The advancement of pedogenesis, particularly in soils with high shrink-swell potential, may be a function of physical development of wedge-shaped aggregates, slickensides and degree of occurrence of structural peds (i.e., angular blocky, subangular blocky and granular). Ships slickensides have a very low frequency and amplitude with slickensided horizons with a total thickness of 66cm. Angular blocky structure occurs throughout the profile thickness, except where bedding structure (BCk) begins, or at the soil surface, where subangular blocky structure is common. Thickness of horizons containing slickensides within the Pledger ML profile is approximately 138 cm and is associated with an increase in wedge-shaped aggregates occurring within the profile. Slickenside development appears to be a strong indicator of soil maturity and is of importance for delineating the advanced stages of Vertisol development. The Burleson ML profile (mature or stage 3) has abundant closely-spaced slickensides that span 161cm, whereas the Lake Charles is 271cm (old age or stage 4). Slickenside development and continuity increases with profile age, which supports a similar trend in pedogenesis. Gilgai or microtopography is likely a function of slickenside continuity and thickness of occurrence. The Ships Pedon contains no surficial expression of gilgai and maintains a very restricted range of slickenside development. These features result in the inability to form distinct chimneys or MH/ML profiles. The remaining pedons do exhibit microtopography and may be distinguished by the spacing and relief (assuming undisturbed surfaces). The Pledger profiles have 10 cm relief and spacing of 2 to 3m. Relief of the Burleson profiles is 10 to 20 cm (due to plowing); spacing reaches 4-6 m. Lake Charles relief is significantly higher than that of the other profiles (30-50 cm). Although the correlation between pedogenic processes and gilgai formation is still debated, there does appear to be a relationship between the extent of development and soil age.

The depth to Bk horizon is used in paleoclimate estimations and may be influenced by increased time of soil formation. This does not appear to be the case for this particular chronosequence. The Burleson and the Ships profiles have the depth to the top of Bk at 39 to 65 cm and 44 to 62 cm, respectively. Similarly, the depth to the Bk in the Lake Charles is 135 to 158 cm and the Pledger is 133 to 171 cm. This trend in depth to Bk is correlative to modern day precipitation regimes, thereby minimizing the affect of historic climate change on translocation in the profile. If, for example, the affect of climate change remained a player through the entire history of the profile (cumulative translocation), then the Burleson profile should be intermediate between the Lake Charles and the Pledger Pedons.

Micromorphology

Micromorphology across the chronosequence is not as straight forward as the macromorphology. Most of the features (Table 2.8) recognized in the micro-scale are derived from the macro-scale features (i.e., slickenfibers and pressure cutans from slickensides). The Ships pedon has an abundance of illuviated clay lining (pores and on ped faces), particularly in the lower portions of the profiles; with advanced stages of pedogenesis, these would be disrupted and dominated by slickenside orientation of clay fabrics (sepic-plasmic and lattice-sepic). Wedge-shaped peds outlined with clay skins are the best diagnostic feature for identification of the extent of development of slickenside surfaces from shrink-swell processes.

Redoximorphic features on ped faces and lithorelicts suggest that advancement of pedogenesis has occurred to the BCk (Ships) horizon. These features occur in much older, more mature profiles, but are typically located along slickenside surfaces, pore linings and within ped interiors. Fe-Mn concentrations occur in a variety of morphologies (i.e., concentrically laminated, dendritic, and weakly-cemented concentrations). These morphologies, however,

Micromorphologic feature	Ships (~400yrs)	Pledger (~3,500yrs)	Burleson (~18,000yrs)	Lake Charles (~35,000yrs)
Pedogenic CO_3				
Matrix (disseminated)	x x xx	xxx	xx	x
Nodules	x	xxx	xxx	xxx
w/ septarian voids	x	xx	xx	x
Redox phases				
Fe-Mn nodules	--	xx	xx	xxx
Segregations	x	xx	xxx	xxx
Dendritic	x	xx	x	xx
Conc. lamina	x	x	x	xx
Depletions	x	xx	xx	xx
Matrix fabric				
Sepic-plasmic	x	xx	xxx	xxx
Lattice sepic	x	x	xx	xx
Slickenfibers	x	xx	xxx	xxx
Burrows	x	x	x	x
Bedded alluvium	xxx	xx	---	---
Clay-lined fabric	xxx	xxx	x	x

Table 2.8 Micromorphologic trends across the chronosequence. The number of x's corresponds to the relative abundance or number of horizons containing the feature.

do not correlate well with profile age. Carbonate nodules and segregations also do not show a clear association with age. Finely disseminated carbonate is abundant throughout portions of each of the profiles. Nodule morphologies are variable (i.e., recrystallized nodules with septarian voids; coarsely crystalline with diffuse boundaries; and dendritic Mn-impregnated) and may vary based on very localized variations in soil moisture regimes (related to gilgai development).

Sedimentary bedding is by far the most definitive indicator for primary or secondary stages of soil development. In thin section, bedding is indicated by slight variations in grains size from clay to silt. Older and better-developed pedons (Burleson and Lake Charles), as mentioned previously, would no longer exhibit this characteristic. The Ships and Pledger profiles have very distinct variations in grain size and may exhibit micro-scale sedimentary structures (i.e., ripples, soft-sediment deformation, and loading structures).

The occurrence of carbonate nodules, particularly in the Ships profile, represents a soil environment conducive to accumulation of carbonate. All of these soils had finely disseminated carbonate, with a significant abundance in the red, clayey alluvium and throughout the Ships profile. The Ships profile also contained 2-5mm carbonate nodules, with some containing septarian voids. Carbonate precipitation is thought to occur over a long period of time, longer than the surface and sediment accumulation of Ships profile. As such, methods of deciphering primary pedogenic or recycled carbonate are discussed in Appendix E (Stable Isotopes). Older soils adjacent to the Brazos River and Permian red bed paleosols may have provided eroded and subsequently recycled nodules, in addition to calcareous matrix.

Bulk Chemistry

Trends in bulk chemistry (Table 2.9) are particularly useful in delineating soil age. Translocation indices (Figures 2.5, 2.9, 2.13 and 2.17) are a first-level indicator of pedogenic development and will be discussed as a preliminary tool to decipher stages of pedogenesis. Salinization, although highly variable with depth within a profile, has experienced more translocation in the older profiles. The Ships profile has values that are +/- <20%, whereas the Lake Charles profile is depleted in Na to 80-90% in the upper portion of the profile. Oxidation is indicative of profile age; the Ships pedon shows limited variation from parent material composition versus 50% loss for both the Burleson and Lake Charles profiles, suggesting either: 1) Fe and Al translocation reaches terminal pedogenesis, to some degree; or 2) rates of Fe and Al mobility decrease over time, possibly as a result of limited liberation from other mineral constituents. Calcification indices are less effective in soils with calcareous parent material, however, there is still a distinction between the Ships (+/- 25%) and the other three profiles (90% reduction in the calcification index.). Ships, Burleson and Lake Charles have exchangeable bases that are consistent across the chronosequence, with increasing losses with soil age. The Pledger profile represents an anomaly in which there is a 150% increase in the upper 120cm of

Table 2.9 Comparison of Chronosequence Pedon Microlows

Characteristics	Ships	Pledger	Burleson (Robinson)	Lake Charles
Calcification index	minor loss (10-15%) to 150cm; gain (45%) at 160cm	major loss (80%) to 120cm; major gain (75%) at 150cm	major loss (85%) to 200cm	major loss (90%) to 140cm; variable gain/loss (25%) to 70cm
Base loss index	base conservation through profile; minor gain (10%) at 60-70cm	major loss (90%) to 120cm; major gain (70%) at 150cm	major loss (90%) throughout profile	major loss (90%) to 150cm; variable gain/loss (25%) to 280cm
Oxidation	minor (5%) loss to 170cm	moderate loss (30%) to 120cm; moderate gain (25%) at 150cm	major loss through profile (50%)	major losses (50%) to 150cm; moderate losses (20-30%) to 240cm
Salinization	minor enrichment (10%) to 70cm; variable loss/gain to 180cm	major loss (50%) to 120cm; major gain (50%) at 150cm	Major loss (50-95%) loss to 200cm	Major loss (50-100%) to 150cm; variable loss (10-20%) to 270cm
Strain (Ti immobility)	<5% dilation to 60cm; 10% collapse to 100cm; 2% dilation/collapse to 180cm	10-35% collapse to 250cm	25% dilation to 120cm; very weak collapse (5%) to 140-170cm	25% collapse to 200 cm; very weak dilation at 200-240cm
Translocations				
Major element (Ti)				
Na2O	highly variable moderate loss (5-20%) through profile; minor gains (5-10%) at 140 and 160cm	major losses (50-75%) to 130cm; minor loss (5-25%) to 190-250cm; peak gain (25%) at 155cm	major losses (25-50%) to 180cm	major losses (50-100%) to 180cm
K2O	minor loss(5%) from 40-120cm; minor gains (<5%) to 170cm	minor loss (5-15%) to 150cm; minor (<5%) to 250cm	minor losses (5-10%) to 180cm	major losses (60%) to 200cm

Table 2.9 (continued) Comparison of Chronosequence Pedon Microlows

Characteristics	Ships	Pledger	Burleson (Robinson)	Lake Charles
Al_2O_3	highly variable, minor losses (5-8%) to 50cm; minor gains (2-8%) to 150cm	moderate gains (15-25%) to 150cm; minor losses (<5%) to 250cm	minor gains (5-10%) to 140cm	moderate losses (20-25%) to 180cm
SiO_2	moderate gains (2-30%) to 180cm	moderate losses (25%) to 150cm; minor losses (5-10%) to 250cm	minor losses (5-10%) to 180cm	weak losses (5-10%) to 160cm; weak gains at 160-180 cm
CaO	moderate losses (5-25%) to 170cm; major peak gain (35%) at 160cm	major losses (80-90%) to 120cm; major gains (50%) at 150cm; minor gains (5-10%) to 250cm	major losses (25-75%) to 160 cm	major losses (80%) to 200cm; weak gains (10-25%) at 200-240cm
MgO	moderate losses (5-20%) to 120cm; minor gains (5%) to 180cm	moderate losses (25-35%) to 140cm; minor gains (5-10%) to 240cm	moderate losses (10-25%) to 160cm	major losses (75%) to 200cm; weak gains (5-10%) at 200-240cm
Fe_2O_3	moderate losses (5-25%) to 100cm; minor gains (5-10%) from 110-180cm	conserved; minor (<5%) gains to 240cm	conserved; minor (<5%) losses to 160cm	major losses (40%) to 200cm
Minor/Trace element (Ti)				
MnO	moderate losses (5-20%) to 70cm and 110 to 120cm; minor gains (5-20%) 120-140cm	moderate gains (10-30%) to 140cm; minor loss (5%) to 240cm	major gains (25-50%) to 60cm and 140-180cm; minor losses (<10%) from 60-140cm	major losses (50%); moderate gains (25%) at 0-40cm, 130-160cm and 200-240cm

Table 2.9 (continued) Comparison of Chronosequence Pedon Microlows				
Characteristics	**Ships**	**Pledger**	**Burleson (Robinson)**	**Lake Charles**
P2O5	Conserved to depth; moderate gain of 25% in upper 30cm	Major loss (>50%) to 120 cm; sporadic gains/losses (~10%) to 300cm	Highly variable loss from (25-80%) to 200cm	major losses (50-100%) to 200cm; weak gains (5-15%) at 220-250cm
Sr	Minor loss (10-25%) to 120cm	Major losses (50%) to 100cm minor gains to conserved to 300 cm	Major loss (50-70%) to 200cm	major losses (50-60%) to 200cm, weak gains (5-10%) at 200-240cm
Zr	Major loss (20-70%) to 100cm and 180cm; variable to minor gain/loss 170	Moderate loss (~25%) to 250cm and major gains (>100%) to >300cm	Very major gains greater than (100%) to 200cm	very major gains (300%) to 200cm
Rb	minor loss (5-15%) to 120cm; minor gains (<5%) 120-180cm	moderate gains (25-35%) to 140cm; conserved to 250cm	moderate losses (5-25%) to 180cm	moderate losses (25%) to 180cm
Cr	Variable minor loss(<10%) to 180 cm	Highly variable with moderate losses (~25%) to very major gains (>100%)	Highly variable gains (0 to >100%) to 200cm	very major gains (50-500%) to 240cm, sporadic losses up to 50% through profile

Table 2.9 (continued) Comparison of Chronosequence Pedon Microlows				
Characteristics	**Ships**	**Pledger**	**Burleson (Robinson)**	**Lake Charles**
Pb	major gains (5-60%) to 170cm	minor loss (2-10%) from 50-250cm	moderate gains of (10-50%) in 10-60cm and 140-180cm; sporadic losses (10%) to 140cm	weak to moderate losses (5-15%), sporadic gains of 10% in upper 20cm
Ni	moderate losses (10-35%) to 100cm; minor gains at 70, 120 and 140cm	major gains (30-50%) to 130 cm; minor loss (<10%) to 200 cm	moderate gains of (15-40%) to 180cm	moderate losses (25%) to depth of 200cm, weak gains (5-10%) from 200-240cm
V	moderate loss (10-40%) to 150cm	major loss (70-85%) to 130 cm; variable gain (10-50%) to 250cm	highly variable losses from (25-85%) to 160cm	major losses (60-75%) to 160cm, moderate gains (25-50%) from 180-260cm
As	major gains (25-60%) to 170cm	moderate loss (10-40%) to 250cm	major losses (25-75%) to 60cm; minor losses (10%) to 180cm	major gains (50-100%) to 200cm, some weak losses (5-10%) from 200-250cm
Co	minor loss (5-15%) to 80cm; minor gains (5-10%) to 180cm	conserved throughout profile (+/-2%)	conserved throughout profile; with minor gains (5%) to 40cm	moderate losses (30%) to 200cm, weak gains (5-10%) from 240-250cm

Translocation trends across the chronosequence are divided into two major areas, increased depth or quantity of translocation. Sodium, K, Mg and Ca exhibit similar trends with soil age demonstrated by an increase in quantity and in depth of translocation. Aluminum and Si are typically functions of grain size. There does, however, appear to be a general decline in amount of gain as profile age increases. The Ships profile may have moderate gains, whereas the Lake Charles may have weak to minor losses. Many of the trace elements are highly variable and may be a function of complexation in the soil matrix. Redox-sensitive cations do not indicate a consistent trend with time and are more strongly associated with the soil moisture regime.

Conclusions

A chronosequence attempts to delineate soil features that form as a function of time. This study has indicated several important tools useful for determining profile maturity. Macromorphologic features, thickness of slickensided horizons, depth of pedogenesis, and gilgai development and topography, provide the most diagnostic morphologic means for determining profile age. Minor expression is associated with primary pedogenesis, whereas maximum expression is indicative advanced or mature stages of pedogenesis. Micromorphology provides valuable information for determining associated soil moisture regimes (e.g., Fe-Mn nodules, redoximorphic concentrations and depletions on ped surfaces and interiors, and carbonate nodule morphology), but is less helpful in delineating additional features beyond those associated with macromorphologic features (i.e., slickenfibers, wedge-shaped aggregates, sepic-plasmic fabrics and bedded alluvium). Micromorphology will provide better control on estimates of depth of pedogenesis based on features such as disruption of bedded alluvium, crack infiling by overlying sediments, and illuviated clays between peds.

Translocation indices and general cation/oxide trends with depth and between profiles of different ages are particularly helpful with delineating stages of pedogenesis. Generally, translocation increases with an increase in profile maturity where 400 yrs of pedogenesis would be indicated by minor translocation and 35,000 yrs indicated by maximum amounts of translocation. Increases in both depletion and depth of translocation of base cations, including Na, K, Ca and Mg, are particularly good indicators of profile maturity. Cations sensitive to the redoximorphic conditions of the soil profile (Fe, Mn and Cr) are highly variable across the chronosequence, suggesting that soil microclimate may be the greater controlling factor in their mobility and concentration. The occurrence of redoximorphic features and associated phases such as dendritic (Mn) concentrations, concentrically laminated nodules, and diffuse staining/depletion within ped interiors and along slickensides may be a function of time, but are not, at this point, definitive. Trace elements consequently do not exhibit consistent trends in translocation with time. This may be due to similar concerns with redox-sensitive elements, in which soil hydrology may play a role in the retention, liberation and mobility of trace elements from more stable mineral phases. Complexation with organic matter and clay surfaces may further impede translocation of a variety of constituents that may otherwise be mobile within the soil profile. These tools may be utilized to further expand the current ideas related to pedogenic processes within the Vertisol order, particularly those soils which are alluvially-derived.

Rates of pedogenesis are influenced by a combination of soil-forming factors, but probably the most important are parent material and time. Unconsolidated, bedded alluvium is particularly susceptible to essentially instantaneous and continuous pedogenesis. This implies that, even at the time of deposition, bioturbation, rooting, and minor translocation are active and culminate in wholesale pedogenesis of the profile once the surface is stabilized. Similarly, with increased duration of landscape stability, the rates of pedogenesis are not constant and tend to decline when advanced stages of pedogenesis are reached.

Pre-Stage 1 soil formation is very rapid (~400yrs), as indicated by the features (e.g, slickensides, lithorelicts lined with illuviated clay, and translocation of some cations/oxides) in the Ships profile. The Pledger Pedon, representing Stage 2 of pedogenesis, has features very similar to both the Ships and Burleson. The Pledger contains bedded alluvium, illuviated clay fabrics in the lower portions of the profile, and an abrupt boundary between the solum and parent material very similar to features of the Ships profile. A thicker interval of slickensides, chimneys (in the MH), gilgai and color distinction between profiles (MH and ML), are all indicative of greater soil maturity of the Burleson. This has two-fold significance: 1) rates of pedogenesis between 400 and 3,500 yrs are very rapid (less than pre-Ships) and 2) rates between 3,500 and 18,000 yrs are much slower (based on the number of features common between the Burleson and Lake Charles Pedons). Stages 3 and 4 exhibit comparable features, suggesting that the rate of soil formation post-18,000 yrs is much slower and is primarily indicated by continued translocation of mobile constituents. It is important to note that translocation (tau) values are not significantly higher for the 35,000 yrs old Lake Charles than for the18,000 yrs old Burleson, for most cations/oxides. The characteristic variation between the later two stages of the pedogenic process are suggestive of terminal pedogenesis, or a maxima beyond which very little morphological changes occur (pedogenic threshold of Chadwick and Chorover, 2001). The general trend of pedogenic processes with time could be described by a general exponential expression, where rapid slope change occurs close to the origin and declines as distance, and in this case time, from the origin (deposition of original bedded parent material) increases. This is consistent with quantitative soil chronofunctions (Y=a +b log X: where X is soil age and Y is the soil property) developed by various authors (Yaalon, 1971; Birkeland, 1974; Bockheim,1980; Harden and Taylor, 1983; Busacca, 1987)

Macromorphologic, micromorphologic and bulk chemistry variations have been established as important tools for deciphering stages of profile development as a function of time. These characteristics, particularly translocation, are very similar to those associated with variable climate conditions. For example, a wetter climate may support increased translocation, mineral weathering, and clay mobility and orientation correlative to those expressed during advanced stages of pedogenesis. Conversely, limited translocation, reduced slickenside and structural development, and absence of gilgai are features suggestive of dry climatic conditions as well as early stages of pedogenic development. Climate studies which use these characteristics as paleoprecipitation estimates may, in fact, over- or under-estimate past moisture conditions due to soil morphological development associated with profile age and maturity.

Chapter III.

A Modern Vertisol Chronosequence Application to PaleoVertisols: Utility for delineating time associated with sequence boundaries

Introduction

The abundance of paleoVertisols, particularly in the Appalachian basin succession, may be linked to the characteristics of the soil prior to burial diagenesis. Bulk density, clay content, and geomorphic position aid in the preservation and limited erosion of Vertisol profiles. The occurrence of macromorphologic pedogenic features (e.g., slickensides, wedge-shaped aggregates, and distinct microtopography), which are significant to characterization in the soil record, are likewise important for paleoVertisol identification. Greater preservation and a potential identification bias over other paleosols have resulted in a plethora of studies devoted to paleoVertisols. PaleoVertisols have occurred throughout geologic time (Proterozoic to Cenozoic) and are very common in the rock record (Button, 1979; Retallack, 1986; Gustavson, 1991; Joeckel, 1994, 2000). A significant number of the paleosols occurring in the Appalachian basin are paleoVertisols or vertic intergrades of other soil types (Driese et al., 1992, 1997; Driese and Mora, 1993, 2000; Mora et al., 1991, 1996; Joeckel, 1995, 2000; Caudill et al., 1996, 1997).

The Appalachian region during the Carboniferous was persistently located in subtropical to tropical paleolatitudes (0-35°) characterized by humid to subhumid climate conditions (Ettensohn et al., 1988). The tectonically uplifted region provided two additional scenarios conducive to paleoVertisols: possible orographic effects and compositionally consistent sediment supply. The fluvio-deltaic region to the southwest of the uplifted region may have been exposed to recurrent seasonal precipitation due to the orographic effects of the Appalachian orogen. Sediment supply increased following the uplift and resulted in an abundance of smectite clays weathering from sourcelands. Together, the depositional conditions are correlative to areas where alluvially-derived, modern Vertisols form: topographically level and geomorphically restricted areas (backbasin facies of floodplains), smectite-rich sediment sources, and seasonal precipitation in an environment conducive to high evapo-transpiration conditions. Vertisol and paleoVertisol formation requires landscape stability for pedogenic processes to occur. These paleoVertisols are associated with sequence boundaries and provide information related to the timing and extent/duration of stable landscape conditions.

This study: 1) describes the macromorphology, micromorphology and bulk chemistry of a paleoVertisol (Paleosol 2, Pennington Fm., White County, TN), 2) compares features of the paleosol with those described in a modern chronosequence analog, and 3) estimates the amount of time associated with deposition, landscape stability and pedogenesis of Paleosol 2 based on a Vertisol chronosequence model developed in Chapter II of this thesis.

Previous Work

During the Late Paleozoic, synorogenic clastic wedges prograded into the adjacent foreland basin from the deforming orogen to the east. Clastic wedges form as a response to thrust loading of continental crust, thereby resulting in sediment redistribution (Hatcher et al., 1989). The foreland basin formed as a result of subsidence, compressional tectonism, and movement along earlier (Ordovician and Silurian) faults. The Allegheny orogeny, and the associated foreland belt of folds and thrust faults, is recorded by sedimentary rocks to the west of the southern and central Appalachians. The Allegheny synclinorium contains one of the largest of the foreland basins and extends from Pennsylvania to the Cumberland Plateau in Tennessee. Geomorphically the Plateau represents a broad, high-standing region, deeply eroded by rivers and streams, with intervening ridges rising to accordant heights and without pattern other than that imposed by erosion (King, 1977). The sedimentary package of the Cumberland Plateau is characterized by rocks that have experienced little deformation, no metamorphic alteration and are mostly of Mississippian and Pennsylvanian age.

During the Mississippian period highlands in the Appalachian Piedmont continued to supply sediment westward to an alluvial apron currently coinciding with the Valley and Ridge and Plateau regions (King, 1977). Further westward of the Valley and Ridge, broad-scale deltaic deposition marks the onset of sequences of marine-terrestrial packages. Hatcher et al. (1989) suggested that for the Pennington-Lee clastic wedge, the single sediment source is to the southeast; alternatively, sediment may be derived from a chain of local sources from southeast of the Virginia recess to southeast of the Tennessee salient. The Mississippian in Tennessee is identified by carbonate rocks deposited on a relatively shallow, stable platform to the west and mixed terrigenous-clastic and carbonate rocks deposited in the foreland basin in the eastern regions (Milici et al., 1979). The geographic placement of the upper delta-plain deposits indicate that there is a general northwest gradation into lower delta-plain facies. Moving through the Pennsylvanian, a general regression is marked by an increase in terrigenous clastics and southwestward progradation of the delta plain. An increase in the thickness and frequency of red mudstone units upward (Vail, 1959) in the Mississippian succession is indicative of increasingly longer duration of pedogenesis and landscape stability at sequence boundaries.

The Pennington Formation is described as a heterogeneous unit composed of many lithologies (Milici et al., 1979). Dolostone, limestone, fine-grained sandstone and red and green shale subunits are indicative of the lithologic diversity occurring within the Pennington Formation. A yellowish gray, cherty dolostone (Calfkiller Dolomite; Vail, 1959) marks the basal contact of the Pennington with the Bangor Limestone. The paleoVertisols discussed in this study occur in the Lower Pennington, just above the contact with the underlying dolostone. The outcrop contains (Figure 3.1) numerous packages of marine limestone or dolostone truncated by terrestrial mudstone to claystone deposits, which represent small-scale transgressive-regressive sequences in which the tops of the paleosols represent sequence boundaries (Harding, 1995). This

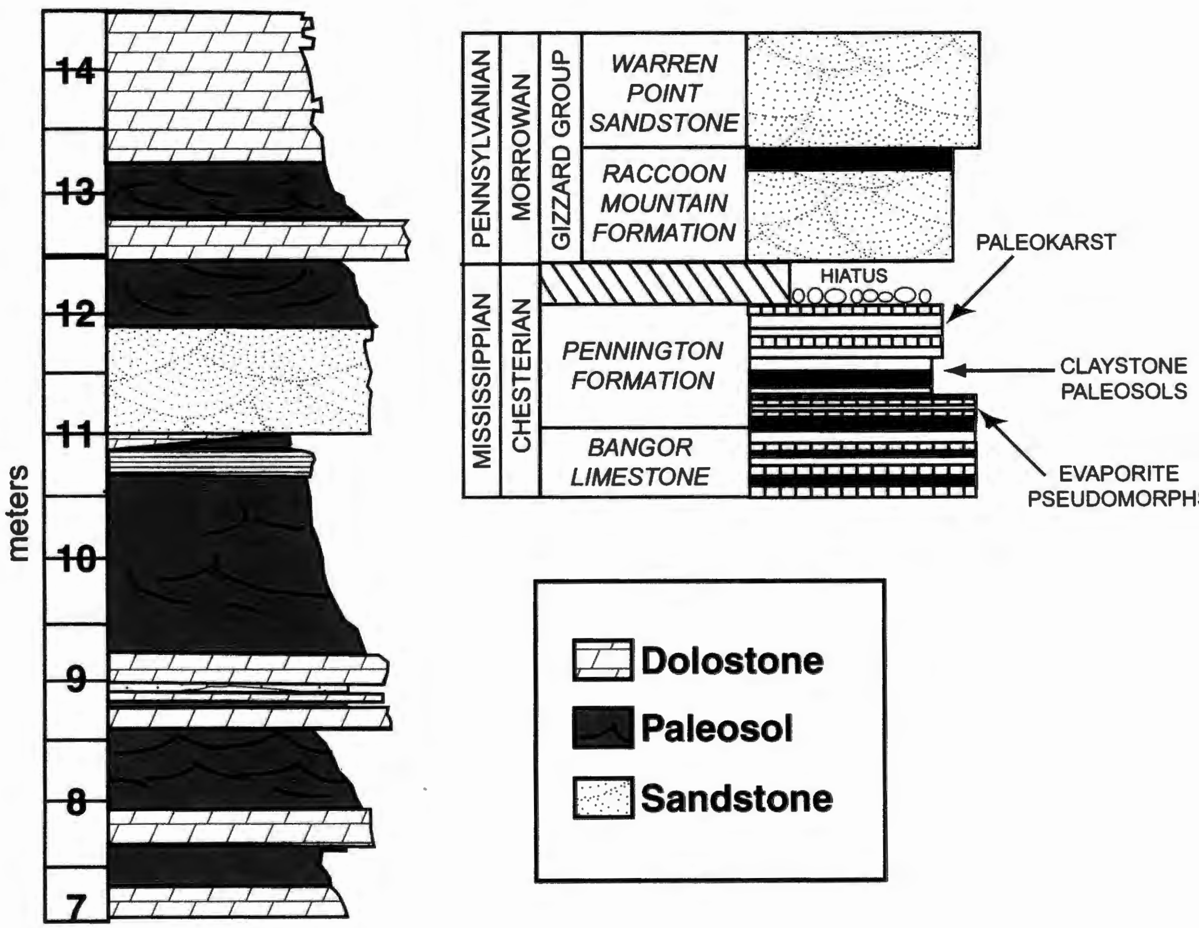

Figure 3.1 General stratigraphy of the Pennington Formation (Upper Mississippian) from Sparta, TN. Stratigraphic column is adapted from Harding (1995). Mississippian and Pennsylvanian stratigraphy from Driese et al., 1998.

study examines one of these sequences in order to gain a better understanding of the timing associated with these sequence boundaries.

The sedimentary package (Figure 3.2) includes a basal marine limestone, marginal-marine green shale and terrestrial red mudstone. This represents a full sequence between maximum flooding of the surface to maximum exposure, terrestrial deposition, and landscape stability (soil formation). The terrestrial deposits at this outcrop and many others throughout the Pennington Formation are typically paleosols, of which, paleoVertisols and vertic intergrades are most common.

Macromorphological features (i.e., pedogenic slickensides, angular to subangular blocky texture, synformal/antiformal structures, wedge-shaped aggregates, and reduction mottling), characteristic of the Holocene Vertisol soil order (Schoeneberger et al., 1998; Dudal and Eswaran, 1988), are present within the paleosols. Micromorphologic fabrics (e.g., masepic plasmic and lattisepic) are diagnostic of soils that have undergone shrink-swell processes related to cycles of wetting and drying (Ahmad, 1983; Wilding and Tessier, 1988). Birefringent clay strings and skins are interpreted as microscopic slickensides and pressure cutans, respectively. The clay composition of modern Vertisols is commonly smectitic (i.e., montmorillinite). A combination of pedogenic processes and burial diagenesis has altered the Pennington paleoVertisols to an illite-dominated clay mineralogy (Mora et al., 1998; Harding, 1995).

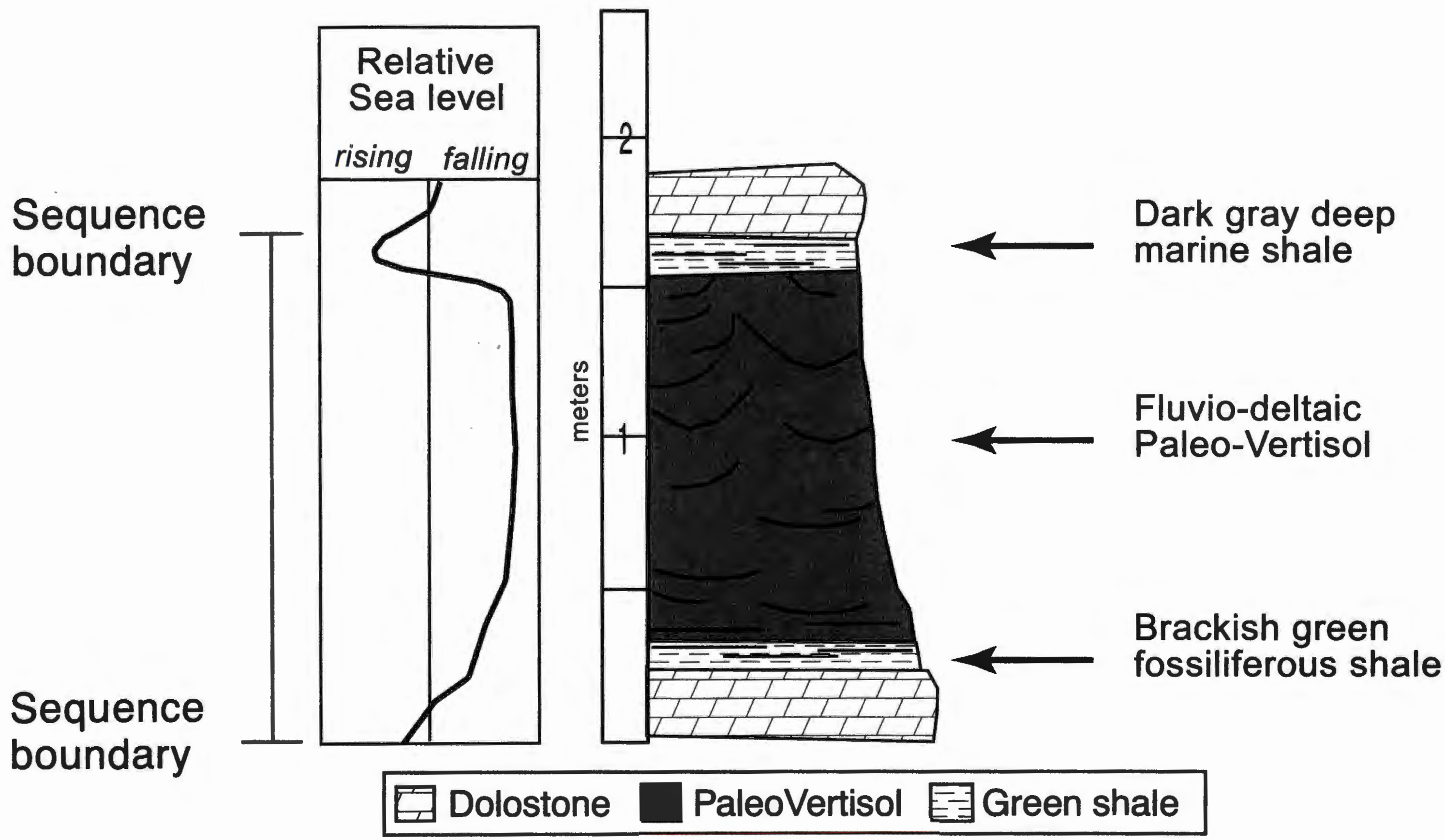

Figure 3.2 Generalized stratigraphy of Paleosol 2 from Mississippian Pennington Fm., Sparta, TN. The three main units include the shallow marine dolostone, transitional green shale, and the claystone paleosol.

Study Area and Methods

The Mississippian-age Pennington Formation outcrop in this study is located along U.S. Highway 70 near Sparta, in White County, Tennessee (Figure 3.3) . Two profiles from Pennington Paleosol 2, as first identified by Harding (1995), were described and sampled by the author.

Methodology for this study followed that utilized by the National Resource Conservation Service and the Paleopedology Group at the University of Tennessee, Knoxville. Macromorphological descriptions were completed according to methods outline in the Field Book for Describing and Sampling Soils (Schoeneberger et al., 1998) and incorporated terminology from Retallack (1988). Horizon designations in paleosols typically require identifying where the upper portion of the solum was removed or reworked. The upper portion of the solum may be indicated by burrowing, granular structure or rooting features that may be preserved, or evidence of removal may include slickensides (Figure 3.4), which normally occur at ~1m depth, that penetrate completely through the marginal unit or may be truncated at the contact with the overlying strata.

Sampling of paleosol profiles occurred as follows: 10cm interval samples were collected for whole-rock chemistry and bulk density and by horizon (delineated by field description) for thin section preparation. Bulk density measurements were conducted using the paraffin coated-clod method (Blake and Hartge, 1986). This method requires air-dried samples be weighed, coated with paraffin, and re-weighed. Each paraffin-coated clod was suspended in a water column and weighed to obtain volumetric displacement with the known

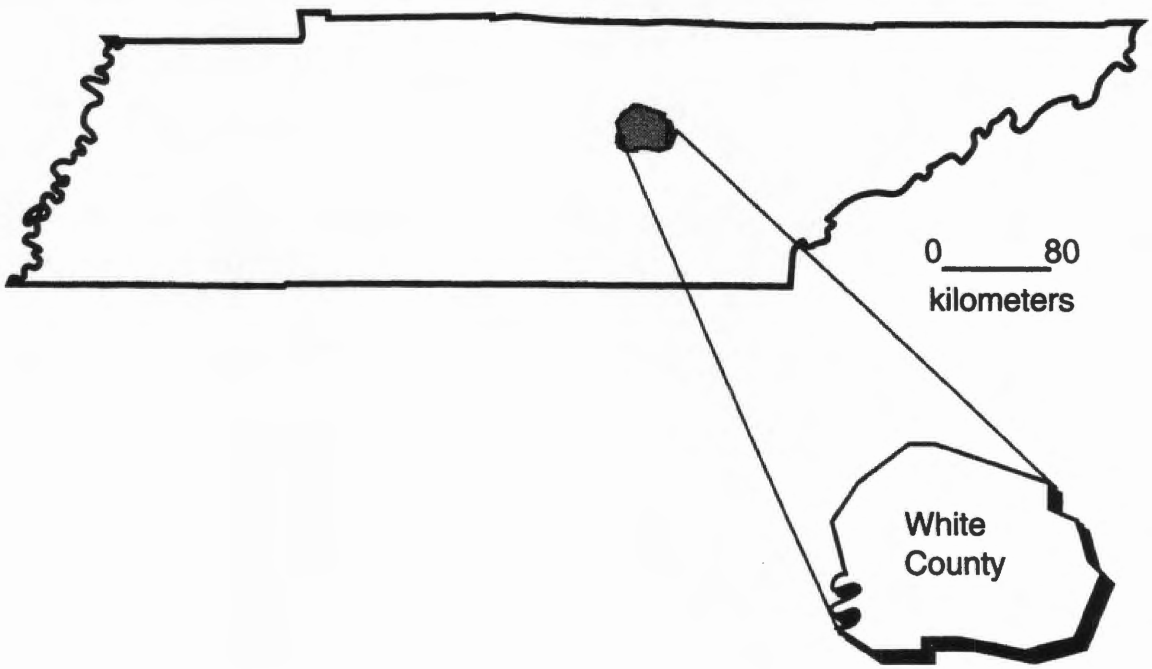

Figure 3.3 Location map for paleoVertisol Application of modern chronosequence. Paleosol 2, Upper Mississippian Pennington Fm., Sparta, Tennessee.

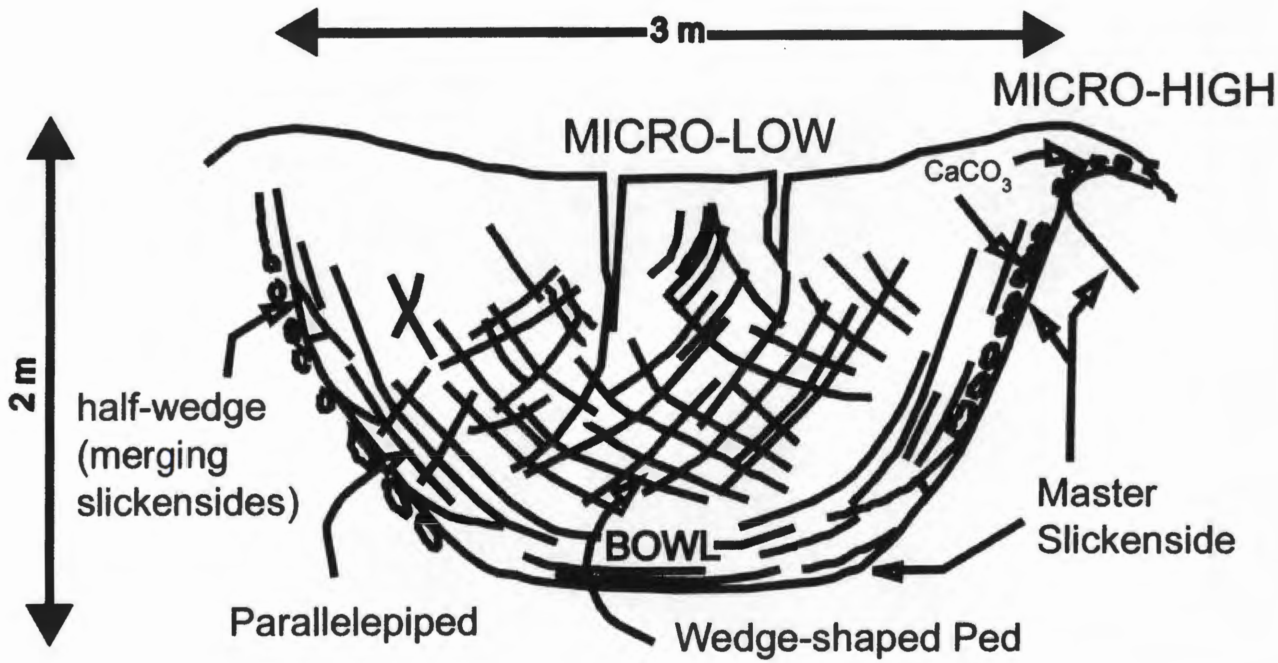

Modified from: Lynn and Williams, Soil Survey Horizons, 1992.

Figure 3.4 Schematic diagram showing structural features of a Vertisol microlow and adjacent microhigh. Master slickensides are located along the edges of the microlow/microhigh contact.

density of water and paraffin used as correction factors in bulk density calculations.

Whole-soil/rock bulk chemistry samples (from 10 cm intervals) were measured into metal tins and allowed to oven dry at approximately 60°C. Each sample was powdered in a shatterbox, followed by standard preparation of pressed pellets and run on the EG & G Ortec X-Ray Fluorescence Analyzer housed at the Department of Geological Sciences, University of Tennessee, Knoxville. Each run utilized appropriate shale and clay soil standards. A mass-balance approach (Brimhall et al., 1991; Driese et al., 2000) was used to examine variation in bulk chemistry within Paleosol 2 (Lower Pennington) profiles.

Oriented samples taken from each horizon were coated with boat resin to enhance durability and maintain the physical properties during transport and treatment. Thin section preparation by water-free methods (Mora et al., 1993) required that void space be filled with epoxy (isotropic in crossed polarized light) to minimize plucking during slide preparation. Each paleosol thin section, prepared to 30 μm thickness, was analyzed under doubly-polarized light using standard petrographic microscopes. Brewer (1964, 1976) and Fitzpatrick (1993) were used as a guide to micromorphological descriptions (see Appendix B) for terminology.

Results

Macromorphology

Macromorphology is an extremely important tool for recognition and characterization of paleoVertisols. Vertisols contain two very distinct microtopographic profiles (microhigh and microlow) formed from movement of the soil along stress failure surfaces (slickensides). Wedge-shaped aggregates form by the intersection of slickensides. Figure 3.4 is a schematic of Vertisol features. Each lithologic description attempts to utilize terminology of pedologists and geologists and is included in Appendix D.

The upper transitional (Figure 3.5; Table 3.1) units (10-30 cm) are noncalcareous, medium- to dark gray-shale to siltstone that appears greenish-gray (drab) in fresh exposure. This unit is typically laminated and nonfissile. Secondary Fe-staining may occur along rock fracture surfaces. The boundary between the transitional unit and the underlying paleosol is gradual with a slight increase in carbonate content, but still maintaining the transitional characteristics of interbedded lamination. There is a slight increase in fissility at the boundary suggesting an increase in clay content. Horizon Bw (30-40cm) represents the first unit primarily assigned as part of the paleosol profile. Structural development of the paleosol is represented by pressure faces, which are associated with shrink-swell processes (in the Vertisol soil order). This Bw unit is characterized as a fissile to nonfissile (due to pressure faces), weakly calcareous claystone. Reduced Fe in the matrix is indicated by a shift from dark gray of the overlying unit to dark greenish-gray (4GY4/1 to 5Y4/1). The matrix reduction

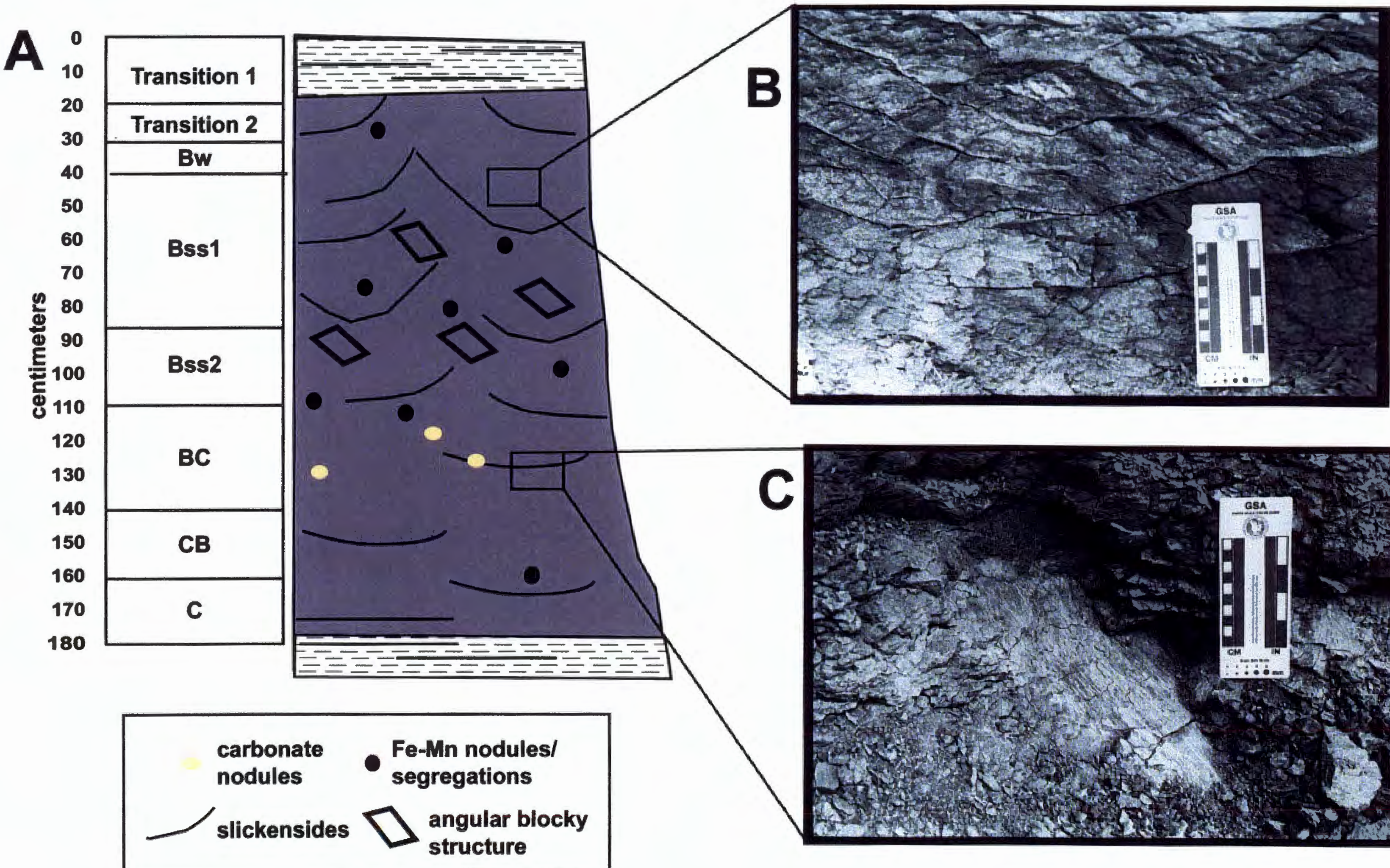

Figure 3.5 Pennington Paleosol 2 Macromorphology. A) Schematic of Vertisol features and related horizons; B) stacked slickenside traces of microlow profile (in outcrop cut); C) Excavated slickenside surface with polished argillan coating. Left side of scale in cm.

Table 3.1 Mississippian Pennington Formation (Paleosol 2 Microlow)- Characteristic Summary

Horizon	Depth (cm)	Slickensides	CO3 nodules	Roots/pores & redox	Structure	Matrix
Transition unit 1	10-20	----	Noncalcareous (no fizz with HCl)	Secondary Fe-staining;	Laminated; nonfissile	Medium dark gray to gray (N4 to N3) shale to siltstone
Transition unit 2	20-30	----	v. weakly calcareous; powdered sample does not fizz	Fe-staining along rock fractures and cracks	Interbedded lamina; increase in fissility	Dark gray (N3)
---	---	*Erosional surface-hiatus*	---	---	---	---
Bw	30-40	Occurrence of pressure faces	Noncalcareous	Reduced (Fe) matrix	Fissile to non-fissile claystone	Dark greenish –gray (4GY4/1 to 5Y4/1)
Bss1	40-85	Pressure faces and weak (not corrugated or polished) slickenside surfaces contain silty material; few polished slickenside faces (thin, lithified argillaceous films)	Weakly effervescent calcareous claystone	Fe-Mn segregations; secondary Fe-staining on slickenside surfaces	Nonfissile, claystone; strong SBK to weak ABK	Brownish gray (5yR4/1); medium dark gray (N3 to N4 mottles) Fe-Mn segregations;
Bss2	85-110	Multiple, well-developed, corrugated slickensides with thin, polished argillan coating	Calcareous (v. weakly effervescent) claystone	Fe-Mn? mottles; Fe-Mn staining on slickenside surfaces	Nonfissile; medium to strong ABK; wedges range in size to greater than 5 cm (long dimension)	Brownish gray to brownish black (5YR4/1 to 5YR2/1); N3 to N4 Fe-Mn mottles

Table 3.1 (con't) Mississippian Pennington Formation (Paleosol 2 Microlow)

Horizon	Depth (cm)	Slickensides	CO3 nodules	Roots/pores & redox	Structure	Matrix
BC	110-140	Argillic coating on slick surfaces and pressure faces	Secondary crack infill effervesces	Fe-Mn mottles	Nonfissile, weak to moderate, medium SBK; appears platy in some areas	Brownish gray (5YR4/1 to 5YR2/1); N3 Fe-Mn mottles
CB	140-160	Rare to common pressure faces	Features similar to carbonate nodules found at (140-150 cm)	Fe-Mn nodules; yellow Fe-staining	Laminated (nonfissile); platy to weak SBK	Brownish gray (5YR4/1)
C	160-180	----	----	Minor dark greenish gray mottles; Fe-staining	Nonfissile to weakly fissile due to platy structure (laminated)	Medium to dark gray (N3 to N4); minor dark greenish gray mottles (5G4/1); Fe-staining (10YR6/6 to 5YR5/6)

may be relict feature from the encroachment or ponding of marine waters into the ML portion of the paleosol.

A transition in color to brownish gray (5YR4/1) and structural development marks the location of significant pedogenic development. The Bss1 horizon is a calcareous, nonfissile claystone exhibiting strong subangular blocky to weak angular blocky structure, with Fe-Mn segregations (N3 to N4 mottles) and secondary Fe-staining on slickenside surfaces. Pressure faces and weakly developed slickensides occur at a depth of 40-85 cm (Bss1). Because this range is not significantly different than the modern Vertisol analog (~35-100cm), there has probably been very little truncation and/or removal (30cm) of soil material prior to inundation and burial. Some slickensides do appear polished and coated by thin, lithified, argillaceous films. The Bss2 horizon (85-110 cm) contains multiple, well-developed corrugated slickensides with thin, polished coatings and wedge-shaped aggregates greater than 5 cm in long dimension. This brownish gray to brownish black unit is a weakly-calcareous, non-fissile claystone with moderate to strong angular blocky structure. Fe-Mn mottles and staining impart an N3 to N4 coloration, particularly on slickenside surfaces.

A decline in structural development, which is associated with horizons containing abundant slickensides, marks the boundary to the BC horizon. This brownish gray horizon is weak to moderate, medium subangular blocky structure and platy (nonfissile) in some areas. Argillaceous coatings and some Fe-Mn mottling occurs on slickenside surfaces and pressure faces. The presence of platy structure is suggestive of the presence of sedimentary layering or bedding.

The CB horizon (140 to 160cm) is laminated (nonfissile), with platy to weak subangular blocky structure, and includes rare to common occurrence of pressure facies. The matrix is brownish gray (5YR4/1) with carbonate and Fe-Mn nodules. The C horizon marks the return of transitional marine deposits mixed with alluvium. Variation in color ranges from medium to dark gray, with minor dark, greenish-gray mottles. Weakly fissile to platy structure is attributable to fine laminations within the parent material.

The Paleosol 2 MH (Table 3.2) transitional unit, a medium gray, fissile claystone, is similar to that for the ML, but is a stratigraphically thicker package. (10-40cm). Moving downward in the profile, the contact between the transitional unit and the Bw horizon is diffuse (~20 cm) particularly because structural features (slickensides) seem to continue into the overlying (transitional) sediment. Pressure faces, minor slickensides, and subangular blocky structure are key indicators of Vertisol pedogenic processes. This (transitional/Bw) unit is characterized as a brownish-gray to medium dark-gray weakly calcareous claystone. An increase in structural development (strong subangular blocky to moderate angular blocky), presence of corrugated slickenside faces and 3.5 to 4 cm wedge-shaped aggregates are indicative of horizons (Bss1) that undergo shrink-swell processes. The Bss1 horizon is a grayish-brown (5YR4/1) to brownish gray (5YR3/2) calcareous claystone.

The gradual boundary between the Bss1 and Bss2 horizons is indicated by an increase in the size of wedge-shaped aggregates (>6 cm in long

Table 3.2 Mississippian Pennington Formation (Paleosol 2 Microhigh)-Characteristic Summary

Horizon	Depth (cm)	Slickensides	CO3 nodules	Roots/pores & redox	Structure	Matrix
Transition	10-40	—	—	Fe-staining	Fissile to platy	Medium gray (N4 to N5) to olive gray (5Y4/1)
Transition/ Bw	40-60	Pressure faces and minor slickensides; truncated by transitional marine unit (diffuse boundary)	—	—	Subangular blocky	Brownish gray (5TR4/1) to medium dark gray (N4)
—	—	*Erosional surface-hiatus*	—	—	—	—
Bss1	60-80	Corrugated slickenside faces; 3.5 to 4 cm wedge-shaped aggregates	—	—	Strong subangular blocky toi moderate angular blocky	Grayish brown (5YR3/2) to brownish gray (5YR4/1); weathered surface 5YR8/1 to 5YR6/1)
Bss2	80-120	Highly polished argillan coatings on corrugated slickenside surfaces; wedge-shaped aggregates greater than 6 cm	Few 0.2 cm carbonate nodules?	Secondary Fe-staining (no surface preference); reduction mottling in lower part of horizon	Moderate to strong angular blocky	Brownish gray (5YR4/1) to grayish brown (5YR3/2)
Bkss1	120-150	Less steep, less well-developed slickensides	Secondary calcite along slickenside plane	Isolated lighter segregations; reduction mottling due to rooting	Strong subangular blocky	Grayish red (5R4/2) to grayish brown (5YR3/2); medium bluish gray (5G6/1 to 5G5/1); grayish green (5G5/2 to 10G4/2)

Table 3.2 (continued) Mississippian Pennington Formation (Paleosol 2 Microhigh)-Characteristic Summary

Horizon	Depth (cm)	Slickensides	CO3 nodules	Roots/pores & redox	Structure	Matrix
Bkss2/C	150-1	Slickenside are very low angle and nearly parallel to bedding; argillan coating on pressure cutans	Weakly cemented carbonate nodules (segregations)	Fe-Mn nodules; Fe-staining on slickensides	Platy to weak subangular blocky	Grayish brown (4YR3/2) to brownish gray (5YR4/1); greenish gray (5GY4/1) and grayish red (5R4/2) mottles
C/B	+	---	---	Grayish red mottles	Fissile, platy structure	Dark greenish gray (5GY4/1 to 5G2-4/1); interlayered with grayish red (10R4/2); grayish red (5R4/2) mottles

dimension) and moderate to strong angular blocky structure. Highly polished argillan coatings occur on corrugated slickenside surfaces. Redox conditions conducive to Fe-Mn mobility are indicated by reduction mottling and occur in the lower portion of the horizon, although secondary Fe-staining is not preferential to surfaces (e.g., slickensides). Few, very small (~2 mm) carbonate nodules were present at the contact between the Bss2 and Bkss1 horizons and throughout the Bkss1 horizon. Less steep and less well-developed slickensides and strong, subangular blocky structure are characteristic of this grayish-red to grayish-brown, weakly-calcareous silty claystone. Reduction due to rooting is indicated by downward branching, medium bluish-gray mottles, in addition to nonsurface-specific, grayish-green mottles.

The Bkss2/C horizon contains very low-angle slickensides that nearly parallel bedding and exhibits platy to weak subangular blocky structural aggregates. Argillan coatings on pressure cutans may have secondary Fe-staining on the surface. Grayish-red and greenish-gray mottles occur along ped faces, suggesting variable redoximorphic conditions. Features similar in appearance to carbonate segregations may represent lithorelicts from underlying material being incorporated into the Bkss2/C horizon. Interbedded grayish-red and dark greenish-gray, noncalcareous claystone marks the occurrence of bedded alluvium within the lowermost horizon (C/B). Basal sedimentary alluvium imparts platy structure or fissility, where parting occurs along minor variations in grain size.

In general, both the Bw to C and Bss1to C/B horizon intervals in the ML and MH, respectively, exhibit features (i.e., subangular blocky to angular blocky structure, polished slickensides, and microtopography) similar to those characteristic of the modern Vertisol analog. Polished slickensides, pressure faces, and subangular to angular blocky structure form from pedogenic processes, particularly shrink-swell processes associated with Vertisol formation. Disruption of very fine sedimentary alluvium indicated by change in structure (subangular blocky to platy/fissile) represents the advancement of pedogenic processes downward in the profile. Fe-Mn and carbonate nodules further support the interpretation of terrestrial processes acting to form Paleosol 2.

Micromorphology

Micromorphology (Figure 3.6) of Paleosol 2 supports the macromorphologic description and characterization as a paleoVertisol. Features such as sepic-plasmic fabric, clay skins, angular blocky pedorelicts, and Fe-Mn nodules are similar to those of the modern Vertisol soil order. The MH and ML profiles from Paleosol 2 will be discussed in terms of three components: Fe-Mn concentrations, matrix fabrics and carbonate accumulations.

Matrix fabrics (Figure 3.6A-B, E) include extremely well-preserved slickenside surfaces and clay skins, as indicated by strong sepic-plasmic and lattice-sepic fabrics and arcuate slickenfibers. The MH and ML profiles each exhibit these features in the Bss1 and Bss2 and Bss2 and Bkss1 horizons, respectively. Wedge-shaped peds (Figure 3.6E) are outlined with oriented clays

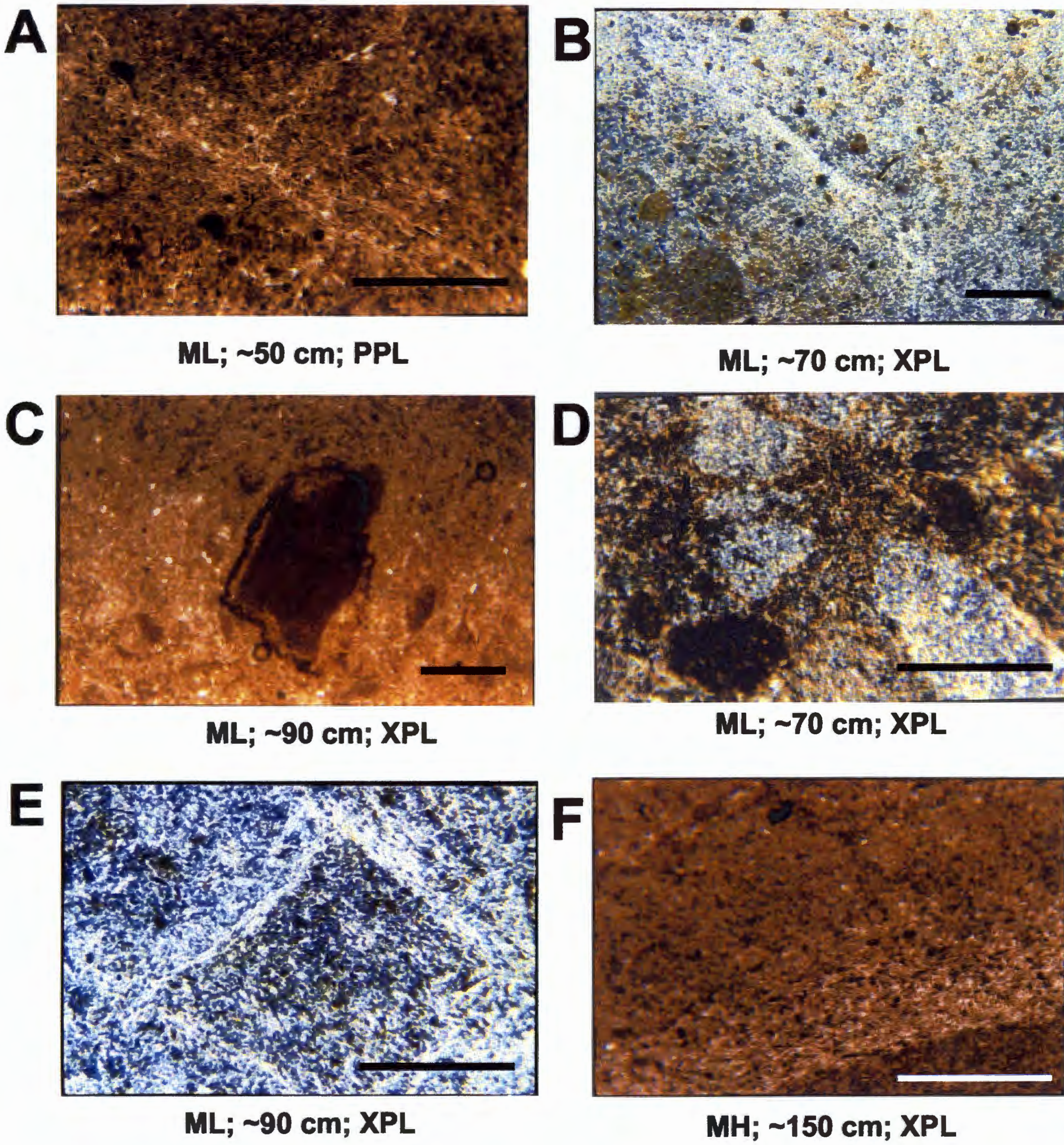

Figure 3.6 Paleosol2, Pennington Fm., Sparta, TN micromorphology. A-B) slickenside fibers cutting across matrix; C) Fe-Mn nodule with concentric laminations; D) pedorelicts indicating advancement of pedogenesis; E) oriented clay fabric around an angular blocky ped; F) variation in grain size in bedded alluvium of parent. A, D-F bar scale is 0.5 mm; B and C bar scale is 1 mm. (XPL=crossed polarized light; PPL=plane polarized light)

and represent micro-scale, angular-blocky structural aggregates. In modern soils, structural development is most pronounced in areas with active shrink-swell processes and slickenside movement. Backfilled burrows, vertical crack infillings, and downward-tapering root traces are indicative of haploidization (Figure 3.6D) or mixing of the soil matrix (BC and C horizons), and mineral transformations (i.e., dolomitization and illitization) may play a minor role in disruption of primary features. Preservation of these features is more pronounced in the basal portions of the paleosol due to less re-orientation of matrix materials during shrink-swell of overlying horizons.

Horizons occurring lower in profiles show distinctive features of original bedding (e.g., bedding-parallel structural features and clay fabrics). Minor grain-size variations are distinct, with gradual to abrupt contacts between very fine layers of sedimentary alluvium. Low-amplitude ripple marks, soft-sediment deformation and sedimentary layering are distinguished by alternation in color between drab gray-green to warm brown (C horizons of MH and ML). Various vug-like features may represent diagenetic or secondary dolomite cementation or may be associated with burrows, because most occur where drab concentration of finer sediment surrounds the coarser size sediment. Quartz silt grains, angular feldspar grains, acicular opaque Fe-Mn minerals and very fine-grained accessory minerals comprise the remaining portion of the matrix, in addition to abundant clay minerals (illite, diagenetic chlorite, and smectite).

Iron and Mn are elements that are particularly susceptible to fluctuating redox conditions that affect their mobility in the soil profile (prior to burial). The

Bss1 horizon of the ML profile contains abundant Fe-Mn nodules (Figure 3.6C) with compact, concentric laminations and dark brown lithorelicts, which may represent weakly- cemented Fe-Mn concentration within the matrix material. The MH profile (Bss1) contains: 1) a much greater proportion of dendritic to very weakly concentric Fe-Mn nodules with engulfed matrix grains, 2) concentric, oblong Fe-Mn nodules with minor quartz inclusions, and 3) dendritic Mn nodules. Redoximorphic (Fe) depletions and concentrations are present in both MH and ML profiles along root traces, burrowing, sedimentary layering and along soil fractures and ped faces. Drab regions (reduced Fe) appear more commonly in areas (throughout MH profile) that are more coarsely crystalline, possibly where calcite nodules have been dolomitized during burial diagenesis.

Carbonate morphologies were difficult to interpret, particularly in areas with highly birefringent clay fabrics. An acid test on most hand samples resulted in very little, or completely absent effervescence, even on powdered samples. Clay abundance and complexation may be responsible for masking the reactive surfaces of the dolomitized (calcareous) fabric. Drab areas (MH and ML profiles) may represent areas that originally contained carbonate segregations, and minimal amounts of coarse dolomite may occur within selected root traces. Relict carbonate nodules (dolomitized) contain oriented clay fabric along their perimeter. The Bkss1 horizon (MH profile) contains two sizeable carbonate nodules juxtaposed to each other. The nodules are separated by shrinkage cracks that are infilled with Fe-Mn oxides. Areas within the nodules are much more coarsely crystalline, which may represent original septarian voids; nodule boundaries with adjacent matrix material are less distinct, when viewed at increased magnification.

Features preserved in Paleosol 2 are consistent with modern Vertisols and may exhibit characteristics associated with early stages of pedogenesis. The occurrence of bedded alluvium at the basal portions of the MH and ML profiles suggests that there has been a limited depth of pedogenesis.

Bulk Chemistry

Soil profile development related to translocation of mobile constituents, weathering and precipitation of various mineral phases, and cumulative moisture status of the soil may be better understood if trends in bulk chemistry are utilized. Mass-balance calculations (Brimhall and Dietrich, 1986; Brimhall et al., 1991; Retallack, 1991; Driese et al., 2000) address the soil volume change (strain) and translocation (tau) of mobile cations/oxides in the soil profile relative to parent material compositions of the same cation or oxide, and normalized to an assumed immobile index element. Translocation indices are indicators of constituent behavior relative to Al (proxy for clay content). For example, calcification refers to the ratio of Ca and Mg to Al, where Ca and Mg may represent stable phases such as calcite or dolomite relative to clay content. Selection of parent material of 160-180cm for Paleosol 2 was based on: 1) profile position, with this being the lowermost siliciclastic sediment horizon identified above the underlying limestone unit and 2) the presence of platy structure (fissility) in the sample, commonly associated with bedded, sedimentary alluvium.

Paleosol 2 strain trends for Zr, Ti and Cr are given in Figure 3.7. Chromium and Ti show the most conservative volume loss (~15%) throughout the ML profile. Zirconium strain values estimate volume losses of approximately 40%. Chromium, Ti and Zr have a coincident inflection point at 150 cm, estimating volume loss of ~60%. Bulk chemical data may facilitate recognition of cause of volume loss. Pennington Paleosol 2 (Figure 3.8) has experienced minor to moderate (+/- 25%) gains or losses for each of the translocation indices. The oxidation trend contains an anomalous peak (75%) at the contact between the transitional marine unit and the upper portion of the soil profile. With depth, the oxidation index has experienced moderate gain (20%) and approaches parent ratios at ~130cm (BC horizon). The calcification index is illustrated by a similar trend with approximately 20-35% loss throughout the profile. There is a peak increase of 10% near the contact between the BC and CB horizons. Other indices, including salinization, oxidation, exchangeable bases, and clayeyness record this transition. The clayeyness index increases to near-parent ratios at this depth may suggest that there is a hydrologic barrier at this depth (due to increase in clay content). The variable trend (~130+ cm) in the clayeyness curve may be used as a proxy for grain size-variation related to the original sedimentary bedding (BC, CB and C horizons). Exchangeable bases show 0 to 10% gain/loss in the parent material region, with gradual increase to 25% gain to the surface, which is suggestive of very limited translocation of base cations in the profile. The salinization index shows significantly more variability through the profile and may be a function of marine-water encroachment in the upper portion

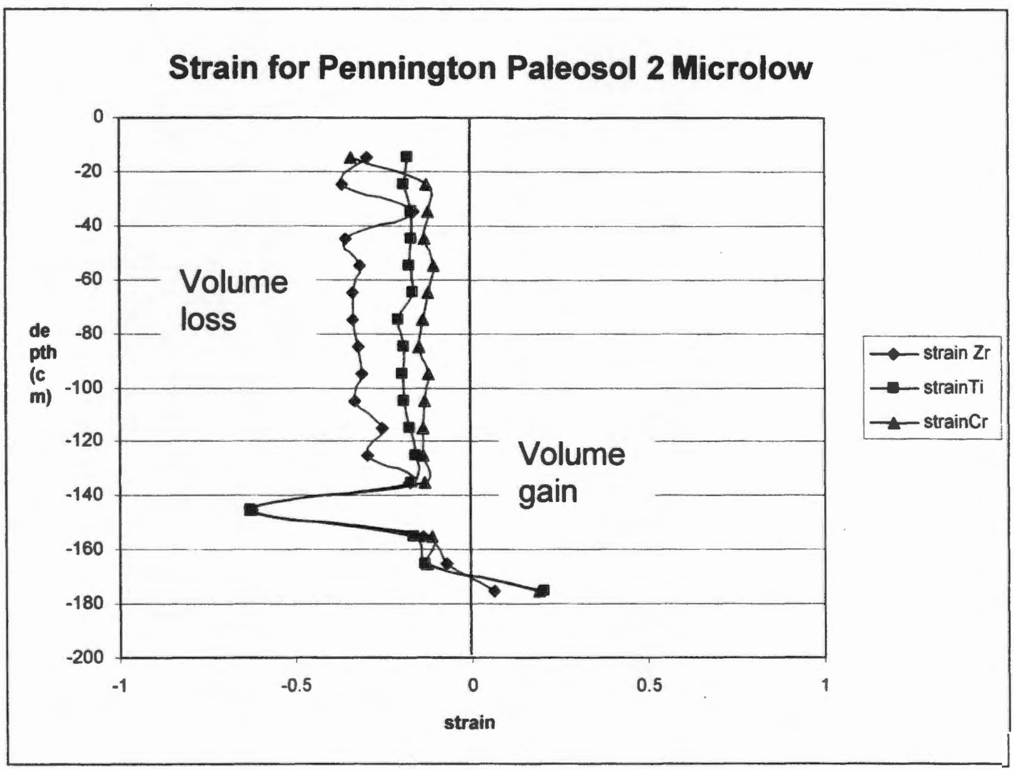

Figure 3.7 Strain trends from Paleosol 2. Zr, Ti and Cr are typically used as immobile trace elements in mass balance calculations. Parent material values are an average for depths ranging 160-180 cm.

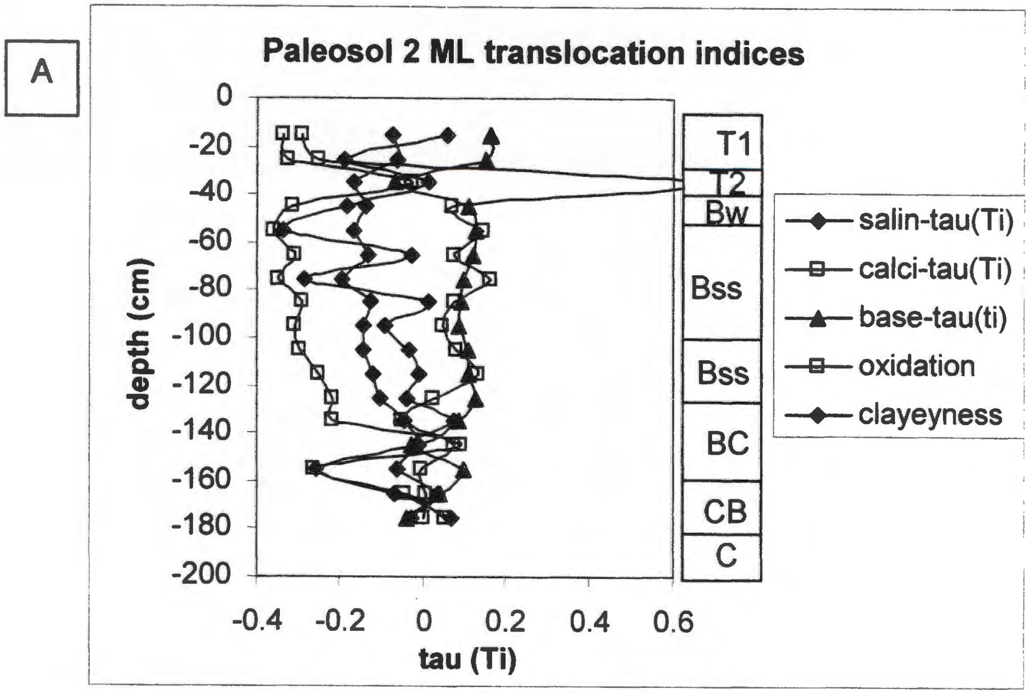

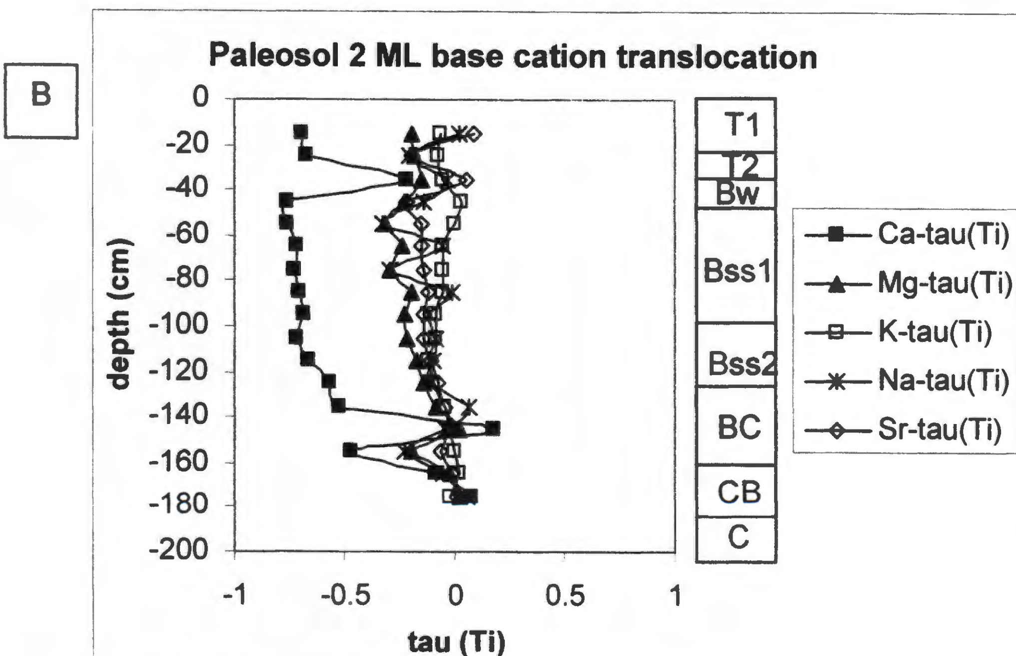

Figure 3.8 Pennington Paleosol 2 ML profile molecular ratios and element translocations calculated using Ti as immobile index element. A) clay (clayeyness), oxid (oxidation), base (base loss), calc (calcification), and salin (salinization) are translocation indices. B) translocation of base cations within soil profile.

C

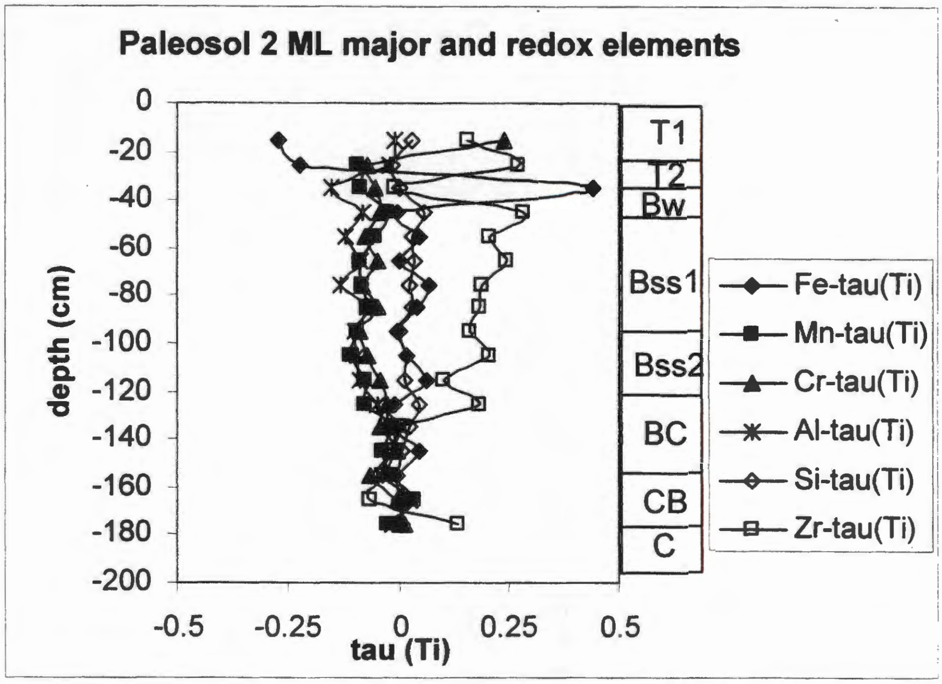

D

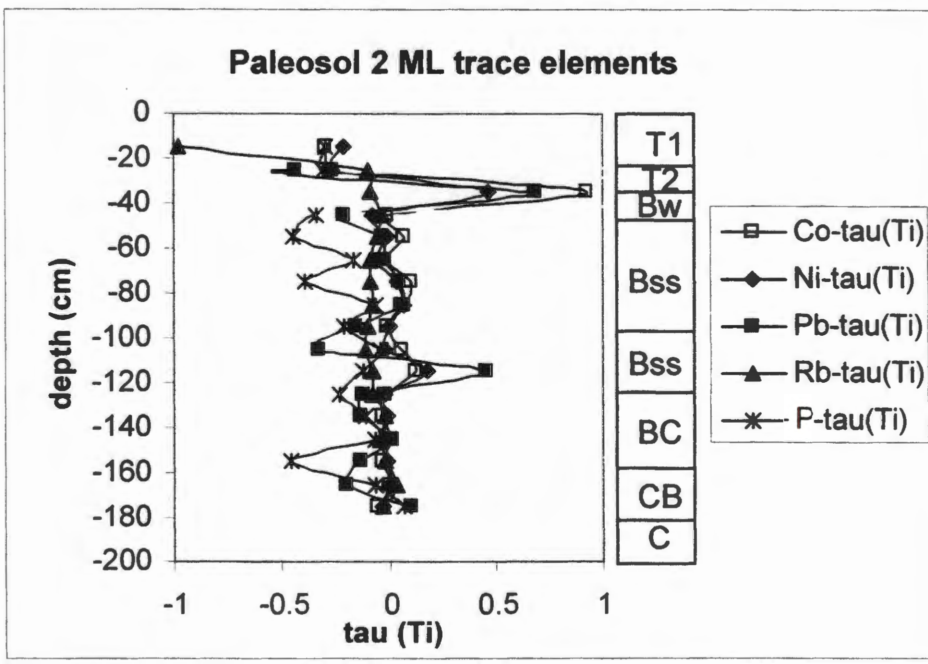

Figure 3.8 (continued) Pennington Paleosol 2 ML profile element translocations calculated using Ti as immobile index element: C) major and redox element translocation. Zr is included because of similarity of trends, and D) trace element trends within the soil profile.

of the solum or Na-rich smectite as the original clay mineralogy (Driese et al., 1992).

Base cation translocation (i.e., Ca, Mg, K, Na, and Sr) is calculated relative to the parent material composition for each respective element. Of these elements, Ca appears to have experienced the most significant amount of translocation, reaching nearly 75% loss through most of the solum. Parent material composition, as indicated by the calcification index, is variable with loss of nearly 50% and gain of 20%. Although many of the major peak losses in Ca-translocation are correlative to similar losses in Na, Mg and Sr trends, their magnitude is significantly reduced (-15 to +10%). Conservation of K throughout much of the profile is likely a result of the illitization process, whereby K is sequestered in the stabilization and transformation of smectite (Driese et al., 2000). The salinization index is calculated based on the ratio of Na to K and therefore, index trends are more significantly affected by the translocation values of Na (-25% to +5). Magnesium exhibits very similar magnitude changes, but more conservative shifts in translocation values. Strontium, however, tends to be conserved, with minor losses within the profile similar to peaks in Ca. The upper portion of the profile has sharp peaks (-10 to 5% variation) suggesting the incorporation of Sr from seawater encroachment.

Major and redoximorphic elements are fairly conservative in oxide and element translocation trends; ~10% gain or loss throughout much of the profile. Zirconium, a trace element in Paleosol 2, is plotted with the major and redox-elements because of similarity in translocation trends. There is gain in Zr of 10 to

35%, which increases upward in the profile. Aluminum and Si are have only minor translocations of -5% and +5%, respectively; these trends indicate limited grain size variation within the profile prior to pedogenic processes, and considering the fact that Si approximates sand and silt particle sizes and Al serves as a proxy for clay content. Iron, Mn and Cr are sensitive to redox conditions, however, each of these elements have experienced very little translocation with depth. There is a peak in Fe and major decline in Mn near the contact between the pedogenic strata (Paleosol 2) and overlying transitional units. Ponding in the ML during early marine encroachment may have resulted in the accumulation of Fe, possibly due to lower Eh conditions and organic complexation, at the interface between transitional and terrestrial strata. If highly (structurally) expansive Na-rich smectites were initially present, the accumulation of Fe would be enhanced due to further impedance of downward migration of mobile constituents. The major decline in Mn may be associated with conditions at the soil-marine interface.

Trace element trends are strikingly similar to previous trends (e.g., Fe, Ca, Na, and Mg). A major inflection point at 30 cm is indicated by gains of 40, 60, 90 and greater than 100% in Ni, Pb, Co and P, respectively. An inflection point this abrupt may support the occurrence of a hydrologic barrier or some type of complexation process (e.g., organic). Phosphorus values are highly variable with a range of 50% loss to greater than 100% gain and may be associated with organometallic complexes indicated by several peaks that correlate well with those of the Fe-translocation trend. Lead, Co and Ni appear to have gains and losses that are in phase with each other, suggesting similar dynamics in the Paleosol 2 profile. Rubidium, which exhibits trends similar to K in paleosol profiles, is conserved throughout the profile with only very minor (<5%) gains and losses.

The bulk chemistry trends presented here generally support very limited translocation of elements/oxides. As such, pedogenic processes must have been very limited in advancement downward in the profile. Major fluctuations in the bulk chemistry trends may be associated with hydrologic boundaries resulting from an increase in clay content or an increase in Na-rich smectite. Fluctuations may also be associated with encroachment of marine waters as the soil was transgressed during rising sea-level.

Discussion

Pennington Paleosol 2 contains features common to the modern Vertisol soil order and maintains excellent preservation of these features, even after burial diagenesis. Primary morphologic features indicative of profile maturity and pedogenesis include thickness and development of slickensided horizons, depth to parent material and occurrence of Fe-Mn masses. The preserved thickness (Table 3.1) of slickensided horizons (Bss1 and Bss2) in the ML is approximately 70 cm. The presence of slickensides suggests active pedogenic processes were occurring at the time of formation. Major slickensides can be traced to the intersection of the paleosol with the overlying transitional unit, suggesting that the upper portion of the MH has been truncated. The original gilgai topography could, therefore not be determined.

Depth of pedogenesis can be determined in several ways. Macromorphology provides the first-level approximation based on color, structural change (angular blocky to platy), and/or retention of sedimentary bedding. Micromorphology allows identification of disruptions in the sedimentary alluvium, mobility of clays and coarser material deposited into vertical soil cracks, and oriented clay fabrics around lithorelicts. A shift to platy to weak subangular blocky structure and occurrence of sedimentary, bedded alluvium are indicative of the depth to which pedogenic processes in Paleosol 2 have occurred. The boundary between the BC and CB horizons marks the lowermost depth exhibiting pedogenic features. Haploidization or mixing within the soil matrix, vertical cracks infilled with coarser sediment, and areas with preserved bedding at 110-140cm are indicative of the lowermost advancement of pedogenesis. Redoximorphic concentrations and depletions on ped surfaces, along root pores, and nodules suggest that mobile constituents were transported, and that pedogenic processes occurred, to this depth.

Bulk chemical trends (Table 3.2) may further support estimates of advancement of pedogenic processes as gains of mobile constituents at a hydrologic break. Peaks in calcification and exchangeable base indices at the BC and CB horizons (140 cm) suggest that the advancement of pedogenesis may have been limited to this boundary. Similar inflections in the salinization and oxidation trendlines occur at this depth. Assuming a depth of 140 cm of the entire profile, ~30 cm must have been removed due to incorporation of the overlying transitional unit into the paleosol profile, and 30 to 40 cm (estimated based average depth to slickensides from modern analog) must be added back to account for the amount of truncation of the upper solum. This calculation results in a depth of pedogenesis estimate of ~140 cm.

An additional hydrologic break at 30-40 cm is indicated by peaks in: 1) calcification, oxidation and exchangeable bases indices, 2) extreme gains in Ni, Pb, Co and P, and 3) inflection points in Fe, Al, Sr, Ca, Na and Zr trendlines. This depth range marks the boundary between the transitional marine flooding unit and the paleosol profile. Although it is difficult to speculate on the original water chemistry and hydrology at the time of deposition of the transitional unit, there must have been ponding, which resulted in reducing conditions and significant Fe accumulation.

Determination of maturity of a soil profile is a function of bulk chemistry trends, in which minor translocation is equivalent to short-term pedogenesis, whereas long-term pedogenic processes may be indicated by major loss, particularly in the upper solum. Exchangeable bases show 0 to 10% gain/loss in the parent material region, with gradual increase to 25% gain to the surface, which is suggestive of very limited translocation of base cations in the profile. The salinization index shows significantly more variability through the profile and may be a function of marine-water encroachment in the upper portion of the solum or Na-rich smectite as the original clay mineralogy. Pronounced Ca translocation through much of the profile, with only limited correlation with Mg, may provide evidence that much of the Ca was translocated prior to burial diagenesis and dolomitization. Shifts in phosphorus are in phase with, but at a greater magnitude than that of Ca, and may indicate similar formation rates of stable mineral phases.

In general, Pennington Paleosol 2 has well developed slickensides, limited translocation of cations/oxides, and macro- and micromorphologic features similar to modern Vertisol analogs. Maturity of the profile can be determined, to some degree, by morphological features and bulk chemistry trends. To better understand the time-significance of this paleoVertisol and others in the rock record, a modern chronosequence must be applied to estimate the duration of pedogenesis on that particular surface. This requires identification of, and comparison between, modern soil profiles and their macromorphologic, micromorphologic, and bulk chemical characteristics.

Chronosequence application: time resolution at sequence boundaries

Paleosol 2 (Pennington Fm., Mississippian, TN) comprises a portion of a depositional package that includes a sequence of dolostone, transitional green shale, claystone paleoVertisol, and green shale. The dolomite represents a period of maximum flooding and well-established marine conditions. There is an abrupt contact between the dolostone and the overlying green shale, indicating that the dolostone was completely lithified prior to deposition of the green shale. Red, calcareous alluvium (brown to reddish gray as a result of diagenesis) was deposited next, creating a gradual boundary dominated by clay-rich fluvio-deltaic deposits. Primary bedding is well preserved in the basal portion of the paleosol. Continued deposition resulted in the ~200+cm thick package of clay-rich sediment and the onset of pedogenic processes. After some period of time, the upper surface of the paleosol became truncated (~30cm), possibly due to encroachment of marine waters associated with the overlying green shale. The green shale is then capped by a second dolostone unit. A sequence is represented by a package of sediment including deposition during maximum marine transgression followed by a regression and development of an exposure surface. This exposure surface corresponds to a sequence boundary or period of nondeposition, prior to the next transgressive phase. The time associated with the hiatus can be determined by estimating the duration of pedogenesis (requires stable land surface) taking place within the soil profile.

To obtain time resolution at sequence boundaries requires an understanding of rates of pedogenesis and the use of modern chronosequences as tools for determining the extent of pedogenic processes. In order to determine the duration of pedogenic processes, as indicated from a chronosequence, requires guidelines on how time is allocated in the profile, from original deposition to full profile development. Profile age estimates include: 1) initiation of original exposure surface, 2) alluvial sediment deposition, including small allowances for each sediment package, and 3) landscape stability and pedogenesis. Whereas the paleosol-chronosequence application provides the opportunity to semi-quantitatively determine ages of the paleosol package, the length of time for deposition of the dolostone and green shale unit can only be considered in the sense of relative time.

A modern Vertisol chronosequence would provide time-related criteria for addressing the duration of pedogenesis question. Paleosol 2 contains an abundance of features (thickness of slickensided horizons, bulk chemical translocation trends, and depth of pedogenesis) that are instrumental in determining the relative maturity of the profile and the stage of pedogenesis (from the modern Vertisol chronosequence) most closely matching features exhibited in Paleosol 2. A detailed comparison of features associated with Stage 1 (~400yrs) and Stage 2 (~3,500yrs) pedogenesis derived from study of the Ships and Pledger Pedons (Chapter II), respectively, can be found in Table 3.1. Although two additional advanced stages of pedogenesis are discussed in Chapter II, the presence of bedded alluvium at the base of Paleosol 2 is suggestive of lower stages of pedogenic development, because more advanced stages characteristically lack bedded alluvium.

The depth to parent material (Table 3.3) and depth of pedogenesis are the best features to use as a first approximation. Stage 1 of Vertisol pedogenesis (Ships) has the depth of parent material present at 130-180 cm, whereas Stage 2 pedogenesis (Pledger) has a depth range of 220 to 265 cm. Paleosol 2 falls intermediate between the two with a depth range of 160-180 cm. Similarly, in Paleosol 2 advancement of pedogenesis range is from 140 to 150 cm depth; this property increases as a function of time and occurs at 110 to 131 cm in the Ships and 182 to 220 cm for the Pledger profile. Vertisol classification requires the

Table 3.3 Comparison of Chronosequence and Paleosol 2 Microlows Macromorphology

Characteristics	Ships (~400 yrs)	Pennington Paleosol 2	Pledger(~3,500 yrs)
Parent Material	bedded, brown to red calcareous silty clay alluvium	bedded, grayish brown to calcareous silty clay alluvium	bedded, brown to red calcareous silty clay alluvium
Depth to Parent	130-180 cm	160-180 cm	220-265 cm
Depth to top of Bk	44-62 cm	120-150 (MH)	33-55 (MH);133-171 cm (ML)
Depth of pedogenesis	110-131cm	140-150 cm (calculated based on estimates of truncation of upper solum)	179-182(MH); 182-220(ML)
Slickenside dev. ; slickenside horizon (thickness)	abundant, closely-spaced (66cm)	Abundant, closely-spaced (70ML; 90-110 MH)	abundant, closely spaced (124MH;138ML)
Gilgai topography	no surface expression of gilgai	no surface expression; truncated by erosion	moderate relief (10 cm); spacing 2-3m
Mukkara	no mukkara developed	Chimney tongues do not penetrate surface (eroded)	chimney tongues do not penetrate to surface in all MH
Sepic-plasmic fabrics	44-62 cm	40-85 cm	44-88 cm
Fe/Mn masses	few masses in Ck1	abundant in ML	common in ML
Redox	rare to common in subsoil (Ck1) along pores and nodules	rare to common in subsoil along root pores, ped surfaces, and nodules	common in subsoil along ped surfaces, pores and fractures
Carbonate morphology	powder CO3 layer following master slickenside and sedimentary layering; nodules typically contain septarian voids; nodule interior similar to matrix	Dolomitized concentrations; some contain weathered Fe-Mn staining?" finely disseminated carbonate is dolomitized	variable nodule morphology; multiple phases of ped. CO3 formation?; some contain dendritic Mn; powder CO3 less common

identification of slickensides, and the thickness of horizons containing slickensides is particularly useful for delineating the stage of pedogenesis, because it increases with increased pedogenic stage. The summation of slickensided horizon thickness for each profile is 66 cm, 70 cm and 138 cm for the Ships, Paleosol 2 and Pledger profiles, respectively. Slickenside formation and development is of particular importance for development of gilgai topography and associated microhigh and microlow profiles. The Ships profile (Stage 1) contains a very limited range of slickensides, such that shrink-swell processes have not occurred for a period of time long enough to form more extensive slickensided horizons and microtopography. The Pledger profile contains very distinct MH and ML profiles with moderate relief (10cm) and spacing of 2 to 3m. Paleosol 2 does have distinctive MH and ML profiles, however, surficial expression of microtopography has possibly been eroded; the spacing between MH profiles is approximately 2 meters. The relationship between slickenside frequency (between adjacent MH profiles) and time is not well understood. Other macro-scale features useful in determining pedogenic stage includes redox concentrations/depletions, Fe-Mn masses, and carbonate morphologies.

Redoximorphic concentrations and depletions increase in occurrence with time in the early stages of pedogenesis. The Pennington Paleosol is intermediate between stage 1 and stage 2, with rare to common depletions/concentrations occurring along root pores, ped surfaces, and nodules. Fe-Mn masses increase in abundance with soil age, with few masses in the Ck1 horizon of the Ships and common throughout the ML of the Pledger. The ML identification of slickensides, and the thickness of horizons containing slickensides is particularly useful for delineating the stage of pedogenesis, because it increases with increased pedogenic stage. The summation of slickensided horizon thickness for each profile is 66 cm, 70 cm and 138 cm for the Ships, Paleosol 2 and Pledger profiles, respectively. Slickenside formation and development are of particular importance for development of gilgai topography and associated microhigh and microlow profiles. The Ships profile (Stage 1) contains a very limited range of slickensides, such that shrink-swell processes have not occurred for a period of time long enough to form more extensive slickensided horizons and microtopography. The Pledger profile contains very distinct MH and ML profiles with moderate relief (10cm) and spacing of 2 to 3m. Paleosol 2 does have distinctive MH and ML profiles, however, surficial expression of microtopography has possibly been eroded; the spacing between MH profiles is approximately 2 meters. The relationship between slickenside frequency (between adjacent MH profiles) and time is not well understood. Other macro-scale features useful in determining pedogenic stage includes redox concentrations/depletions, Fe-Mn masses, and carbonate morphologies.

Redoximorphic concentrations and depletions increase in occurrence with time in the early stages of pedogenesis. The Pennington Paleosol is intermediate between stage 1 and stage 2, with rare to common depletions/concentrations occurring along root pores, ped surfaces, and nodules.

Fe-Mn masses increase in abundance with soil age, with few masses in the Ck1 horizon of the Ships and common throughout the ML of the Pledger. The ML profile of Paleosol 2 contains abundant Fe-Mn masses throughout, with some concentrically laminated, dendritic and weakly-cemented phases. These phases are more characteristic of advanced pedogenesis.

Carbonate morphology, particularly nodule morphology does not have as clear of a correlation with age. Nodules with dendritic Mn may be indirectly a function of increased soil moisture, but may also represent a true increase in occurrence across the chronosequence. The utility of this as primary tool is not recommended until processes related to the formation of nodules with Mn-dendrites are better understood. The percentage of matrix carbonate or finely-disseminated carbonate may vary as a function of time, and longer duration of pedogenesis is reflected in a reduction of matrix diffuse carbonate. Dolomitization and clay transformations associated with burial diagenesis may have obliterated conclusive evidence on the quantity of matrix carbonate.

Micromorphology provides a secondary tool for delineating soil maturity. Extensive development of slickenside fibers, sepic-plasmic fabrics and clay translocation are useful in determining advancement of pedogenesis. Slickenside fibers, pressure faces, and sepic-plasmic fabric are better defined and occur as distinct domains within the thin section. This tool is better used as an addition to macromorphology, or when a complete set of samples will allow for estimations of horizon thickness containing these shrink-swell related fabrics. The Ships, Paleosol 2 and Pledger each have similar ranges of sepic-plasmic fabric occurrence. Clay translocation is particularly helpful when determining the depth to which parent material has been reworked by soil-forming processes. The depth of pedogenesis is usually indicated by vertical cracking, haploidization of the soil matrix, and variable Fe-Mn redox-depletions and enrichments on lithorelict surfaces. Because the Ships (Stage1) and Pledger (Stage 2) both have parent material preserved within the basal portions of their profiles, delineation of profile maturity based on disruption of the bedding is not as conclusive as other tools. There are features similar to the Ships and Pledger found in the BC and CB horizons of Paleosol2.

Bulk chemistry (Table 3.4) is another useful tool for determining relative profile maturity. Increased translocation, particularly of base cations, is an indicator of advanced pedogenesis. The Ships profile shows a general trend of minor to moderate translocations throughout the profile. Base cations (Ca, Mg, K, and Na) typically experience losses (15-20%) relative to the original parent material composition. In some cases, at depth (150-180cm) there is an enrichment or accumulation (5-10%) of the translocated cations. Base cation translocation trends of Paleosol 2 are variable, but in general have conservative to moderate losses (5-30%) to 180cm. The Pledger profile represents increased translocation with moderate to major losses of base cations to 120 to 140cm.

Redox-sensitive elements do not exhibit trends across the chronosequence that are consistent. Their mobility within the soil profile is subject to localized variations in soil moisture conditions. Localized grain-size

Table 3.4 Comparison of Chronosequence and Paleosol 2 Microlows

Characteristics	Ships	Pennington Paleosol 2	Pledger
Calcification index	minor loss (10-15%) to 150cm; gain (45%) at 160cm	moderate loss (5-30%) to 160cm ; minor gain (10%) at 150 and 180cm	major loss (80%) to 120cm; major gain (75%) at 150cm
Base loss index	base conservation through profile; minor gain (10%) at 60-70cm	moderate gain (0-25%) to 180cm	major loss (90%) to 120cm; major gain (70%) at 150cm
Oxidation	minor (5%) loss to 170cm	moderate loss (25%) to 30cm; major gain (75%) at 30cm; minor gain (0-15%) to 180cm	moderate loss (30%) to 120cm; moderate gain (25%) at 150cm
Salinization	minor enrichment (10%) to 70cm; variable loss/gain to 180cm	variable loss (0-25%) to 130cm; minor gains (10%) at 140 and 180cm; loss of 25% at 150	major loss (50%) to 120cm; major gain (50%) at 150cm
Strain (Ti immobility)	<5% dilation to 60cm; 10% collapse to 100cm; 2% dilation/collapse to 180cm	10-15% volume loss, with a 60% volume loss at 145cm	10-35% collapse to 250cm
Translocations			
Major element (Ti)			
Na_2O	highly variable moderate loss (5-20%) through profile; minor gains (5-10%) at 140 and 160cm	Variable loss (0-25%) to 180cm; peak loss at 60, 80 and 160 cm	major losses (50-75%) to 130cm; minor loss (5-25%) to 190-250cm; peak gain (25%) at 155cm
K_2O	minor loss(5%) from 40-120cm; minor gains (<5%) to 170cm	Conserved to minor gain/loss (<10%)	minor loss (5-15%) to 150cm; minor (<5%) to 250cm
Al_2O_3	highly variable, minor losses (5-8%) to 50cm; minor gains (2-8%) to 150cm	Minor loss (<10%) to 140 cm; conserved to 180cm	moderate gains (15-25%) to 150cm; minor losses (<5%) to 250cm

Table 3.4 (continued) Comparison of Chronosequence and Paleosol 2 Microlows

Characteristics	Ships (~400 yrs)	Pennington Paleosol 2	Pledger(~3,500 yrs)
SiO2	moderate gains (2-30%) to 180cm	Conserved to minor loss (<~5%) to 180cm	moderate losses (25%) to 150cm; minor losses (5-10%) to 250cm
CaO	moderate losses (5-25%) to 170cm; major peak gain (35%) at 160cm	major loss (60-75%) at 20-30 and 50-140cm; moderate gain (10-20%) at 150 and 180cm; loss of 50% at 160 cm	major losses (80-90%) to 120cm; major gains (50%) at 150cm; minor gains (5-10%) to 250cm
MgO	moderate losses (5-20%) to 120cm; minor gains (5%) to 180cm	moderate losses (0-30%) to 180cm; peak losses at 60 and 80 cm	moderate losses (25-35%) to 140cm; minor gains (5-10%) to 240cm
Fe2O3	moderate losses (5-25%) to 100cm; minor gains (5-10%) from 110-180cm	Moderate loss (30%) to 30cm; major gain at 40cm; conserved to minor gains (<5%) to180cm	conserved; minor (<5%) gains to 240cm
Minor/Trace element (Ti)			
MnO	moderate losses (5-20%) to 70cm and 110 to 120cm; minor gains (5-20%) 120-140cm	Major loss (~100%) at 20cm; minor loss (<5%) to 180cm	moderate gains (10-30%) to 140cm; minor loss (5%) to 240cm
P2O5	Conserved to depth; moderate gain of 25% in upper 30cm	Extremely variable from gains of more than 100% to loss of near 50% to 180cm	Major loss (>50%) to 120 cm; sporadic gains/losses (~10%) to 300cm
Sr	Minor loss (10-25%) to 120cm	Minor gains (10%) at 20 and 40cm; minor loss (0-20%) to 180cm	Major losses (50%) to 100cm minor gains to conserved to 300 cm
Zr	Major loss (20-70%) to 100cm and 180cm; variable to minor gain/loss 170	Moderate gains (0-30%) to 180cm; peak loss correspond to 30cm and 170cm	Moderate loss (~25%) to 250cm and major gains (>100%) to >300cm
Rb	minor loss (5-15%) to 120cm; minor gains (<5%) 120-180cm	Conserved to minor loss (<10%) to 180 cm	moderate gains (25-35%) to 140cm; conserved to 250cm
Cr	Variable minor loss(<10%) to 180 cm	Conserved to minor loss (~5%) to 180 cm	Highly variable with moderate losses (~25%) to very major gains (>100%)

variation can result in concentration of Fe, Mn and Cr, particularly when there is organic matter present with which to complex. Translocations of these elements are similar between the Ships and Paleosol 2, thus indicating that similar conditions may have been present during soil formation.

In general, the duration of pedogenesis for Pennington Paleosol 2, as estimated using the modern Vertisol chronosequence, is in the range of 400 to 3,500 years. Based on the data presented here, characteristics of the Paleosol 2 are indicative of a time closer to 400 years. Regardless, this type of study has provided time resolution not normally seen in geologic materials, particularly those from the Paleozoic Era. Using this information, we can allocate time (Figure 3.9) through the entire sequence to determine if the current estimates are feasible. Sea-level fluctuations during this time are considered to be on the Milankovitch scale (100,000 to 400,000 yrs). Vail (1959) suggested that shorter cycles may be superimposed on longer-term cycles. Sedimentation rates for shale and dolomite range from 20-1000m/Ma and 20-200m/Ma (Alterman and Nelson, 1998), respectively. Based on the stratigraphic thicknesses of these units, limestone (.25 m), green shale (.125 m) and red claystone paleosol (1.5 m), time allocation ranges for each unit are 1.25-12.5 ky, 0.0125-6.25 ky, and 1.5-75 ky (using shale sediment accumulation rate), respectively. Total profile time allocation ranges from 2.7625-93.75 ky, which suggests that these units may not account for the total time associated with a complete Milankovitch-scale sea level fluctuation cycle. The time estimate for Paleosol 2, between 400 and 1000 years, indicates that there is still a significant amount of time not accounted for by rock, if these deposits represent 100,000 to 400,000 yr duration cycles. Figure 3.9 is a schematic diagram representing time allocation, in which the larger arrows indicate longer time intervals, and the smaller arrows indicate shorter time intervals. If these sea-level fluctuations are, in fact of Milankovitch scale, then significant periods of time are not represented in the rock units. As such, fairly large hiatuses may be associated with: 1) erosional surfaces between the dolostone and the green shale, and 2) erosional truncation due to encroachment and flooding of marine waters (upper green shale) over the paleosol surface. Re-evaluating similar sections in the rock record may prove that Vail's (1959) proposed shorter transgressive-regressive cycles during the Mississippian are significantly "shorter" than originally thought.

Conclusions

Pennington Paleosol 2 contains very distinct morphological and bulk chemical features analogous to those of modern Vertisols. The occurrence of paleoVertisols at sequence boundaries is particularly useful in determining landscape and environmental conditions at the time of deposition and pedogenesis. Time-dependent criteria such as thickness of slickensided horizons, estimated depth of pedogenesis, occurrence of original bedded parent material, and translocation of base cations, are particularly useful in determining profile maturity in both modern Vertisols and Mississippian paleoVertisols. The duration of pedogenesis may have been greater than a few hundred years, but probably was less than a few thousand years, as recorded by Paleosol 2. Only

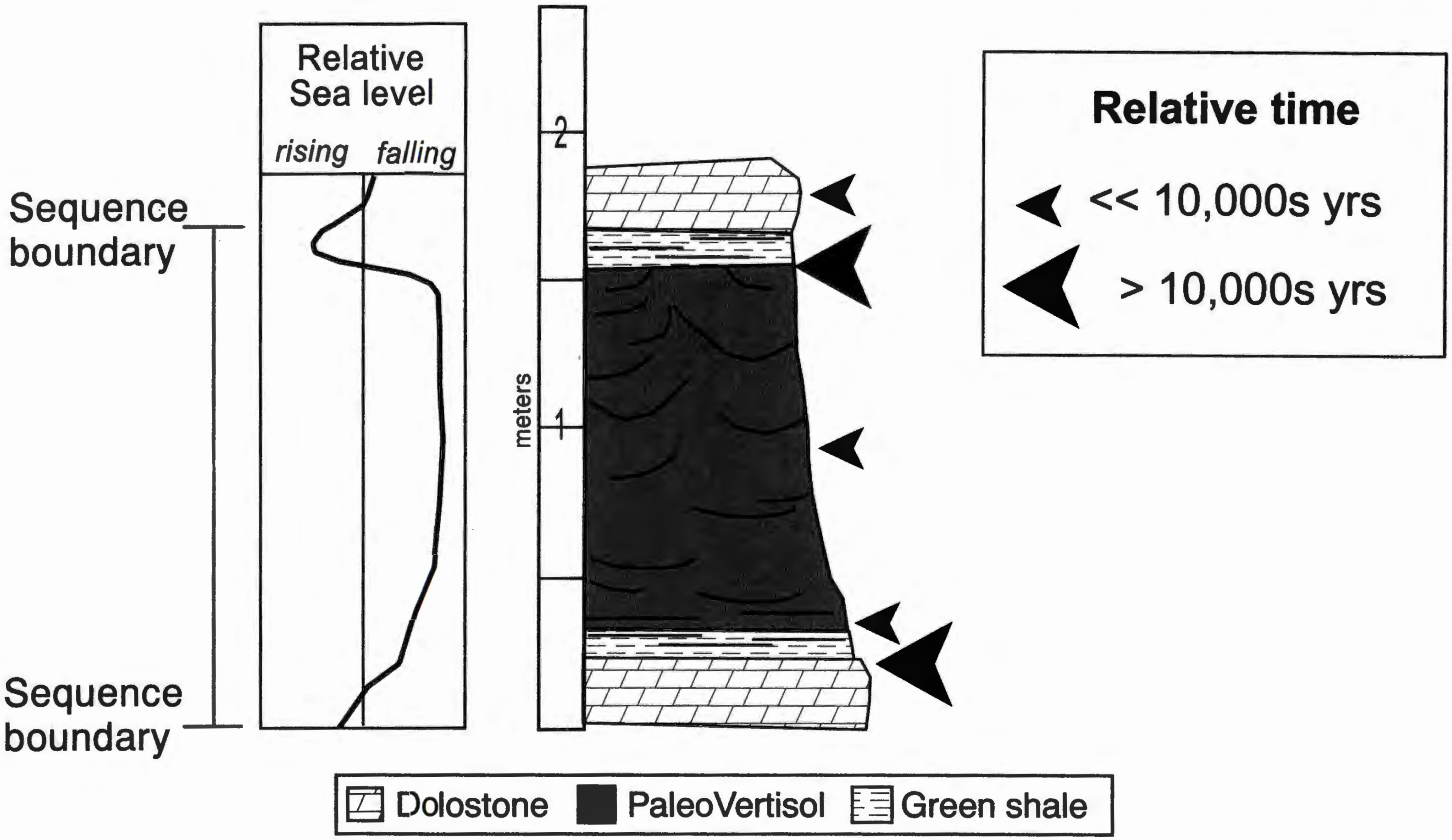

Figure 3.9 Generalized stratigraphy of Paleosol 2 from Mississippian Pennington Fm., Sparta, TN. The size of the arrow increases with increasing allocated time.

through the application of the modern Vertisol chronosequence (Chapter II) to the rock record can semi-quantitative estimates be made on duration of pedogenesis.

Application of the chronosequence study to additional paleoVertisol profiles in the Pennington Fm. (late Mississippian, TN) may require re-evaluation of sequence cyclicity and duration. Considering the age estimates for Paleosol 2 (~400-3,500 yrs), there is a significant reduction in the time duration associated with surface stability during sea-level lowstand. This estimate for Paleosol 2, in addition to sedimentation rates for the other non-pedogenic strata, requires that: 1) a significant hiatus must have occurred to account for time not represented by the sedimentary package, or 2) the cycles between marine and terrestrial conditions are much shorter than current estimates.

Chapter IV.

General Conclusions from the Modern Vertisol Chronosequence and Application to PaleoVertisols

The modern Vertisol chronosequence creates a semi-quantitative method for determining pedogenic stage and rates of pedogenesis of alluvially-derived soils formed on terraces of the Brazos River, TX. Several important conclusions from this study are as follow:

1) Morphological and bulk chemical trends serve as tools useful for identifying time-related characteristics. Increased thickness of slickensided horizons and depth to the pedogenic development front, as well as greater relief of gilgai topography correlates well with increasing profile age. Micromorphologic features such as: slickenfibers, sepic-plasmic fabric, Fe-Mn segregations, and carbonate phases are more distinct and better defined with increasing pedogenic development. Translocation indices, loss of base cations and redox variation are bulk chemical characteristics that vary as a function of time.
2) Rates of pedogenesis, in alluvially derived soils, appear to be much faster in early stages of pedogenesis (Stages 1 and 2, 400-3500 yrs) where there is minimal to significant expression of the characteristics discussed in Chapter II and summarized in 1 (above). Later stages (Stages 3 and 4, 18,000-35,000 yrs) of pedogenesis occur at slower rates, as indicated by

a minor characteristic differential. There appears to be a limit in pedogenic processes, where morphological expression of continued pedogenesis is minimal or absent (terminal pedogenesis).

3) Correction factors, based on stages of profile development, may be useful in paleoclimate reconstructions (depth vs. time) and deciphering climate/time signals preserved in the profile. For example, if a soil is determined to be in early stages of pedogenesis then the climatic influence on soil-forming processes may be magnified, whereas with increased duration of profile development, pedogenesis may be the dominant process overprinting or convoluting the pure climate signal.
4) The chronosequence model is useful for obtaining greater time resolution associated with paleoVertisols, which occur at sequence boundaries in Mississippian carbonate-clastic sequence sets. Milankovitch sea-level fluctuation cycles (100,000-400,000 yrs) have been suggested for the Mississippian in Tennessee. Time allocation estimates for each sequence package indicate that there may be a significant amount of time not represented by rock.

Chapter IV.

Suggestions for future work

Avenues of future work related to the chronosequence model and application of the chronosequence model to paleoVertisols are suggested. The model requires additional testing on additional paleoVertisols within the Pennington Fm. and also applied to paleosols from other depositional basins along the Appalachian basin succession (e.g., Maccrady Fm., West Virginia; Mauch Chunk Fm., Pennsylvania).

Completion of the stable C isotopic compositions of each profile across the chronosequence should better enable one to: 1) determine the origin of the pedogenic nodules in the Ships profile, 2) create higher time-resolution climate studies, and 3) determine if depth-equals-time is a valid approach to climatic reconstructions, particularly when the soils may be at different pedogenic stages.

Conventional or existing chronofunctions typically do not correctly access the morphological development of Vertisols for several reasons: 1) the presence and abundance of slickenside features, 2) the minimal variation in texture, 3) the color indices (e.g., melanization) would vary between MH and ML profiles within the same pedon, 4) clay films due to illuviation are secondary in importance to shrink-swell oriented clays, and 5) structural aggregates are a function of shrink-swell processes. Development of a Vertisol-specific chronofunction that includes these as well as other features outlined in chronosequence studies may provide a more quantitative approach to rates of Vertisol pedogenesis and age estimates based on morphologic features.

References

REFERENCES

Ahmad, N., 1983, Vertisols, *in* Wilding, L.P., Smeck, N.E., and Hall, G.F., eds., Pedogenesis and Soil Taxonomy, II. The Soil Orders: Developments in Soil Science 11B, New York, Elsevier, p. 91-123.

Altermann, and Nelson, D.R., 1998, Sedimentation rates, basin analysis and regional correlations of three Neoarchaean and Paleoproterozoic sub-basins of the Kaapvaal Craton as inferred from precise U-Pb zircon ages from volcaniclastic sediments: Sedimentary Geology, v. 120, p. 225-256.

Aniku, J. and Singer, M., 1990, Pedogenic iron oxide trends in a marine terrace chronosequence. Soil Science Society of America Journal, v. 54, p. 147-152.

Bal, L., 1982, Zoological Ripening of Soils, Center for Agricultural Publishing and Documentation, Wageningen, 365 p.

Bilzi, A.F. and Ciolkosz, E.J., 1977, A field morphology rating scale for evaluating pedological development: Soil Science, v. 124, no.1, p. 45-48.

Birdseye and Aronow, 1991, New evidence for a young late Wisconsin age for the Prairie Formation in southwestern Louisiana: Boulder, CO, Geological Society of America, GSA Abstracts with Programs, v. 23, no. 5, p.223.

Birkeland, P., 1974, Pedology, Weathering and Geomorphogical Research: Oxford, Oxford University Press, 285p.

Birkeland, P.W., 1984, Soils and Geomorphology: New York, Oxford University Press, 372 p.

Blake, G.R. and Hartge, K.H., 1986, Bulk density. In: Kulte, A. (Ed.), Methods of Soil Analysis: Part I. Physical and Mineralogical Methods. 2nd edn. Soil Science Society of America Agronomy Monograph 9, p. 363-375.

Blum, M.D. and Valastro, S. Jr., 1994, Late Quaternary sedimentation, lower Colorado River, Gulf Coastal Plain of Texas: Geological Society of America Bulletin, v. 106, p. 1002-1016.

Bockheim, J.G.,1980, Solution and use of chronofunctions in studying soil development: Geoderma, v. 24, p. 71-85.

Bouma, J. and Loveday, J., 1988, Characterizing soil water regimes in swelling clay soils, *in* Wilding, L.P. and Puentes, R., eds., Vertisols: Their Distribution, Properties, Classificiation, and Management: College Station, Texas, Texas A&M University Press, p. 83-96.

Brewer, R., 1976, Fabric and Mineral Analysis of Soils: New York, R.E. Krieger Publishing, 482 p.

Brewer, R., 1964, Fabric and Mineral Analysis of Soils: New York, Wiley Publishers, 470 p.

Brimhall, G.H., and Deitrich, W.E., 1987, Constitutive mass balance relations between chemical composition, volume, density, porosity, and strain in metasomatic hydrochemical systems; results on weathering and pedogenesis: Geochimica et Cosmochimica Acta., v. 51, p. 567-587

Brimhall, G.H., Chadwick, O.A., Lewis, C.J., Compston, W., Williams, I.S., Danti, K.J., Dietrich, W.E., Power, M.E., Hendricks, D., Bratt, J., 1991, Deformational mass transport and invasive processes in soil evolution: Science, v. 255, p. 695-755.

Brimhall, G.W., Lewis, C.J., Ford, C.R., Bratt, J., Taylor, G., and Warin, O., 1991; Quantitative geochemical approach to pedogenesis; importance of parent material reduction, volumetric expansion, and eolian influx in lateritization: Geoderma, v. 51, no. 1-4, p.51-91.

Buol, S.W., Hole, F.D., and McCracken, R.D., 1989, Soil Genesis and Classification (3rd ed.): Ames, Iowa, Iowa State University Press.

Busacca, A.J., 1987, Pedogenesis of a chronosequence in the Sacramento Valley, California, U.S.A., I. Application of a soil development index. Geoderma, v. 41, p. 123-148.

Busacca, A.J. and Singer, M.J., 1989, Pedogenesis of a chronosequence in the Sacramento Valley, California, U.S.A., II. Elemental chemistry of silt fractions: Geoderma, v. 44, p. 43-75.

Button, A., 1979, Early Proterozoic weathering profile on the 2200 million year old Hekpoort Basalt, Pretoria Group, South Africa: preliminary results: University of Witwatersrand (Johannesburg, South Africa) Economic Geology Research Unit Information Circular 35, 38 p.

Caudill, M.R., 1996, Paleoclimate, Burial Compaction, and Perched Water Tables; Carboniferous Vertic Paleosols, Ohio and Tennessee: unpublished Doctoral dissertation, University of Tennessee-Knoxville, 171 p.

Caudill, M.R., Driese, S.G., and Mora, C.I., 1997, Physical compaction of vertic palaeosols: implications for burial diagenesis and palaeo-precipitation estimates: Sedimentology, v. 44, p. 673-685.

Caudill, M.R., Driese, S.G., and Mora, C.I., 1996, Preservation of a paleo-Vertisol and an estimate of late Mississippian paleoprecipitation: Journal of Sedimentary Research, v. 66, no. 1, p. 58-70.

Chadwick, O.A., Derry, L.A., Vitousek, P.M., Huevert, B.J., and Hedin, L.O., 1999, Changing sources of nutrients during four million years of ecosystem development: Nature, v. 397, p. 491-497.

Chadwick, O.A., and Chorover, J., 2001, The chemistry of pedogenic thresholds: Geoderma, v. 100, p. 321-353.

Chorover, J., DiChiaro, M.J., and Chadwick, O.A., 1999, Structural change and cesium retention in a chronosequence of tephritic soils: Soil Science Society of America Journal, v. 63, p. 169-177.

Coulombe, C.E., Dixon, J.B., and Wilding, L.P., 1996, Mineralogy and chemistry of Vertisols, *in* Ahmad, N. and Mermut, A., ed., Vertisols and Technologies for their Management: Amsterdam, Elsevier, p. 115-197.

Crowley and North, 1991, Paleoclimatology: Oxford, Oxford University Press, 349 p.

Driese, S.G., and Mora, C.I., 1993, Physio-chemical environment of pedogenic carbonate formation in Devonian vertic paleosols, central Appalachians, U.S.A.: Sedimentology, v. 40, p. 199-216.

Driese, S.G., Caudill, M.R., and Srinivasan, K., 1998, Late Mississippian to Early Pennsylvanian paleokarst in east-central Tennessee; field, petrographic, and stable isotope evidence: Southeastern Geology, v. 37, p. 189-204.

Driese, S.G., Mora, C.I., Cotter, E., and Foreman, J.L., 1992, Paleopedology and stable isotope chemistry of Late Silurian vertic Paleosols, Bloomsburg Formation, central Pennsylvania: Journal of Sedimentary Petrology, v. 62; p. 825-841.

Driese, S.G., Mora, C.I., and Elick, J.M., 1997, Morphology and taphonomy of root and stump cast of the earliest trees (Middle to Late Devonian) Pennsylvania and New York, U.S.A.: Palaios, v. 12, p. 524-537.

Driese, S.G., Mora, C.I., Stiles, C.A. R.M. Joeckel, and Nordt, L.C., 2000, Mass-balance reconstruction of a modern Vertisol: implications for interpreting the geochemistry and burial alteration of paleoVertisols: Geoderma, 95, p. 179-204.

Dudal, R., 1965, Dark clay soils of tropical and subtropical regions: FAO Agriculture Development Paper, Rome.

Dudal, R., and Eswaran, H., 1988, Distribution, properties and classification of Vertisols, *in* Wilding, L.P., and Puentes, R. eds., Vertisols: Their distribution, properties, classification and management: College Station, Texas A & M University Printing Center, p. 1-22.

Ettensohn, F.R., Pashin, J.C., and Jacobs, G.W., 1986, Shallow-water marine siltstones in Paleozoic shelf deposits of Kentucky: American Association of Petroleum Geologists Bulletin, v. 70, p. 588-598.

FitzPatrick, E.A., 1993, Soil microscopy and Micromorphology: New York, John Wiley & Sons, 304 p.

Gile, L.H., Peterson, F.F., and Grossman, R.B.G., 1966, Morphology and genetic sequences of carbonate accumulation in desert soils: Soil Science, v. 101, p. 347-360.

Golden, D.C., Turner, F.T., Sittertz-Bhatkar, H. and Dixon, J.B., 1997, Seasonally precipitated iron oxides in a Vertisol of Southeast Texas: Soil Science Society of America Journal, v. 61, p. 958-964.

Gustavson, T.C., 1991, Buried Vertisols in lacustrine facies of the Pliocene Fort Hancock Formation, Hueco Bolson, West Texas and Chihuahua, Mexico: Geological Society of America Bulletin, v. 103, p. 448-460.

Hallsworth, E.G., and Crawford, D.V., eds., 1965, Experimental Pedology, Proceedings of the Eleventh Easter School in Agricultural Science, University of Nottingham.

Harden, J.W., 1982, A quantitative index of soil development from field descriptions: examples from a chronosequence in central California: Geoderma, v. 28, p. 1-28.

Harden, J.W., and Taylor, E.M., 1983, A quantitative comparison of soil development in four climatic regimes: Quaternary Research, v.20, p. 342-359.

Harding, S.D., 1995, The Stratigraphy and Paleoenvironments of Paleosols and Associated Strata of the Lower Pennington Formation (Upper Mississippian) at Sparta, Tennessee: unpublished senior honors thesis, University of Tennessee, 41 p.

Hatcher, R., Jr., Thomas, W.A., Vieleet, G. W., et al., 1989, The Appalachian-Ouachita orogen in the United States: Geological Society of America, Boulder, Colorado, 767p.

Hoefs, J. 1987, Stable isotope geochemistry, Springer-Verlag, New York, 241 p.

Hoefs, J. 1987, Stable isotope geochemistry, Springer-Verlag, New York, 241 p.

Jenny, H., 1941, Factors of Soil Formation: New York, McGraw-Hill, 281 p.

Jenny, H.J., 1961, Derivation of state factor equations of soils and ecosystems: Soil Science Society of America Proceedings, v. 25, p. 385-388.

Joeckel, R.M.,1994, Virgilian (Upper Pennsylvanian) Paleosols in the upper Lawrence Formation (Douglas Group) and its Snyderville Shale Member (Oread Formation, Shawnee Group) of the northern Midcontinent, USA; pedologic contrasts in a cyclothem sequence: Journal of Sedimentary Research, Section A: Sedimentary Petrology and Processes, v.64, no. 4, p. 853-866.

Joeckel, R.M., 1999, Paleosol in Galesburg Formation (Kansas City Group, Upper Pennsylvanian), northern Midcontinent, U.S.A.; evidence for climate change and mechanisms of marine transgression: Journal of Sedimentary Research, v. 69, no. 3, p. 720-737.

Jongerius, A., and Rutherford, G.K., 1979, Glossary of soil micromorphology, Centre for Agricultural Publishing and Documentation, Wageningen, Netherlands, 138p.

King, 1977, The evolution of North America, Princeton University Press, Princeton, N.J., 197 p.

Knight, M.J., 1980, Structural analysis and mechanical origins of gilgai at Boorook, Victoria, Australia: Geoderma, v. 23, p. 245-283.

Kunze, G.W., Oakes, H., and Bloodworth, M.E., 1963, Grumusols of the Coast Prairie of Texas: Soil Science Society of America Proc., v. 27, p. 412-421.

Lin, H.S., McInnes, K.J., Wilding, L.P., and Hallmark, C.T., 1998, Macroporosity and initial moisture effects on infiltration rates in Vertisols and vertic intergrades: Soil Science, v. 163, p. 2-8.

Lynn, W., and Williams, D., 1992, The making of a Vertisol: Soil Survey Horizons, v. 33, no. 2, p. 45-50.

Markewich, H.W. and Pavich, M.J., 1991, Soil chronosequence studies in temperate to subtropical, low-latitude, low-relief terrain with data from the eastern United States: Geoderma, v. 51, p. 213-239.

Marsan, F.A., Barberis, E. and Arduino, E., 1988, A soil chronosequence in Northwestern Italy: morphological, physical and chemical characteristics: Geoderma, v. 42, p. 51-64.

Machette, M.N., 1985, Calcic soils of the Southwestern United States, *in* Weide, D.L., ed., Soils and Quaternary geology of the Southwestern United States: Geological Society of America Special Paper 203, p. 1-21.

McCarthy, P.J. and Plint, A.G., 1998, Recognition of interfluve sequence boundaries: integrating paleopedology and sequence stratigraphy: Geology v. 26, p. 387-390.

Miller, D.L., 2000, Occurrence and Stable Isotope Compositions of Soil Carbonate and Organic Matter Within a Climatic Transect of Modern Vertisols Along the Coastal Prairie of Texas: unpublished M.S. thesis, University of Tennessee, 83 p.

Milici, R.C., Briggs, G., Knox, L., Sitterly, P.D., and Statler, A.T., 1979, The Mississippian and Pennsylvanian (Carboniferous)systems in the United States: U. S. Geological Survey Professional Paper, Report: P 1110 G, p. G1-G38.

Mora, C.I., Driese, S.G., and Colarusso, L.A., 1996, Middle to Late Paleozoic atmospheric CO_2 levels form soil carbonate and organic matter: Science, v. 271, p. 1105-1107.

Mora, C.I., and Driese, S.G., 1993, A steep, mid- to late Paleozoic decline in atmospheric CO_2; evidence from the soil carbonate CO_2 paleobarometer: Chemical Geology, v. 107, p. 217-219.

Mora, C.I., and Driese, S.G., 1999, Palaeoenvironment, palaeoclimate and stable carbon isotopes of Palaeozoic red-bed Palaeosols, Appalachian Basin, USA and Canada, *in* Thiry, M and Simon, C.R., ed., Palaeoweathering, palaeosurfaces and related continental deposits: Special Publication of the International Association of Sedimentologists, v. 27, p. 61-84.

Mora, C.I., Sheldon, B.T., Elliott, W.C., and Driese, S.G., 1998, An oxygen isotope study of illite and calcite in three Appalachian Paleozoic vertic paleosols: Journal of Sedimentary Research, v. 28, p. 456-464.

Nordt, L.C., 1996, Development of a soil chronosequence in late Quaternary alluvium in central Texas; a stable C isotope and mass balance approach, unpublished Doctoral dissertation, College Station, TX, Texas A&M University, 155 p.

Nordt, L.C., Hallmark, C.T., Wilding, L.P., and Chervenka, W.G., 1992, Soils and Geomorphology Tour of Brazos and Eastern Burleson Counties, Texas: Soil Science Institute.

Probert, M.E., 1987, The Properties and Management of Vertisols: Wallingford, UK, CSIRO Division of Soils, 369 p.

Puentes, R., 1992, Microspatial variability and sampling concepts in soil porosity studies of Vertisols: Geoderma v. 53, no. 3-4, p. 373-385.

Retallack, G.J., 1988, Field recognition of paleosols, *in* Reinhardt, J. and Sigleo, W.R., ed., Paleosols and Weathering Through Geologic Time: Special Publication of Geological Society of America, v. 216, p. 1-20.

Retallack, G.J., 1991, Untangling the effects of burial alteration and ancient soil formation: Annual Reviews of Earth and Planetary Science, v. 19, p. 183-206.

Retallack, G.J., 1986, The fossil record of soils, *in* Wright, V.P., ed., Paleosols: Their Recognition and Interpretation: Oxford, Blackwell Science, p. 1-57.

Runge, E.C.A., 1973, Soil development sequences and energy models: Soil Science, v. 115, p. 183-193.

Schoeneberger, P.J., Wysocki, D.A., Benham, E.C., and Broderson, W.D., 1998, Field Book for Describing and Sampling Soils: Lincoln Nebraska, National Soil Survey Center, NRCS and USDA, 91 p.

Simonson, R.W., 1959, Outline of a generalized theory of soil genesis: Soil Science Society of America Proceedings, v. 23, p. 152-156.

Stevens, P.R., and Walker, T.W., 1970, The chronosequence concept and soil formation: Quarterly Review of Biology, v. 45, p. 333-350.

Stiles, C.A., 2001, Pedogenic Relationships in a Texas Vertisol Climosequence Defined by Geochemical Mass Balance of Whole Soil and Chemistry of Iron-Manganese Nodules: unpublished Doctora dissertation, University of Tennessee, 264 p.

Stiles, C.A., Mora C.I., and Driese, S.G., 2001, Pedogenic iron-manganese nodules in Vertisols: A new proxy for paleoprecipitation?: Geology, v. 29, p. 943-946.

Vail, P., 1959, Stratigraphy and lithofacies of Upper Mississippian rocks in the Cumberland Plateau. Unpublished Doctoral dissertation: Evanston, IL, Northwestern University, 378 p.

Vidic, N., Pavich, M. and Lobnik, F., 1991, Statistical analyses of soil properties on Quaternary terrace sequence in the upper Sava River Valley, Slovenia, Yugoslavia: Geoderma, v. 51, p. 189-212.

Vitousek, P.M., Chadwick, O.A., Crews, T.E., Fownes, J.H., Hendricks, D.M., and Herbert, D., 1997, Soil and ecosystem development across the Hawaiian Islands: GSA Today, v. 7, no. 9, p. 1-10.

White, G.N. and Dixon, J.B., 1996, Iron and manganese distribution in nodules from a young Texas Vertisol: Soil Science Society of America Journal, v. 60, p. 1254-1262.

Wilding, L.P. and Tessier, D., 1988, Genesis of Vertisols: shrink-swell phenomena, *in* Wilding, L.P. and Puentes, R., eds., Vertisols: Their Distiribution, Properties, Classification and Management: Technical Monograph 18: Texas A&M Univertsity Printing Center, p. 55-81.

Yaalon, D.H., 1975, Conceptual models in pedogenesis: can soil-forming functions be solved?: Geoderma, v. 14, p. 189-205.

Yaalon, D.H. and Kalmar, D., 1978, Dynamics of cracking and swelling clay soils: displacement of skeletal grains, optimum depth of slickensides, and rate of intra-pedonic turbation: Earth Surface Processes, v. 3, p. 31-42.

http://encarta.msn.com

http://www.ncdc.noaa.gov/ol/climate/climatedata.html

Appendices

See attached CD ROM (plate 1) for Appendix material.

The Appendices stored on the CD ROM include the following:

APPENDIX	TOPIC
A.	Macromorphology
B.	Micromorphology
C.	Bulk Chemistry
D.	Particle Size Analyses and Clay Mineralogy
E.	Stable Isotopes
F.	Pennington Paleosol 2
G.	Preliminary Study of Stable Isotopes

The CD contains Appendices created using Microsoft Word 97. To access the data in the Appendices, insert the CD ROM. If the autorun feature is enabled on your computer, a window will open automatically. If not, you will need to run the file autorun.exe located on the CD ROM. When the program runs a window will open, allowing the user to link to various parts of the Appendices. When scrolling over the Appendix options, each will become highlighted. The item of interest may then be selected by clicking the mouse button on the Appendix of choice.

VITA

Amelia Carol Robinson was born in Union City, Tennessee on December 14, 1973. She attended UC Elementary, East Side, and UC Middle School. She moved to Martin, attended Martin Jr. High and graduated from Martin Westview High School in 1992. Two science fair projects allowed her to work with Dr. Michael Mullen, at the University of Tennessee-Martin. The following August, Amelia majored in Environmental Management and Chemistry at UTM. An exercise in Historical Geology (with Dr. Michael Gibson) included reconstruction of the depositional history of a set of samples. This lab peaked Amelia's interest and an encouraging note from the instructor, resulted in a change to major in geology. During her time at UT Martin, Amelia served as math lab, soil science lab and P.A.C.E. teaching assistants. On her birthday in 1997, she received two degrees, a Bachelor of Science in Natural Resources Management and a Bachelor of Science in Geology. The following January, Amelia began her Master of Science in Geology at the University of Tennessee. The combination of her background in soils, chemistry and geology provided a good foundation to do research in paleopedology with Dr. Steve Driese at the University of Tennessee. The Master of Science Degree was granted May, 2002. She began her doctoral work at the University of California-Davis in September, 2001.